

# **„Aluminium and Iron Catalysts as sustainable Alternatives in Synthetic Processes“**

Dissertation

zur Erlangung des Doktorgrades der Naturwissenschaften

**Dr. rer. nat.**

an der Fakultät für Chemie und Pharmazie

der Universität Regensburg



vorgelegt von

**Josef Bernauer**

aus Passau

Regensburg 2020



The experimental part of this work was carried out between December 2015 and March 2018 at the University of Regensburg, Institute of Organic Chemistry, and between April 2018 and April 2019 at the University of Hamburg, Institute of Inorganic and Applied Chemistry.

Doctoral application submitted on 10 June 2020

The dissertation was supervised by Prof. Dr. Axel Jacobi von Wangelin

Board of examiners:

Apl. Prof. Dr. Rainer Müller	(Chairman)
Prof. Dr. Axel Jacobi von Wangelin	(1st Referee)
Jun.-Prof. Dr. Ivana Fleischer	(2nd Referee)
Prof. Dr. Frank-Michael Matysik	(Examiner)

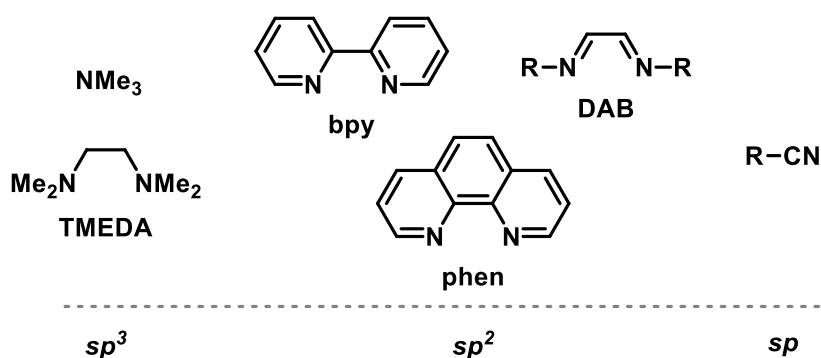
# Table of Contents

<b>1</b>	<b>INTRODUCTION</b>	<b>1</b>
1.1	Nitrogen Donors in Homogeneous Catalysis	1
1.2	Bis(imino)acenaphthene (BIAN) Synthesis	4
1.3	BIAN Ligands in Catalysis	8
1.4	Conclusion	25
1.5	References	26
<b>2</b>	<b>APPLICATION OF REDUCED BIAN ALUMINIUM HYDRIDE COMPLEXES IN CATALYSIS</b>	<b>30</b>
2.1	Introduction	31
2.2	Results and Discussion	32
2.3	Conclusion	41
2.4	Experimental	42
2.4.1	<i>Complex Synthesis</i>	43
2.4.2	<i>Preparation of Imines</i>	49
2.4.3	<i>Catalytic Reactions</i>	54
2.5	References	65
<b>3</b>	<b>IRON-CATALYZED ALLYLATION-HYDROGENATION SEQUENCES AS MASKED ALKYL-ALKYL CROSS-COUPPLINGS</b>	<b>67</b>
3.1	Introduction	68
3.2	Results and Discussion	70
3.3	Conclusions	81
3.4	Experimental	82
3.4.1	<i>Preparation of Starting Materials</i>	83
3.4.2	<i>Iron-catalyzed cross-coupling reactions</i>	96
3.4.3	<i>Mechanistic Investigations</i>	118
3.5	References	125
<b>4</b>	<b>THESIS SUMMARY</b>	<b>128</b>
4.1	Summary	128
4.2	Zusammenfassung	129
<b>5</b>	<b>APPENDIX</b>	<b>130</b>
5.1	List of Abbreviations	130
5.2	Acknowledgements	132
5.3	Curriculum Vitae	133
5.4	Eidesstattliche Erklärung	135

# 1 Introduction

## 1.1 Nitrogen Donors in Homogeneous Catalysis

Nitrogen containing ligands have been around for centuries. In 1893 investigations by Alfred Werner on the coordination of ammonia to platinum set the foundation for modern coordination chemistry.<sup>[1]</sup> However, *N*-donor ligands were only rarely used in catalytic reactions until the 1990s,<sup>[2]</sup> when the ease of generating chiral *N*-containing compounds led to a major increase of interest in the organometallic community.<sup>[3]</sup> On this path, they became the second pillar alongside established phosphorus donor ligands. A small excerpt of common nitrogen ligands is shown in Figure 1.1.



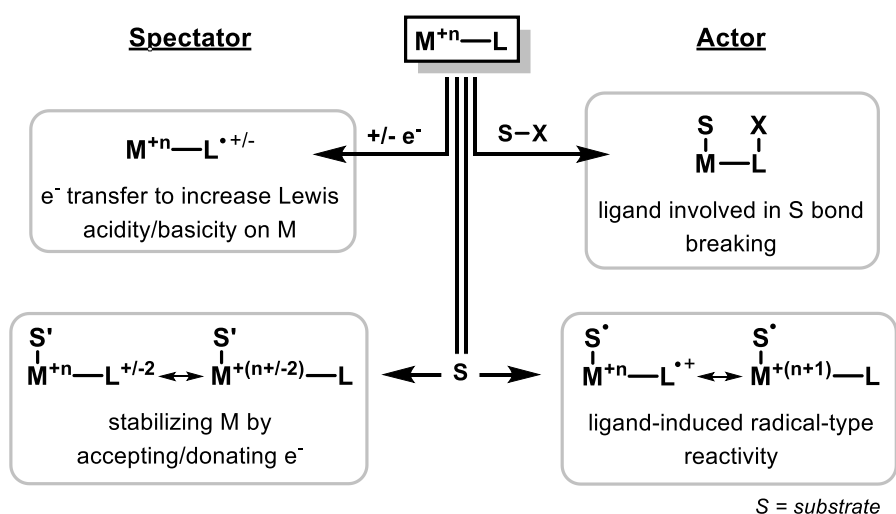
**Figure 1.1** Classification of nitrogen ligands based on the hybridization of *N*.

abbr.: *N,N,N',N'*-tetramethylethylenediamine (TMEDA), 2,2'-bipyridine (bpy), 1,4-diazabutadiene (DAB), 1,10-phenanthroline (phen).

While ligands containing  $\text{sp}^3$ -hybridized nitrogen atoms merely serve as  $\sigma$ -donors, a very extensive coordination chemistry is at hand by employing  $\text{sp}^2$ -hybridized nitrogen ligands due to the possibility of  $\pi$ -interactions.  $\text{sp}^2$ - and partially also  $\text{sp}^3$ -hybridized nitrogen ligands became key players in organometallic chemistry. Thanks to their complexity, they are established in a wide diversity of fields, namely coordination, inorganic, pharmaceutical and medicinal chemistries, biologically active compounds, electrochemistry, C–H bond activation and functionalization, catalysis, etc.<sup>[4]</sup> Ligands containing  $\text{sp}$ -hybridized nitrogen atoms on the other hand are solely represented by nitriles. Nitriles generally show only weak coordination and therefore mostly function as labile placeholders.

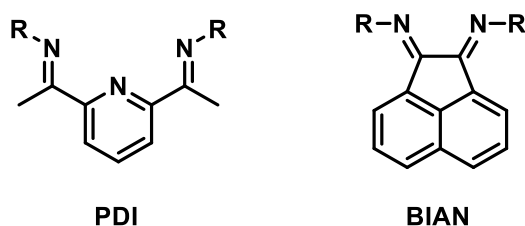
The purpose of ligands in catalytic reactions was known to be very diverse early on. Generally, ligands were employed to modulate the electron density on the central metal atom and/or to block coordination sites at the metal center to arrange the desired

symmetry of available valence orbitals. However, the ability of ligands to directly interfere in catalytic cycles has captured the attention of researchers only since the mid-2000s.<sup>[5,6]</sup> Society's demand for environmentally benign and earth abundant alternatives to noble metal based catalysts made more influential ligands indispensable.<sup>[7]</sup> These so-called non-innocent ligands are differentiated in the literature between occupying a spectator or an actor role. An actor ligand will engage directly with the substrate, while the spectator ligand exerts its effect on the metal center (examples shown in Figure 1.2).



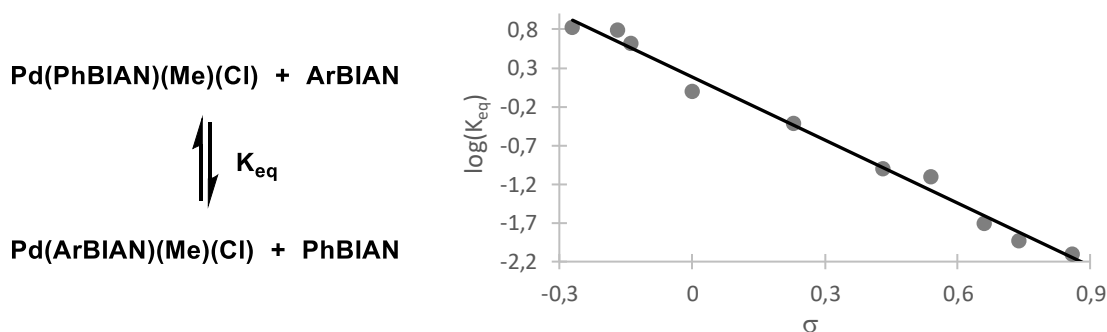
**Figure 1.2** Examples for possible non-innocent ligand behaviour.<sup>[5]</sup>

Among the first non-innocent ligands were the bis(imino)pyridines (PDIs), (*NNN*)-pincer type ligands (Figure 1.3). Even though the redox non-innocent behaviour of this ligand was known long before, it took until 2006 to highlight the influence on a catalytic cycle.<sup>[8]</sup> Structural, spectroscopic, and computational studies by Chirik *et al.* revealed that the ligands capability to accept electrons was the key feature of the catalytic iron-PDI system in [2+2] cycloaddition reactions.<sup>[9]</sup> This and similar reports led to a revival of a whole set of redox active ligands. Among them, bis(imino)acenaphthene (BIAN) ligands constitute promising candidates for catalytic applications (ArBIAN redox behaviour: see Chapter 1.3, Scheme 1.6).<sup>[10,11]</sup>



**Figure 1.3** Redox non-innocent ligands PDI and BIAN.

Structurally, BIANs can be considered a 1,4-diazabutadiene (DAB) unit merged on a naphthalene moiety. This union provides a series of advantages in organometallic applications. The exocyclic imines are expected to lead to better  $\sigma$ -donating as well as  $\pi$ -accepting properties as comparable chelating nitrogen ligands 2,2'-bipyridine (bpy) and 1,10-phenanthroline (phen). These qualities facilitate stabilization of metal ions in both higher and lower oxidation states.<sup>[12–14]</sup> Additionally, BIAN derivatives are more rigid than related acyclic diimine ligands, which imparts a high chemical stability towards both hydrolysis and rupture of the central C–C-bond.<sup>[15]</sup> Moreover, the aromatic backbone enforces the anti-anti conformation on the  $\alpha$ -diimine moiety, thus encouraging strong chelation to a metal center.<sup>[12]</sup> It should be noted that the coordination strength of ArBIAN ligands was still found to be weaker than e.g. bpy and phen. In case of ArBIAN, however, this attribute is adjustable. Investigations by Ragaini revealed a linear correlation between the coordination strength towards Pd and the Hammett  $\sigma$  constants of the aryl substituents of the ligand (Figure 1.4).<sup>[16]</sup>



**Figure 1.4** Plot of  $\log K_{eq}$  for the ligand exchange reaction as a function of the Hammett  $\sigma$  constants for the aryl substituents of ArBIAN.<sup>[16]</sup>

Their results show that the stabilities of ArBIAN metal complexes can be controlled by a reasoned choice of the aryl substituent. Better electron donating substituents lead to a more stable coordination with Pd(0)- and Pd(II)-complexes.<sup>[16]</sup> Speaking of the Hammett constants, a similar correlation was also observed with respect to the UV-Vis lowest energy absorption band of free ligands. According to UV-Vis spectra of ArBIANs

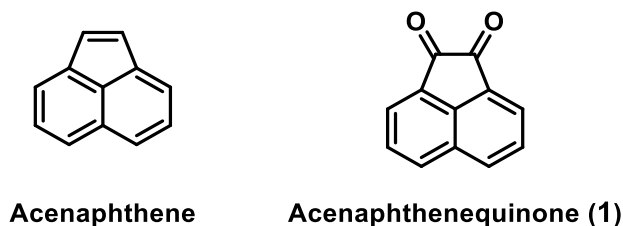
recorded by the group of Zysman-Colman, electron rich substituents promote a red shift of the lowest absorption band.<sup>[17]</sup>

Although ArBIAN compounds were first described in the 1960s,<sup>[18,19]</sup> it was not until the 1990s that they appeared in catalytic applications. Early investigations in that regard are derived from the group of Elsevier<sup>[20]</sup> and later from Brookhart.<sup>[21]</sup> The former will be discussed in more detail in chapter 1.3. The research of Brookhart focused primarily on polymerization chemistry, a field in which BIAN ligands fit naturally. Thanks to their highly tunable capacities,  $\alpha$ -diimines are widely employed in this area. Resulting polymers can be customized with respect to molecular weight, branching density or comonomer incorporation via simple ligand adjustments.<sup>[22]</sup> Even though the application of ArBIAN ligands in polymerization reactions would justify a review on its own, it shall not be part of this survey. Instead, our aim is to focus on catalytic applications in synthetic chemistry and the ligands' influence thereof.

To this day, ArBIAN ligands have been reported to efficiently coordinate to almost all main group elements<sup>[23–27]</sup> and transition metals.<sup>[21,28–31]</sup> And yet, despite all the desirable properties regarding coordination, customizability, and the possibilities as a non-innocent ligand, they are still largely underrepresented in catalysis – a subject as extensive and diverse as the BIAN ligands themselves.

## 1.2 Bis(imino)acenaphthene (BIAN) Synthesis

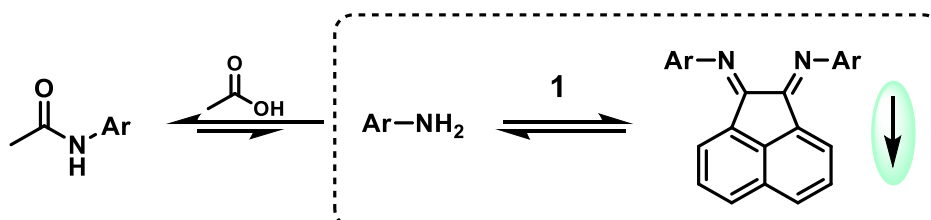
The main building block for BIAN syntheses is the acenaphthenequinone **1**, a compound commonly used as an intermediate for dyes, pharmaceuticals, and pesticides. It is derived from the oxidation of acenaphthene, which in turn is directly extracted from coal tar (Figure 1.5).<sup>[32]</sup> This makes it an easily accessible and inexpensive basis for ligand syntheses.



**Figure 1.5** Acenaphthenequinone as building block.



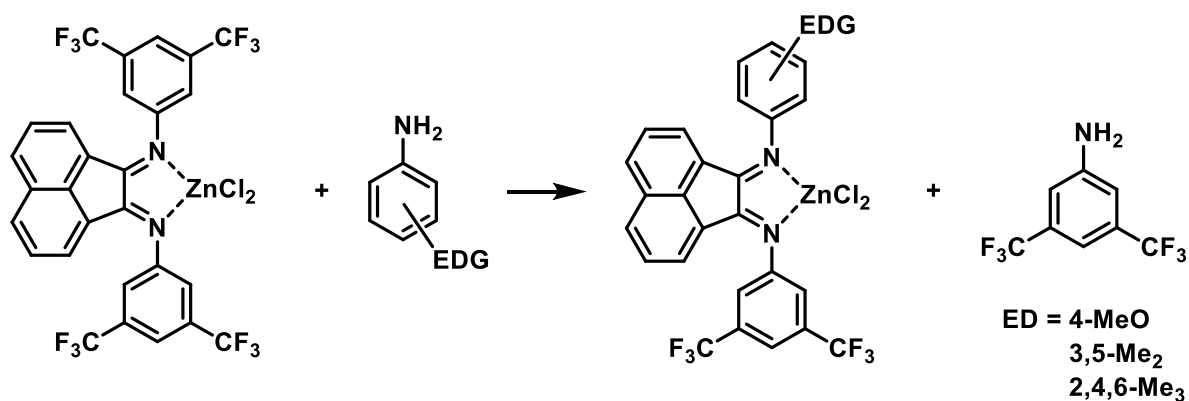
Most ArBIANs are synthesized via acetic acid catalyzed imine formation. However, in 2002 Ragaini uncovered that the reaction equilibrium is actually on the amide side of the side reaction with the catalyst.<sup>[33]</sup> According to their work, the key to a successful ArBIAN synthesis is to force the reaction outcome to the favored product by precipitation (Scheme 1.1).



**Scheme 1.1** General approach of ArBIAN synthesis.

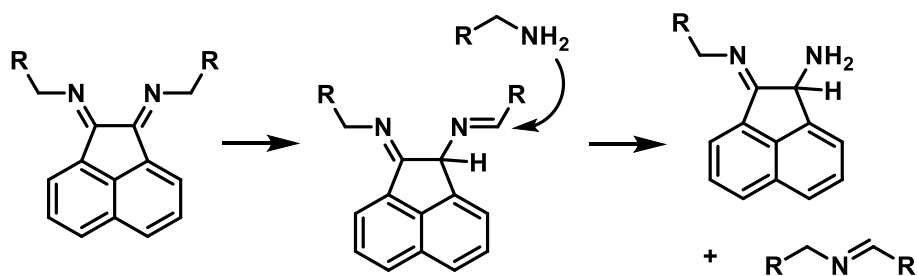
Unknowingly, this was applied practice via the formation of Zn or Ni adducts in many reported ArBIAN syntheses.<sup>[23]</sup> These adducts are usually not soluble in acetic acid and are easily filtered off. Free ligand is then obtained by simple base-treatment. The deeper understanding of the background mechanisms opened the door for the synthesis of more challenging ArBIANs. Anilines containing strongly electron withdrawing  $\text{CF}_3$  groups were hardly accessible before, but they can be obtained with slight solvent changes that lead to precipitation of the otherwise soluble Zn adducts.<sup>[33]</sup> The uncommon solubility behaviour in this case demonstrates a unique trait among BIAN, which led to a new synthetic strategy for asymmetric ArAr'BIAN syntheses.<sup>[15]</sup>

Generally, the synthesis of asymmetric ArAr'BIANs remains a challenge to this day. First attempts of Ragaini in 2004 have shown that a route via monoimination of acenaphthenequinone is problematic.<sup>[15]</sup> Asymmetric ArAr'BIANs could be generated this way, but sterically extremely congested anilines are necessary to yield the monoimine.<sup>[34]</sup> A different approach employs a transimination pathway, in which one electron poor substituent is replaced by an electron rich aniline. Unfortunately, the transimination was found to require the Zn-BIAN adducts to deliver good yields. This limits the starting material to the previously mentioned  $\text{CF}_3$  containing ArBIAN complexes, due to their inherent solubility properties.<sup>[33]</sup> Further investigations are necessary to implement those strategies in a more broad variety of substances, but it could be shown that transiminations are a promising field in providing asymmetric ArAr'BIAN ligands (Scheme 1.2).<sup>[15]</sup>



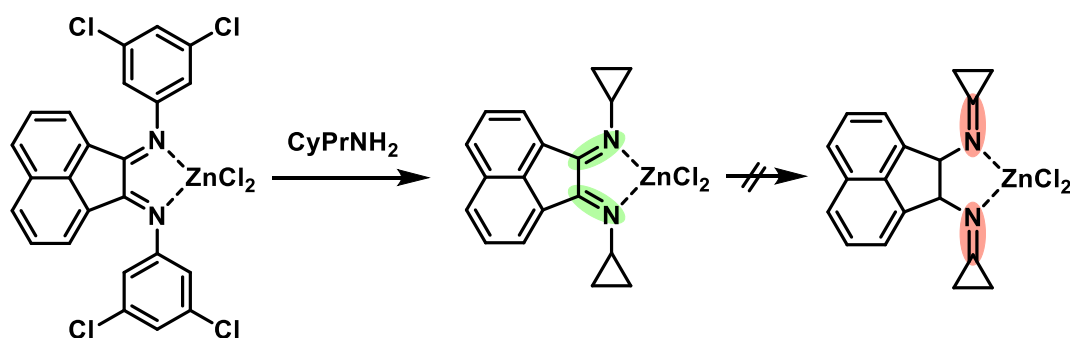
**Scheme 1.2** Asymmetric ArAr'BIAN synthesis via transimination.

Early efforts to expand the BIAN library with alkyl-substituted derivatives have met with failure.<sup>[35]</sup> First of all, the oxidizing power of the acenaphthenequinone can lead to oxidations of the aliphatic amines. That is why these syntheses need to be carried out via transiminations of ArBIAN. The second and more severe problem is that the alkyl substituents tend to undergo rapid isomerization, followed by further unwanted side reactions (Scheme 1.3).<sup>[35,36]</sup>



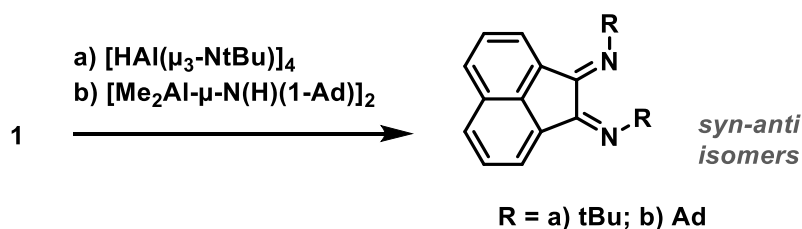
**Scheme 1.3** Isomerization of alkyl BIAN.

In his reports, Ragaini could demonstrate that the cause for the undesired isomerization is the relief of the ring strain.<sup>[36]</sup> This could be proven by the fact that transiminations run smoothly, if aliphatic amines are applied that carry even stronger strained rings (e.g. cyclopropylamine, Scheme 1.4). By employing chiral cyclopropylamines in this procedure, asymmetric alkyl BIANs can be obtained.<sup>[37,38]</sup>



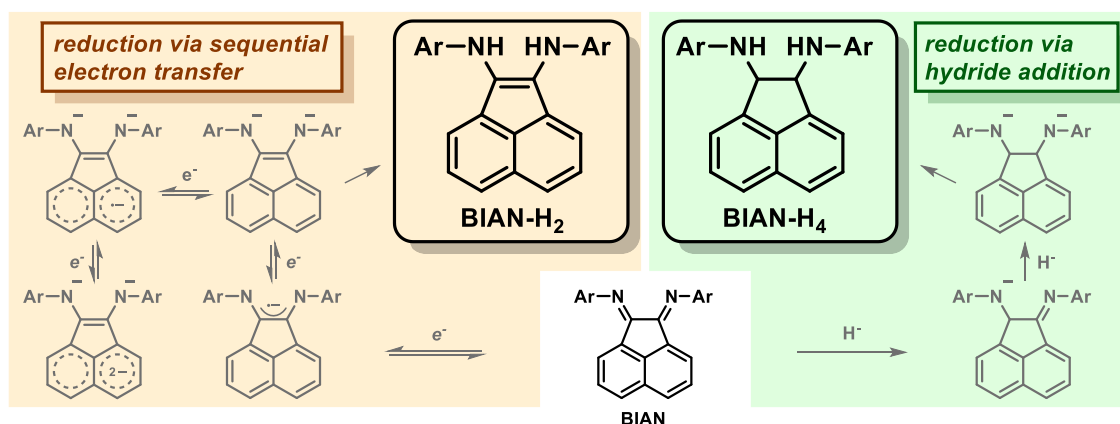
**Scheme 1.4** Synthesis of cyclopropyl BIAN.

The usage of aliphatic amines that lack the problematic  $\alpha$ -hydrogen, such as *tert*-butyl- and 1-adamantylamine, initially failed. It is believed that tertiary amines are sterically too demanding for a transimination. However, it was Cowley in 2011 who could show that the syntheses of these kind of alkyl BIAN are feasible in a different reaction setup. Special aminoalanes react directly with the acenaphthenequinone to deliver the corresponding alkyl BIANS (Scheme 1.5). Interestingly, in contrast to crystal structures of ArBIAN ligands, these are mainly found in the syn-anti isomeric form.<sup>[39]</sup>



**Scheme 1.5** Synthesis of alkyl BIAN using aminoalanes.

Another key element that makes BIAN ligands such a versatile and viable option is that they cannot only be modified by the choice of the substituents, but also by reduction. Besides the reduction to the diamine *BIAN-H<sub>4</sub>* with e.g. lithium aluminium hydride, it was shown that ArBIAN are capable of accepting up to four electrons.<sup>[11]</sup> The dienamine *BIAN-H<sub>2</sub>* can be isolated after reduction and represents a low valent depiction of the redox active BIAN ligand family (Scheme 1.6).<sup>[40]</sup>

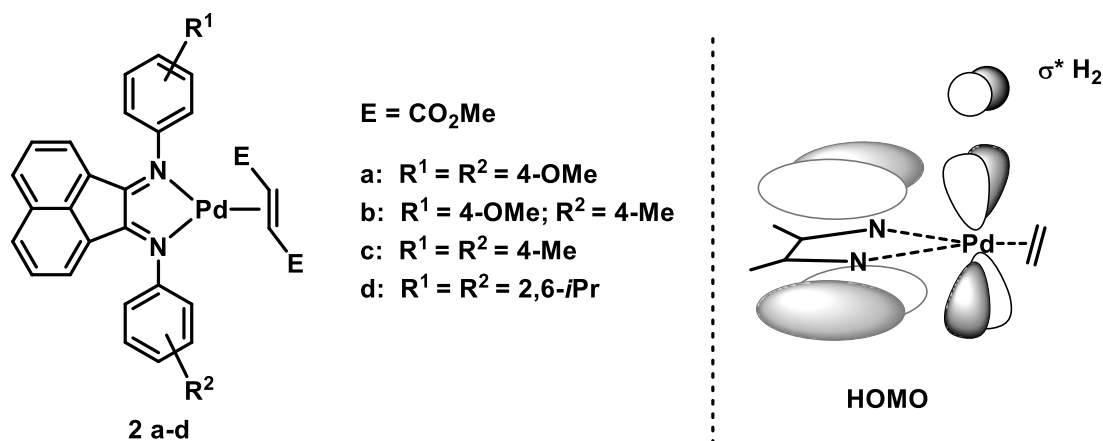


**Scheme 1.6** Reduction of ArBIAN compounds.

### 1.3 BIAN Ligands in Catalysis

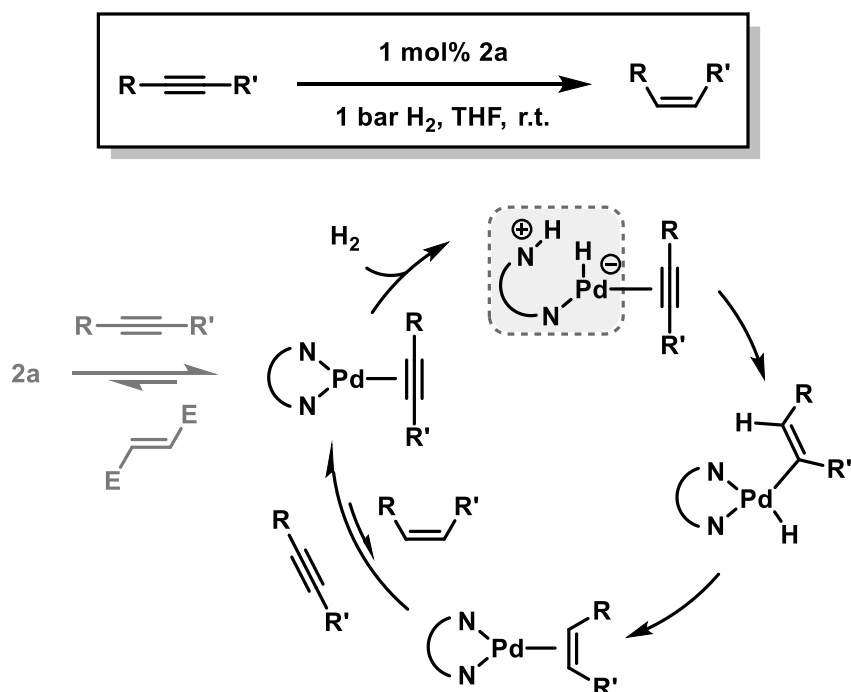
BIAN ligands were tested in countless reactions, which makes some restrictions inevitable. In order to make this excerpt of catalytic reactions appropriate and meaningful, we will focus on protocols, in which the usage of ArBIAN is key to achieve high activities and selectivities.

**Hydrogenation.** Hydrogenation reactions constitute one of the key chemical transformations in academic laboratories and industrial production plants.<sup>[41,42]</sup> Before ArBIAN ligands became popular in polymerization reactions, the group of Elsevier was working on catalytic hydrogenations. In 1991 they published ArBIAN palladium complexes **2a-d** which are operating as an homogeneous catalysts in hydrogenations of electron deficient alkenes (Scheme 1.7, left).<sup>[20]</sup> Other olefins were hydrogenated as well, but in these cases the complexes decompose and Pd particles run the reaction. The improved reactivity of the (BIAN)Pd(alkene) complexes contrary to e.g. bis(phosphine)Pd(alkene) relies on a change of the HOMO, induced by the filled  $\pi$ -orbitals of ArBIAN, thus facilitating the interaction with the  $\sigma^*$ -orbitals of  $H_2$  (Scheme 1.7, right).<sup>[20]</sup>



**Scheme 1.7** Hydrogenation catalyst **2** and HOMO –  $\sigma^*$  interaction.<sup>[20]</sup>

Based on these findings it was possible to develop a catalytic system for the semihydrogenation of alkynes to (*Z*)-alkenes in 1999.<sup>[43]</sup> Since analogues of **2** with electron rich alkenes were known to be unstable it could be assumed that alkenes would be readily substituted with alkynes. In presence of molecular hydrogen, repeated hydrogenation and subsequent substitution delivers a viable catalytic cycle. The results of further DFT calculations, kinetic and spectroscopic studies are summarized in the mechanism depicted in Scheme 1.8.<sup>[44,45]</sup>



**Scheme 1.8** Semihydrogenation of alkynes to alkenes.<sup>[43–45]</sup>

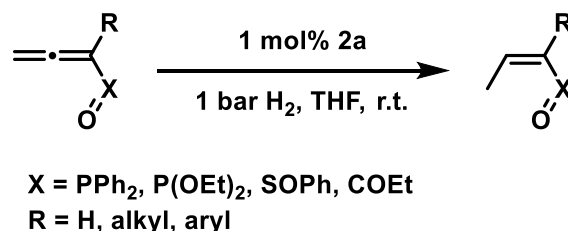
The results of the DFT calculations suggest the formation of a zwitterion after a heterolytic addition of  $H_2$  across one Pd–N-bond. The active participation of BIAN in

the catalytic cycle implies the significance of the efforts that go into ligand design. In their opening work they tested several BIAN ligands, which differed electronically and sterically (Table 1.1). The results show a decrease in selectivity for (*Z*)-alkenes with decreasing electron-donor character of the substituents on the *N*-aryl groups. The sterically congested complex **2d** delivers larger amounts of alkane (Entry 4). This is believed to be a result of steric crowding, since **2d** may form more stable complexes with (*Z*)-alkenes than with alkynes.<sup>[43]</sup>

**Table 1.1** Product distribution in the hydrogenation of 1-phenyl-1-propyne.<sup>[43]</sup>

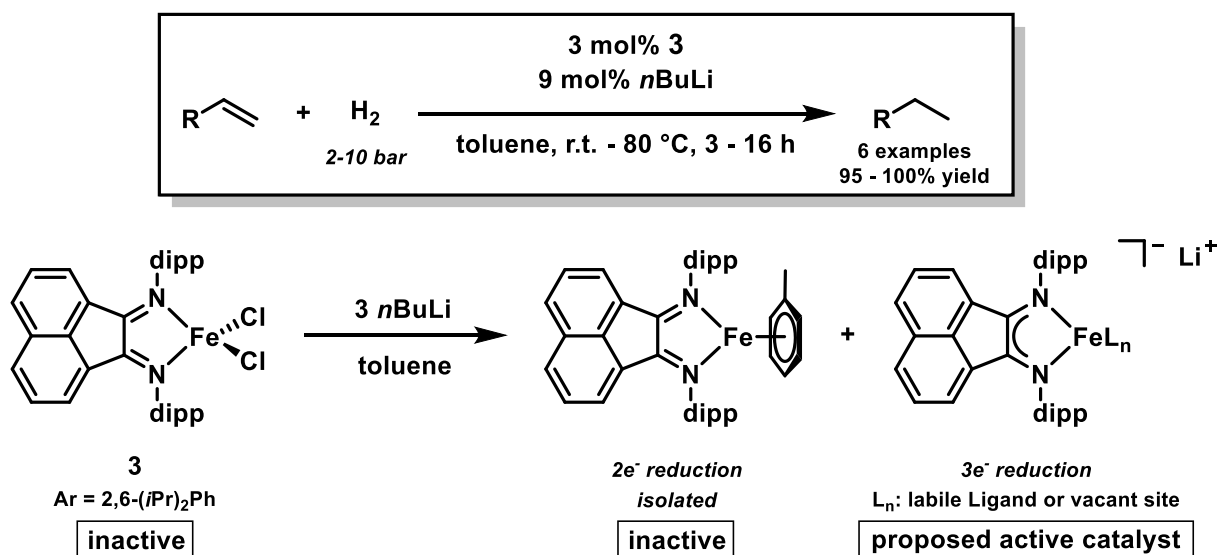
Entry	Precatalyst	Product distribution [%]		
		<i>Z</i> -alkene	<i>E</i> -alkene	alkane
1	<b>2a</b>	92	2	6
2	<b>2b</b>	85	5	10
3	<b>2c</b>	80	7	13
4	<b>2d</b>	62	3	35

In 2006 it could be shown by the same group that this reaction setup can also be applied on the semihydrogenation of allenes. The general mechanistic backgrounds are believed to work in a similar fashion (Scheme 1.9).<sup>[46]</sup>



**Scheme 1.9** Semihydrogenation of allenes.<sup>[46]</sup>

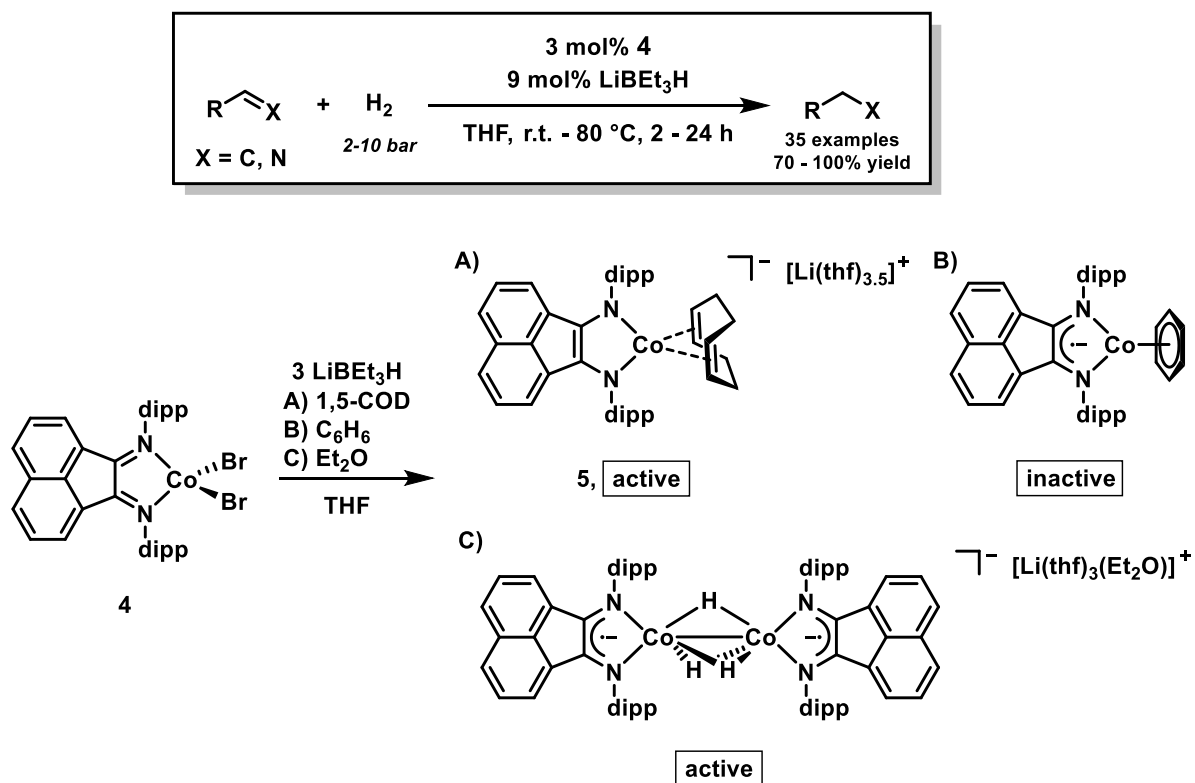
Further aspirations to find applications for BIAN ligands in hydrogenation reactions have been advanced recently by our group. In 2017 we employed 2,6-diisopropylphenyl (dipp) BIAN iron complex **3** as a precatalyst in hydrogenations of alkenes under mild conditions (Scheme 1.10).<sup>[30]</sup> The usage of less bulky *N*-aryl substituents gave inactive octahedral (metal:ligand = 1:3) complexes.



**Scheme 1.10** DippBIANFeCl<sub>2</sub> as precatalyst in the hydrogenation of alkenes.<sup>[30]</sup>

At elevated temperature and H<sub>2</sub> pressure more challenging tri- and tetrasubstituted olefins were cleanly hydrogenated. The catalyst is prepared *in situ* by reduction with three equivalents of *n*BuLi. Attempts to disclose the chemical identity of the active catalyst have not been successful. But it was shown that the Fe(0) analogue of **3** is formed in the reduction process, which however displayed no catalytic activity. Therefore, a low valent (BIAN)Fe species with BIAN in the radical anion or dianion state is postulated as the active catalyst.<sup>[30]</sup>

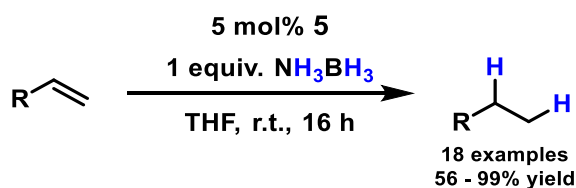
In collaboration with the group of Wolf we could extend this reaction to dippBIAN cobalt complex **4**.<sup>[47]</sup> A broad variety of substrates, including tri- and tetrasubstituted alkenes as well as imines and quinolines could be hydrogenated smoothly (Scheme 1.11).



**Scheme 1.11** DippBIANCoBr<sub>2</sub> as precatalyst in hydrogenation reactions.<sup>[47]</sup>

In the identification process for the active reduced species, we added labile coordination placeholders for the stabilization of potential catalyst intermediates. This method gave two catalytically active cobaltates which might be present in the catalytic cycle in these or analogue forms. With aid of 1,5 cyclooctadiene (COD) we could isolate cobaltate **5** with dippBIAN in the dianionic BIAN-H<sub>2</sub> form and cobalt in the oxidation state +1. By running the reduction in presence of Et<sub>2</sub>O we received an active cobaltate dimer with three hydride bridges. In this case we observe the single electron reduced dippBIAN and cobalt in the +2 state.<sup>[47]</sup>

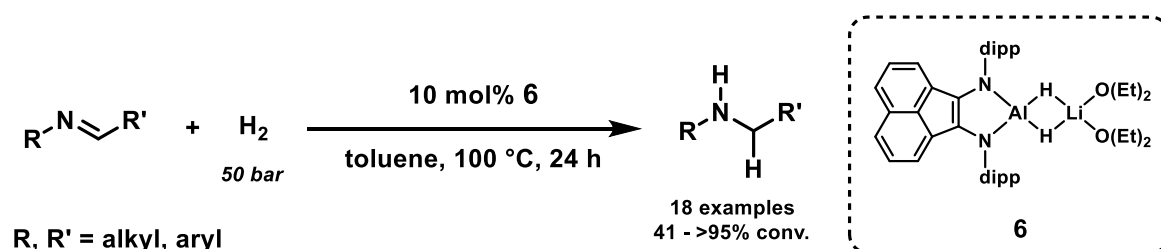
Cobaltate **5** was also found to catalyze the dehydrogenation of amine-boranes. The released hydrogen could be used subsequently for mild hydrogenation reactions (Scheme 1.12).<sup>[48]</sup>



**Scheme 1.12** DippBIAN-H<sub>2</sub>-cobaltate as catalyst in transfer hydrogenation reactions.<sup>[48]</sup>

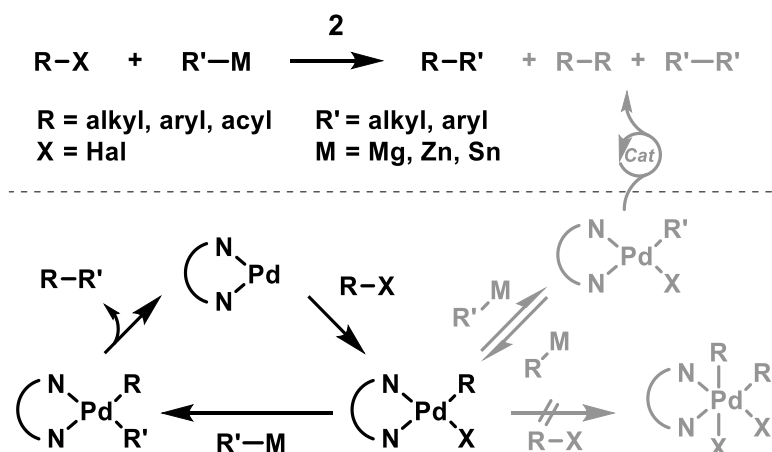


Lastly, we could demonstrate that the dippBIAN- $\text{H}_2$  ligand enhances the catalytic activity of aluminium hydride catalyzed imine hydrogenations (Scheme 1.13, for more details see Chapter 2). Based on calculations by the group of Harder,<sup>[49]</sup> which identified the catalytically active species in  $\text{LiAlH}_4$  catalyzed imine hydrogenations, we can assume that complex **6** mimicks the active bimetallic species. The presence of the Li-cation proposedly accelerates the hydrogen activation. We found that the usage of complex **6** makes the reaction applicable on a broader variety of substrates, while the formation of inactive dimers is prevented through steric crowding.<sup>[50]</sup>



**Scheme 1.13** Aluminium hydride catalyzed imine hydrogenation.

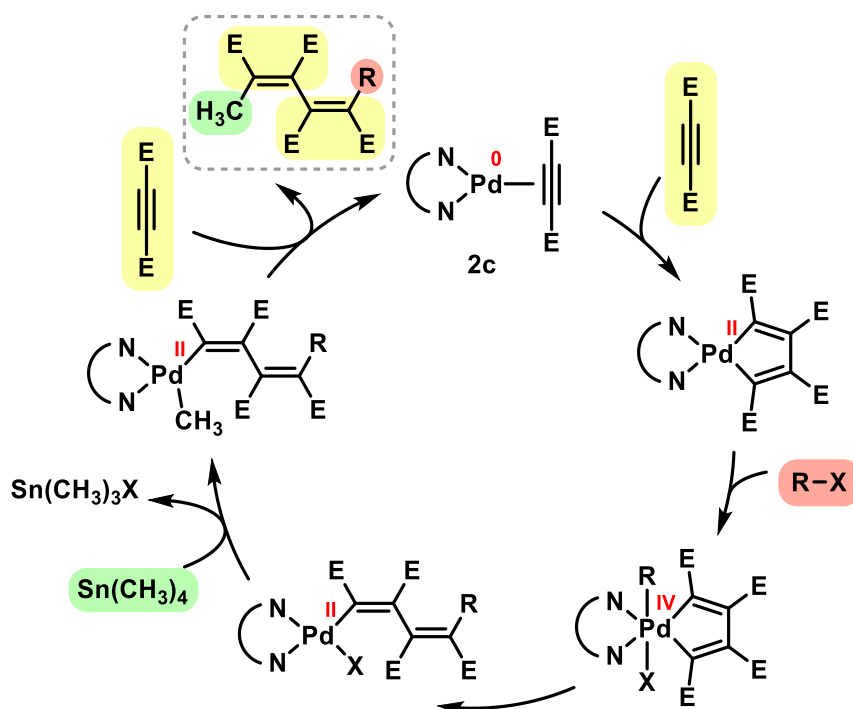
**C–C-bond formation.** As of today, cross-coupling and related reactions are among the most versatile and useful tools for performing organic syntheses in both lab scale reactions as well as industrial manufacturing.<sup>[51]</sup> Despite their versatility in established polymerization reactions, BIAN ligands are largely underutilized in other C–C-bond formations. Again, the few publications build up upon early efforts by the group of Elsevier.<sup>[52]</sup> Next to hydrogenation reactions, they also targeted a variety of different cross coupling reactions. Interestingly, the results were complementary to the commonly employed palladium(phosphine) compounds: When employing Pd complexes with BIAN (or other nitrogen) ligands, side reactions leading to homo-coupling are usually lowered compared to the same reactions with phosphine ligands. For coupling of aryl bromides, however, the phosphine ligands give better results in terms of conversion as well as selectivity.<sup>[53]</sup>



**Scheme 1.14** Application of complex **2** in cross coupling reactions by Elsevier *et al.*<sup>[53,54]</sup>

Except for the coupling of allylic halides, the aromatic substituent of the ArBIAN ligand had no significant influence on product distribution or catalytic activity. This is in accordance with the anticipated *oxidative addition - transmetalation - reductive elimination* mechanism, which does not involve sterically congested or electronically demanding intermediates.<sup>[53]</sup> However, these results allowed mechanistic insights into the formation of the undesired homo coupling products. A second oxidative addition, leading to sterically crowded Pd(IV) during the mechanism, could be ruled out. Therefore an exchange of the organic groups between the transmetalating agent and the organopalladium complex was stated to be the most plausible explanation for the emergence of the side products (Scheme 1.14).<sup>[54]</sup>

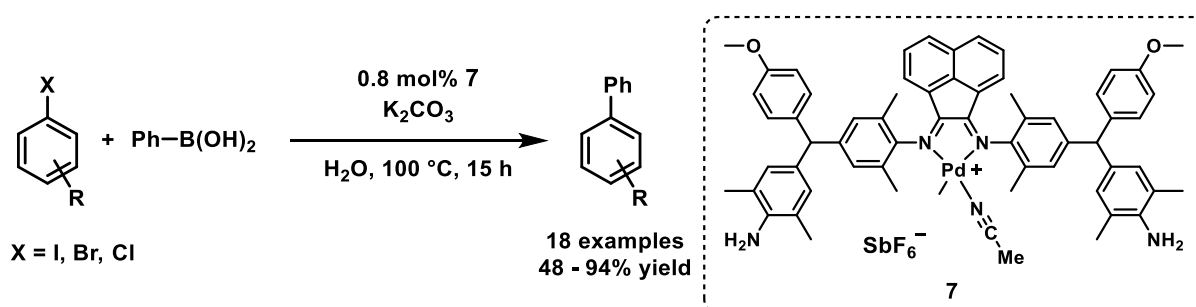
The group of Elsevier could also show that BIAN and similar bidentate nitrogen ligands are able to stabilize Pd complexes in the oxidation states 0, II and IV within a single catalytic cycle.<sup>[55]</sup> The mechanism depicted in Scheme 1.15 displays an example of the development of a catalytic reaction based on the corresponding stoichiometric reactions.<sup>[56,57]</sup> This led to a new Pd-catalyzed three-component synthesis of conjugated dienes employing alkynes, an organic halide and tetramethyltin.<sup>[58]</sup>



**Scheme 1.15** Pd/BIAN catalyzed alkyne coupling developed by Elsevier *et al.*<sup>[58]</sup>

The occurrence of the sterically demanding Pd(IV) intermediate resonates with the demands on the BIAN ligand design. Bulky aromatic substituents hinder a second oxidative addition at the Pd(II) center and lower catalytic activity drastically. Interestingly no cross coupling between the organo halide and organotin reagent was observed.<sup>[58]</sup>

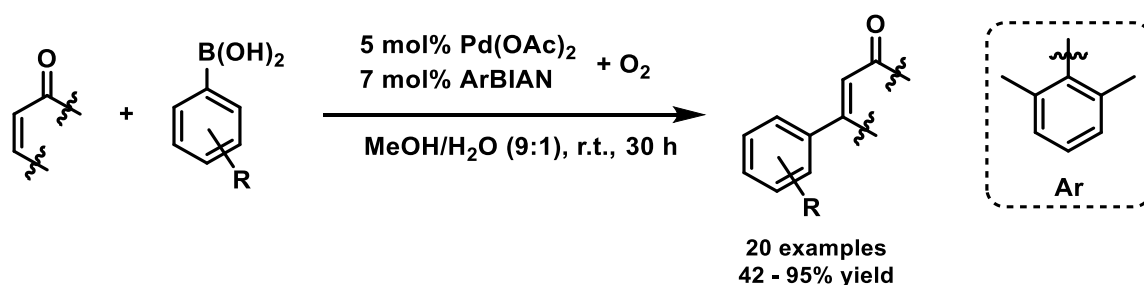
After these initial investigations, the subject of BIAN ligands in cross-coupling reactions became rather silent. One noteworthy example, however, is the Suzuki-Miyaura coupling of aryl halides in water published by Kim *et al.* in 2013.<sup>[59]</sup> The idea was to strongly increase the electron richness and the steric bulk through the aryl substituents. The electron density should accelerate oxidative additions, while the steric bulk should promote reductive eliminations (Scheme 1.16).



**Scheme 1.16** Suzuki-Miyaura coupling supported by bulky BIAN ligand.<sup>[59]</sup>

The developed complex was found to be a highly active catalyst in Suzuki-Miyaura couplings in water. Aryl bromides and iodides gave high to excellent yields, while aryl chlorides still gave moderate results. Additionally, thanks to the heterogeneity of the system, the airstable catalyst can easily be separated from the reaction mixture and recycled for a couple of runs with slightly decreasing activity.<sup>[59]</sup>

Another C–C-coupling in which BIAN ligands have been successfully utilized is the oxidative Heck reaction. In 2011 the group of Minaard unveiled a highly active Pd/BIAN catalyst system for challenging Michael acceptors as substrates (Scheme 1.17). Commonly these reactions suffer from catalyst deactivation by dimerization or ligand decomposition in the oxidative environment. The customizable BIAN ligands satisfied the criteria of both, resistance towards oxidation and dimerization, of which the latter could be discouraged with steric bulk. Their kinetic data show a substantial increase in selectivity and catalytic activity with ArBIAN compared to established phenantroline ligands. These findings constitute a breakthrough in the oxidative Heck reaction as most of these products could not be synthesized by Heck procedures beforehand.<sup>[60]</sup>

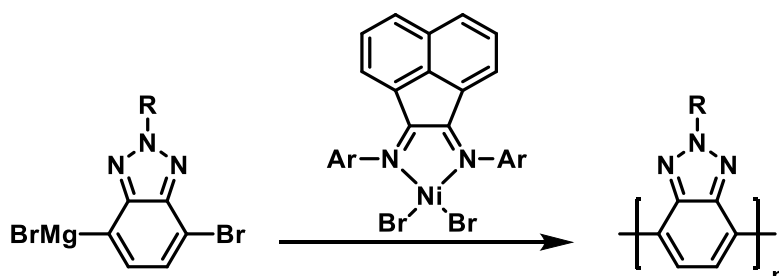


**Scheme 1.17** Oxidative Heck reaction for challenging substrates.<sup>[60]</sup>

The developed procedure allowed coupling reactions with various challenging Michael acceptors, including aldehydes. For the phenylboronic acids, meta- and para-substituted substrates generally gave high to excellent yields, while ortho-substitution still delivered moderate results.<sup>[60]</sup>

The next reaction fits into the categories of cross couplings as well as polymerizations and highlights the perception that BIAN ligands are more common in the minds of chemists dealing with the latter.<sup>[61]</sup> In fact, the nickel catalyzed polymerization featured in Scheme 1.18 proceeds via Kumada type cross couplings. Mechanistically, this represents a living polymerization in which the catalyst initiates the chain reaction and continues catalyzing the chain growth. Thus, in an ideal situation, one catalyst molecule starts and synthesizes a single polymer chain. However, challenging

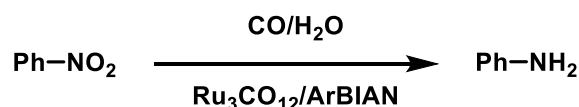
monomers, namely electron deficient substrates, commonly give uncontrolled reactions due to weak catalyst coordination. In this regard, the application of this Ni/BIAN system portrays a significant advance towards the synthesis of electron deficient polymers.<sup>[62]</sup>



**Scheme 1.18** Nickel catalyzed polymerization of electron deficient monomers.<sup>[62]</sup>

BIAN ligands with electron rich substituents led to controlled chain growth even with challenging electron poor monomers. The exceptional high level of control also made block copolymerization possible by simply adding different monomers sequentially. Electron rich as well as electron deficient monomers could be used to generate novel donor-acceptor block copolymers.<sup>[63]</sup>

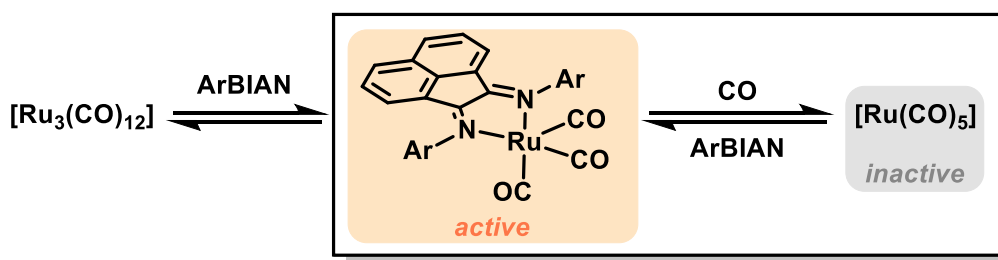
**Nitroarene reduction and C–N-bond formation.** The reduction of nitro compounds by CO, catalyzed by different metal complexes, affords a variety of *N*-containing compounds e.g. indoles, pyrroles, oxazines and allylic amines.<sup>[64–66]</sup> ArBIAN ligands have shown early on to be particularly efficient in activating  $[\text{Ru}_3(\text{CO})_{12}]$  in catalytic reductions of nitrobenzene to aniline (Scheme 1.19).<sup>[67]</sup> Unsurprisingly, the substituent of the aryl ring in BIAN has a sensible effect on the activity of the reaction. However, the preferred substitution of the aryl ring following the order  $4\text{-H} > 4\text{-CH}_3 > 4\text{-Cl} > 4\text{-OMe}$  was unexpected, as electron donating ligands are commonly suited to accelerate reductive reactions.<sup>[68]</sup>



**Scheme 1.19** Ru-catalyzed reduction of nitrobenzene to aniline.

It was shown that  $[\text{Ru}_3(\text{CO})_{12}]$  reacts with ArBIAN under CO pressure and elevated temperatures to  $[\text{Ru}(\text{CO})_3(\text{ArBIAN})]$ . This complex is believed to be the active catalyst in the nitrobenzene reduction. However, it was found to enter an equilibrium by incorporating CO, yielding inactive  $[\text{Ru}(\text{CO})_5]$  (Scheme 1.20). This equilibrium is

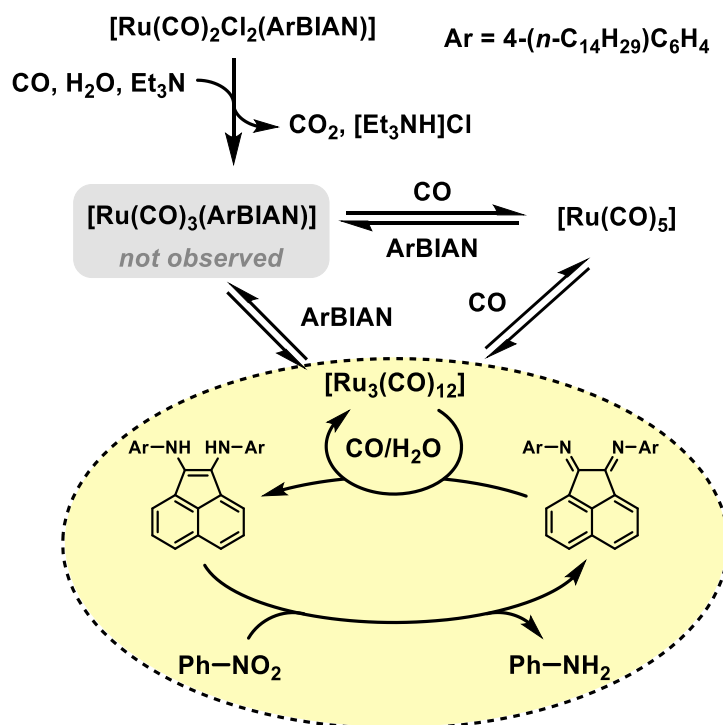
determined by the choice of the ArBIAN ligand. The low oxidation state of ruthenium favours  $\pi$ -acidic ligands and disfavours electron rich substituents, which will be replaced by CO more easily and therefore lead to catalyst deactivation.<sup>[68]</sup>



**Scheme 1.20** Active Ru-catalyst formation and deactivation.<sup>[68]</sup>

In summary, electron donating substituents on the ligand afford high initial catalytic activities, but lead to ligand exchange and inactive  $[\text{Ru}(\text{CO})_5]$ , while electron withdrawing groups lead to lower activities in general.<sup>[68]</sup>

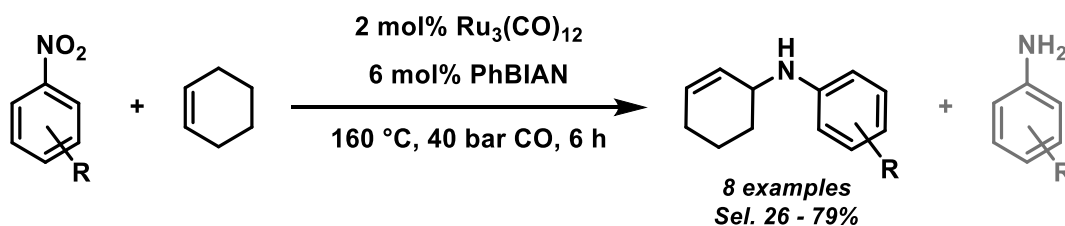
As these complexes are highly air-sensitive, the idea of catalyst recycling turns into an overwhelming challenge. To overcome these difficulties, the concept was to implement the catalyst on a polymer membrane. With aid of long-chain substituents on the ligand, ruthenium ArBIAN complexes could be embedded on a polymer membrane by simple steric interactions. However, to surmount the conditions during the membrane polymerization, stable  $[\text{Ru}(\text{CO})_3\text{Cl}_2(\text{ArBIAN})]$  had to be used. Consequently, this oxidized version of the active catalyst required a reduction step prior to the catalytic reactions. The chosen polymer PEEK-WC (a modified polyether ether ketone) showed high thermal and chemical stability and no catalyst leaching was observed.<sup>[69]</sup>



**Scheme 1.21** Reduction of nitrobenzene on catalytic polymer membranes.

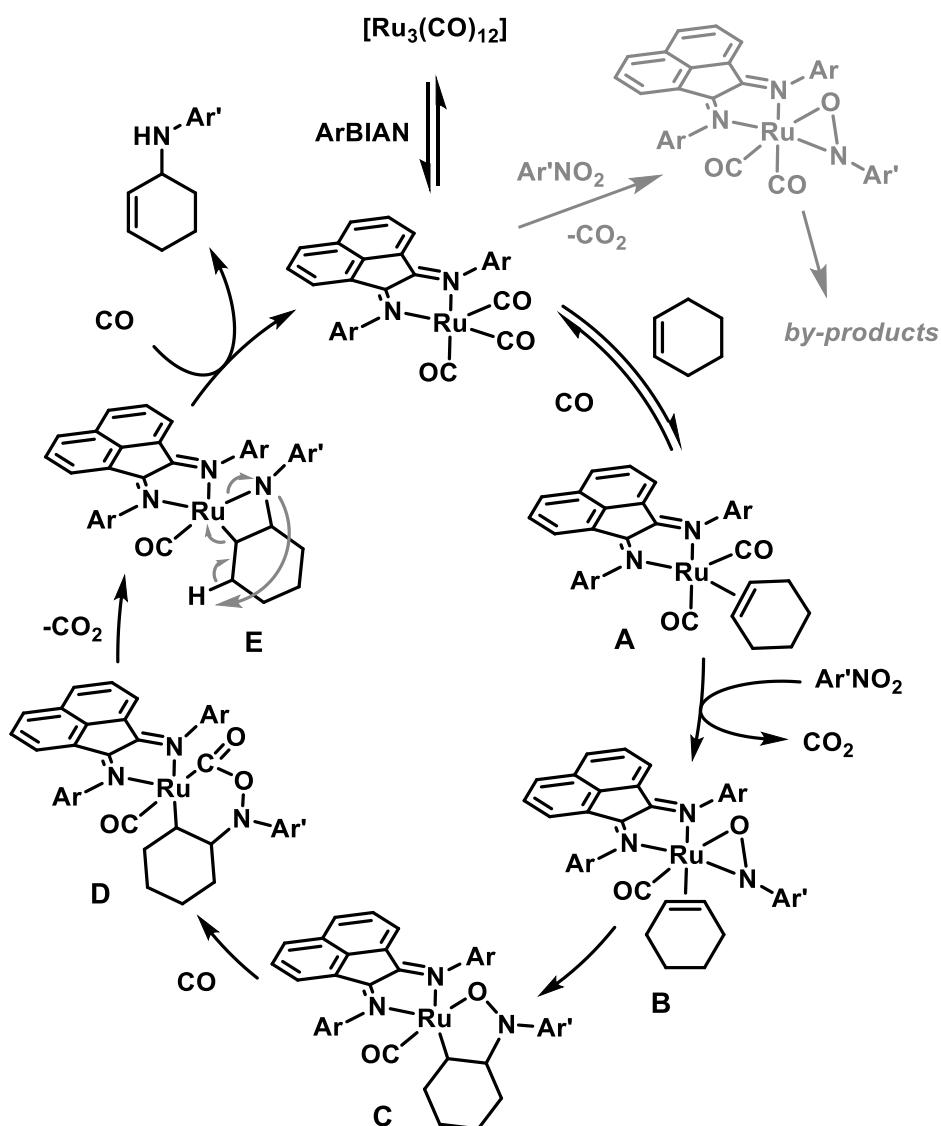
The catalytic membrane could be successfully utilized for the reduction of nitrobenzene and was recycled for multiple runs with decreasing activity. However, closer examination of the mechanism revealed that no  $[\text{Ru}(\text{CO})_3(\text{ArBIAN})]$  was present during the reaction. An IR spectrum of the membrane displayed  $[\text{Ru}_3(\text{CO})_{12}]$  as the only carbonyl-containing complex. Model reactions could show that catalytic amounts of  $[\text{Ru}_3(\text{CO})_{12}]$  are able to reduce ArBIAN to ArBIAN- $\text{H}_2$ , which can subsequently reduce nitrobenzene in a stoichiometric reaction (full mechanism see Scheme 1.21). Consequently, it is assumed that ArBIAN is not acting, or not only acting as a ligand, but rather as an electron and proton shuttle in this catalytic cycle.<sup>[69]</sup>

As indicated before, the reduction of nitroarenes is accompanied by a series of follow-up reactions. One of them is the allylic amination of olefins, which was reported in 1996 by the group of Ragaini. This work constitutes the first intermolecular C-N bond formation using nitroarenes as the aminating species (Scheme 1.22).<sup>[70]</sup>



**Scheme 1.22** Allylic aminations of unactivated olefins from nitroarenes.

Nitroarenes carrying electron-withdrawing groups or mildly electron donating groups give full conversions with high selectivities towards the allylic amine. Strong donating groups, e.g. 4-methoxybenzene show incomplete conversion and poor selectivity. The influence of the ArBIAN substituents is based on the same pattern as discussed earlier (Scheme 1.20), but is extended by the involvement of olefin coordination and steric crowding in the reaction mechanism (Scheme 1.23).<sup>[71]</sup>



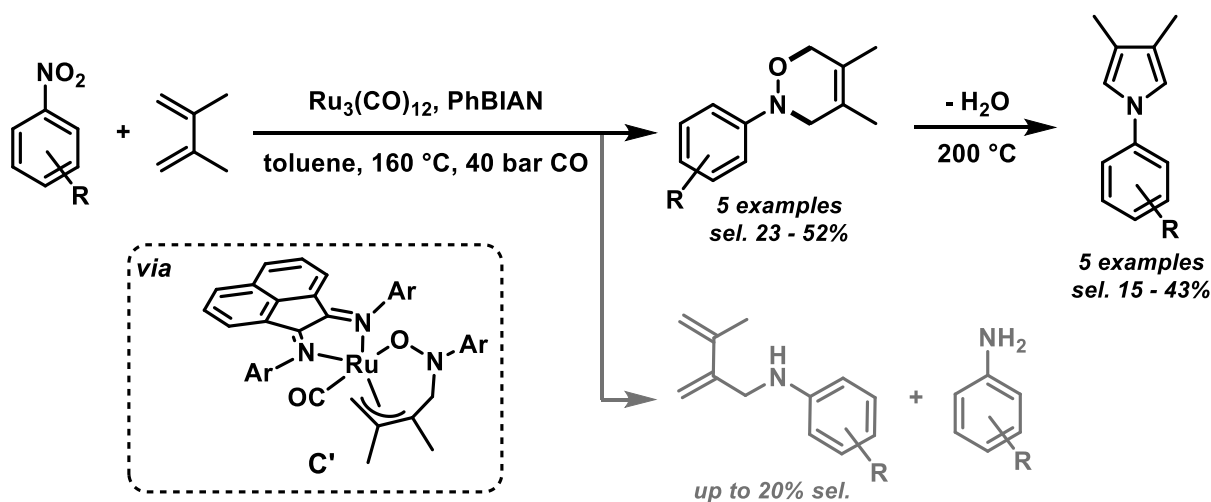
**Scheme 1.23** Mechanism of [Ru(CO)<sub>3</sub>(ArBIAN)]-catalyzed allylic amination.

This detailed mechanism is the result of in-depth investigations performed by Ragaini *et al.* As the selectivity of the reaction is determined by the olefin coordination vs. nitroarene reduction, strong electron donating substituents on the ArBIAN are believed to accelerate both, therefore leading to a less selective reaction outcome. More bulky



dippBIAN showed lowered conversion and selectivity, presumably as a result of steric congestion.<sup>[71]</sup>

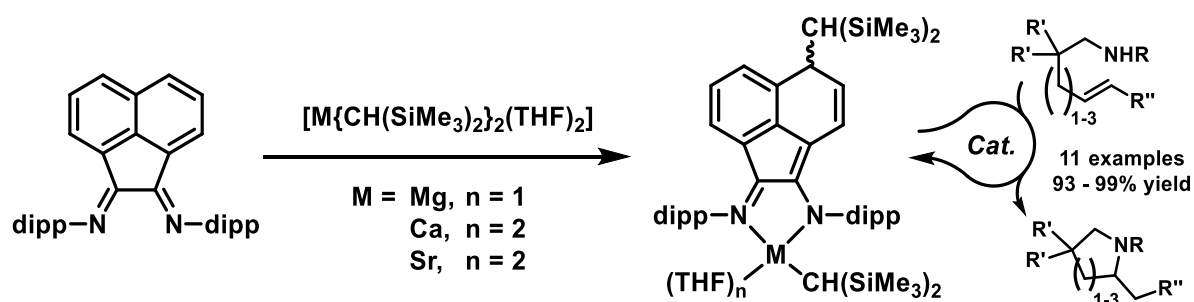
When unfunctionalized conjugated diene 2,3-dimethylbutadiene was employed in this reaction, the formation of oxazines and, by increasing the reaction temperature, pyrroles can be obtained (Scheme 1.24).<sup>[72]</sup>



**Scheme 1.24** Synthesis of oxazines and *N*-arylpyrroles from nitroarene reduction.

Basically, this reaction is believed to follow the same mechanism as depicted in Scheme 1.23 until intermediate C' is formed. Here, instead of inserting CO, direct reductive elimination takes place and releases the oxazine. Due to the close relationship of this reaction with the allylic amination, it should be no surprise that similar observations were made with regard to BIAN ligand effects.<sup>[72]</sup>

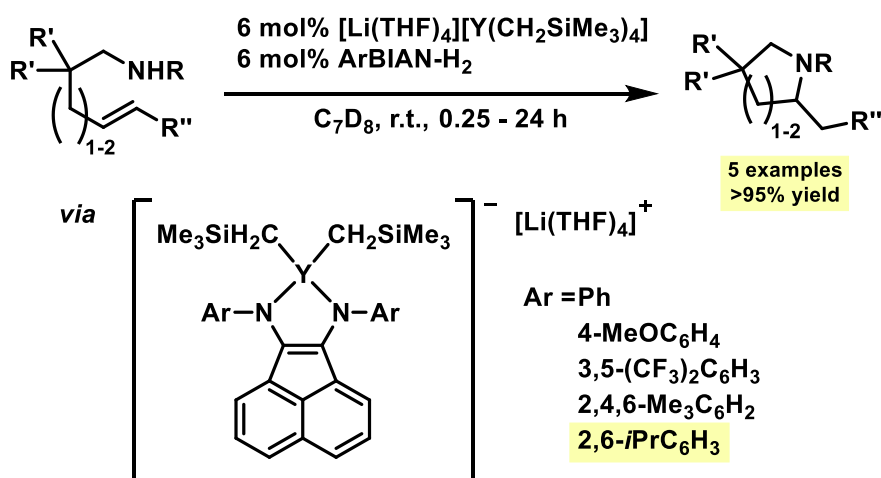
Another class of C–N-bond formation reactions are hydroaminations of olefins. This reaction constitutes one of the most straightforward atom-economical processes for the synthesis of valuable nitrogen-containing compounds from relatively low cost and accessible starting materials. A severe challenge for this reaction, however, is the poor reactivity of internal compared to terminal olefins. In 2011 Hill and coworkers published a series of alkaline earth metal complexes, bearing a dearomatized BIAN backbone. It was uncovered that these complexes were active catalysts in the highly desirable hydroamination of internal olefins (Scheme 1.25).<sup>[73]</sup>



**Scheme 1.25** Hydroamination catalyzed by alkaline earth metals.<sup>[26]</sup>

The calcium analogue showed superior catalytic activity in the transformations, following the trend  $Ca > Sr \gg Mg$ . However, the Mg complex was found to be the only candidate to catalyze the formation of seven membered *N*-heterocycles under forcing conditions. The highly active Ca complex showed excellent yields, with some internally substituted alkenes being converted under even milder conditions than the terminal alkene model substrate.<sup>[26]</sup>

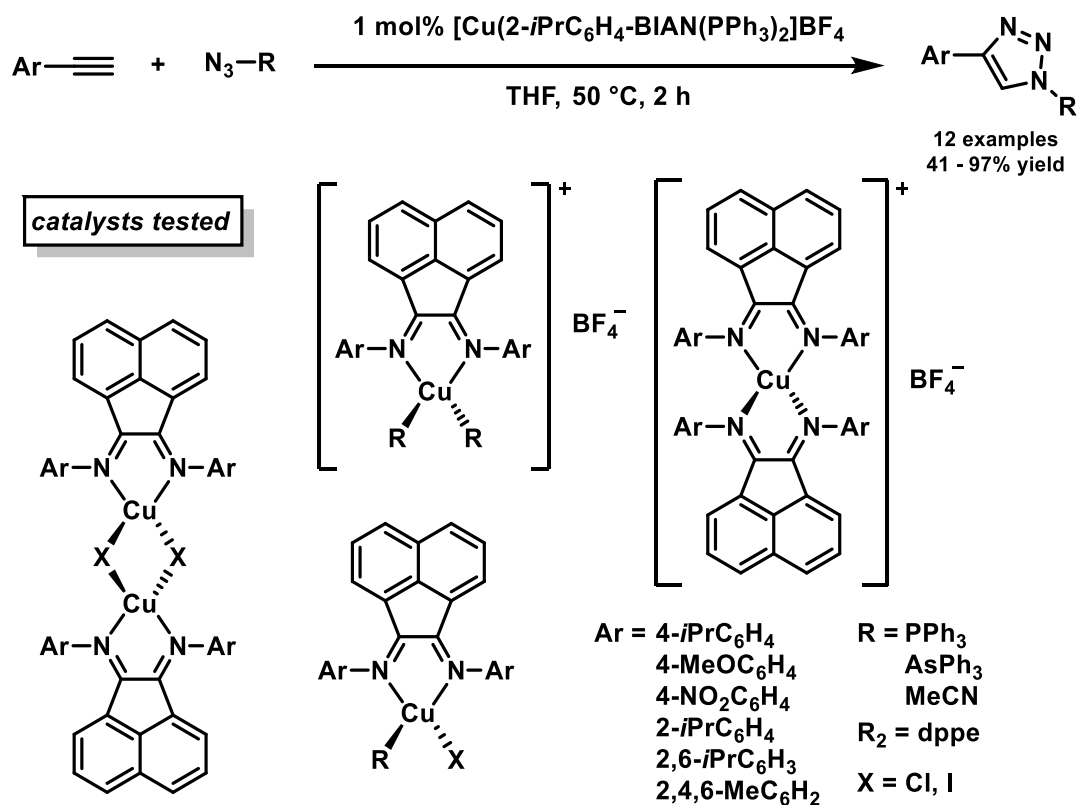
The same reaction was found to be catalyzed by Zr and Y complexes, applying reduced BIAN- $H_2$  as the catalyst backbone. The Zr complex, however, was less active than the Zr precursor used for the complexation, so the investigations focused on the highly active Y-BIAN- $H_2$  catalyst. A neutral analogue of the complex shown in Scheme 1.26 also displayed high activity but was easily outperformed by the anionic complex. This catalyst gave excellent yields in the formations of five and six membered *N*-heterocycles as well as convenient cyclisation with both, terminal and internal alkenes.<sup>[74]</sup>



**Scheme 1.26** Hydroamination catalyzed by Y-BIAN- $H_2$  catalysts.<sup>[74]</sup>

It is proposed, that the BIAN ligand occupies an important role in preventing catalyst deactivation through aggregation or over-coordination, as more sterically demanding aryl-substituents provided superior catalytic activity.<sup>[74]</sup> In 2018 the library of active hydroamination catalysts has been extended to Ca- and Mg-BIAN-H<sub>2</sub> complexes by the group of Fedushkin. In this report a mechanism was postulated, in which the BIAN ligand fulfills an active role by transferring the amine proton.<sup>[75]</sup>

In 2012 the groups of Aviles and Gomes reported a series of novel ArBIAN-copper(I) complexes, which are active catalysts in the azide-alkyne cycloaddition reaction. The variety of complexes allowed them to closely examine the effect of the ligands (Scheme 1.27).<sup>[76,77]</sup>

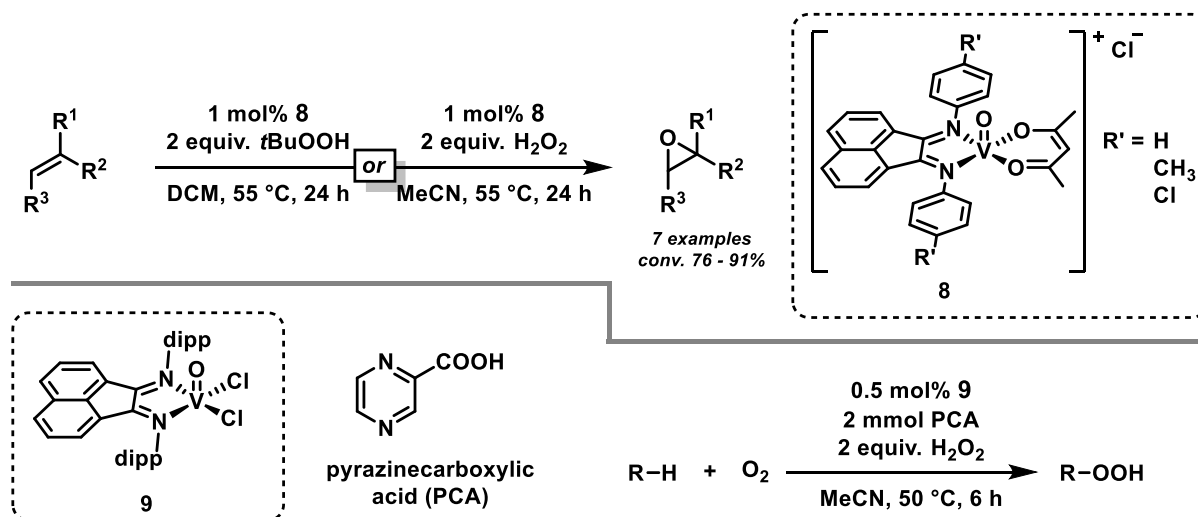


**Scheme 1.27** Azide-Alkyne Cycloaddition.

The results of the catalyst screenings are summarized below: for the neutral complexes, the chloride ligand was superior to the iodide. However, the cationic complexes delivered better results overall. The dimeric and bischelated catalysts showed significantly decreased catalytic activity compared to their monochelated counterparts. For the labile ligands R, acetonitrile gave better results than the arsine, but both were surpassed by the triphenylphosphine. Lastly, also the substituents of the BIAN ligands have a great impact on the reaction outcome. Electron withdrawing group

$\text{NO}_2$  delivered the worst results, while bulky substituents showed excellent yields. These findings support the notion of preventing the deactivation of the catalyst by overcoordination.<sup>[76,77]</sup>

**Oxidation reactions.** Organic oxidation chemistry is a huge and vibrant field of research, partially thanks to inspirations derived from biochemical processes. The activity of vanadium enzymes in oxidation reactions set the direction for the development of vanadium complexes, that commonly employ  $\text{H}_2\text{O}_2$  as an environmentally friendly alternative compared to organic peroxides. The group of Calhorda published in 2015 a V-BIAN complex that catalyzes the epoxidation of olefins (Scheme 1.28, top).<sup>[78]</sup>



**Scheme 1.28** V-BIAN-catalyzed oxidation reactions.

The impact of the ligand was tested with three different aryl substituents. Their results presume a significant ligand-substrate dependency: phenyl- and 4-chlorophenyl-substituents showed a high selectivity towards specific substrates, while TolBIAN gave the highest activity overall and is thus less substrate-selective. Additionally, it was demonstrated by cyclic voltammetry experiments that BIAN ligands support the stabilization of V(IV) against oxidation to presumably inactive V(V).<sup>[78]</sup> Due to these outstanding properties, a similar V-BIAN complex could be employed as a catalyst for the oxidation of alkanes to the corresponding peroxides more recently (Scheme 1.28, bottom).<sup>[79]</sup>

## 1.4 Conclusion

In summary, it was our aim to highlight the diversity of BIAN ligand applications in catalysis and to inspire researchers to make use of this exceptionally highly adaptable, easily accessible, but still underrepresented class of diimine ligands. Many dormant potentials still need to be brought to light, since topics such as alkyl BIAN and asymmetrical BIAN have largely remained untouched. The application of reduced BIAN ligands, however, has gradually gained momentum in recent years. Their increased  $\sigma$ -donor capacities extend the range of coordinatable metals and make them an exciting and emerging topic.

In the couple of protocols discussed in this report, the BIAN ligands have a diverse spectrum of tasks. It was shown to act as an electron and/or proton sponge, immobilize the catalyst on a membrane, hinder the formation of dimers, stabilize the metal in demanding oxidation states or influence other significant reaction equilibria. Underlying patterns are yet hard to discern. The research in this field has not progressed to a point in which we can accurately predict distinctive effects on catalytic cycles based on the choice of the BIAN ligand.

However, efforts put into the design of these ligands are often rewarded with increased catalytic efficiencies and provide mechanistic insights into the investigated reaction. For mechanistic studies, the use of BIAN ligands was found to be especially advantageous, because the steric and electronic properties are easily controlled and customized by variation of the imine substituent.

## 1.5 References

- [1] A. Werner, *Z. Anorg. Chem.* **1893**, 3, 267–330.
- [2] A. Togni, L. M. Venanzi, *Angew. Chem. Int. Ed. Engl.* **1994**, 33, 497–526.
- [3] F. Fache, E. Schulz, M. L. Tommasino, M. Lemaire, *Chem. Rev.* **2000**, 100, 2159–2232.
- [4] A. J. L. Pombeiro, *Dalton Trans.* **2019**, 48, 13904–13906.
- [5] V. Lyaskovskyy, B. de Bruin, *ACS Catal.* **2012**, 2, 270–279.
- [6] O. R. Luca, R. H. Crabtree, *Chem. Soc. Rev.* **2013**, 42, 1440–1459.
- [7] P. J. Chirik, K. Wieghardt, *Science* **2010**, 327, 794–795.
- [8] M. W. Bouwkamp, A. C. Bowman, E. Lobkovsky, P. J. Chirik, *J. Am. Chem. Soc.* **2006**, 128, 13340–13341.
- [9] S. C. Bart, K. Chłopek, E. Bill, M. W. Bouwkamp, E. Lobkovsky, F. Neese, K. Wieghardt, P. J. Chirik, *J. Am. Chem. Soc.* **2006**, 128, 13901–13912.
- [10] W. Kaim, *Dalton Trans.* **2019**, 48, 8521–8529.
- [11] I. L. Fedushkin, A. A. Skatova, V. A. Chudakova, G. K. Fukin, *Angew. Chem. Int. Ed.* **2003**, 42, 3294–3298.
- [12] R. van Asselt, C. J. Elsevier, W. J. J. Smeets, A. L. Spek, R. Benedix, *Recl. Trav. Chim. Pays-Bas* **1994**, 113, 88–98.
- [13] K. J. Cavell, D. J. Stufkens, K. Vrieze, *Inorg. Chim. Acta* **1981**, 47, 67–76.
- [14] J. Reinhold, R. Benedix, P. Birner, H. Hennig, *Inorg. Chim. Acta* **1979**, 33, 209–213.
- [15] M. Gasperini, F. Ragaini, E. Gazzola, A. Caselli, P. Macchi, *Dalton Trans.* **2004**, 3376–3382.
- [16] M. Gasperini, F. Ragaini, *Organometallics* **2004**, 23, 995–1001.
- [17] K. Hasan, E. Zysman-Colman, *J. Phys. Org. Chem.* **2013**, 26, 274–279.
- [18] I. Matei, T. Lixandru, *Bul. Inst. Politeh. Iasi* **1967**, 13, 245–255.
- [19] M. Dvolaitzky, *C. R. Acad. Sci. Ser. C* **1969**, 268, 1811–1813.
- [20] R. van Asselt, C. J. Elsevier, *J. Mol. Catal.* **1991**, 65, L13–L19.
- [21] L. K. Johnson, C. M. Killian, M. Brookhart, *J. Am. Chem. Soc.* **1995**, 117, 6414–6415.
- [22] S. D. Ittel, L. K. Johnson, M. Brookhart, *Chem. Rev.* **2000**, 100, 1169–1204.
- [23] N. J. Hill, I. Vargas-Baca, A. H. Cowley, *Dalton Trans.* **2009**, 240–253.
- [24] I. L. Fedushkin, M. V. Moskalev, A. N. Lukoyanov, A. N. Tishkina, E. V. Baranov, G. A. Abakumov, *Chem. Eur. J.* **2012**, 18, 11264–11276.
- [25] I. L. Fedushkin, A. A. Skatova, N. L. Bazyakina, V. A. Chudakova, N. M. Khvoinova, A. S. Nikipelov, O. V. Eremenko, A. V. Piskunov, G. K. Fukin, K. A. Lyssenko, *Russ. Chem. Bull.* **2013**, 62, 1815–1828.
- [26] M. Arrowsmith, M. S. Hill, G. Kociok-Köhn, *Organometallics* **2014**, 33, 206–216.
- [27] J. Wang, R. Ganguly, L. Yongxin, J. Díaz, H. S. Soo, F. García, *Inorg. Chem.* **2017**, 56, 7811–7820.
- [28] V. Rosa, C. I. M. Santos, R. Welter, G. Aullón, C. Lodeiro, T. Avilés, *Inorg. Chem.* **2010**, 49, 8699–8708.

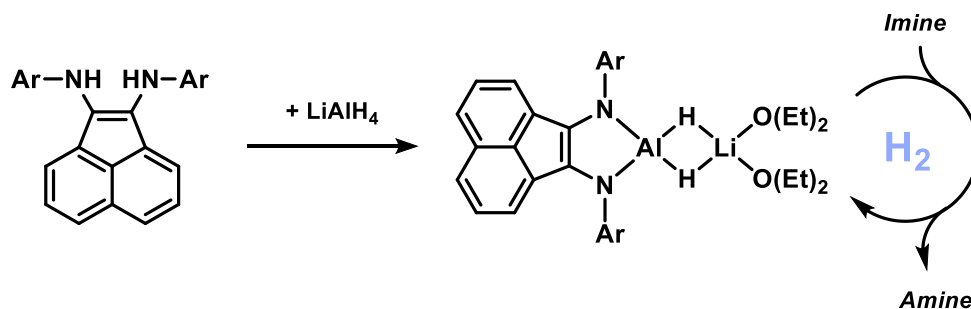
- [29] I. L. Fedushkin, V. M. Makarov, V. G. Sokolov, G. K. Fukin, M. O. Maslov, S. Y. Ketkov, *Russ. Chem. Bull.* **2014**, 63, 870–882.
- [30] M. Villa, D. Miesel, A. Hildebrandt, F. Ragaini, D. Schaarschmidt, A. Jacobi von Wangelin, *ChemCatChem* **2017**, 9, 3203–3209.
- [31] S. Quintal, M. J. Pires da Silva, S. R. M. Martins, R. Sales, V. Félix, M. G. B. Drew, M. Meireles, A. C. Mourato, C. D. Nunes, M. S. Saraiva, M. Machuqueiro, M. J. Calhorda, *Dalton Trans.* **2019**, 48, 8449–8463.
- [32] R. Schmidt, K. Griesbaum, A. Behr, D. Biedenkapp, H.-W. Voges, D. Garbe, C. Paetz, G. Collin, D. Mayer, H. Höke in *Ullmann's encyclopedia of industrial chemistry* (Hrsg.: W. Gerhartz, Y. S. Yamamoto), VCH Verlagsgesellschaft, Weinheim **1985-1996**.
- [33] M. Gasperini, F. Ragaini, S. Cenini, *Organometallics* **2002**, 21, 2950–2957.
- [34] H. Liu, W. Zhao, X. Hao, C. Redshaw, W. Huang, W.-H. Sun, *Organometallics* **2011**, 30, 2418–2424.
- [35] F. Ragaini, M. Gasperini, P. Parma, E. Gallo, N. Casati, P. Macchi, *New J. Chem.* **2006**, 30, 1046.
- [36] F. Ragaini, M. Gasperini, E. Gallo, P. Macchi, *Chem. Commun.* **2005**, 1031–1033.
- [37] M. Hagar, F. Ragaini, E. Monticelli, A. Caselli, P. Macchi, N. Casati, *Chem. Commun.* **2010**, 46, 6153–6155.
- [38] M. Viganò, F. Ferretti, F. Ragaini, P. Macchi, *Inorg. Chim. Acta* **2018**, 483, 305–309.
- [39] J. A. Moore, K. Vasudevan, N. J. Hill, G. Reeske, A. H. Cowley, *Chem. Commun.* **2006**, 2913–2915.
- [40] M. Viganò, F. Ferretti, A. Caselli, F. Ragaini, M. Rossi, P. Mussini, P. Macchi, *Chem. Eur. J.* **2014**, 20, 14451–14464.
- [41] S. Nishimura, *Handbook of heterogeneous catalytic hydrogenation for organic synthesis*, Wiley, New York **2001**.
- [42] J. G. de Vries, C. J. Elsevier, *The Handbook of Homogeneous Hydrogenation*, Wiley **2006**.
- [43] M. W. van Laren, C. J. Elsevier, *Angew. Chem. Int. Ed.* **1999**, 38, 3715–3717.
- [44] A. Dedieu, S. Humbel, C. Elsevier, C. Grauffel, *Theor. Chem. Acc.* **2004**, 112.
- [45] A. M. Kluwer, T. S. Koblenz, T. Jonischkeit, K. Woelk, C. J. Elsevier, *J. Am. Chem. Soc.* **2005**, 127, 15470–15480.
- [46] H. Guo, Z. Zheng, F. Yu, S. Ma, A. Holuigue, D. S. Tromp, C. J. Elsevier, Y. Yu, *Angew. Chem. Int. Ed.* **2006**, 45, 4997–5000.
- [47] S. Sandl, T. M. Maier, N. P. van Leest, S. Kröncke, U. Chakraborty, S. Demeshko, K. Koszinowski, B. de Bruin, F. Meyer, M. Bodensteiner, C. Herrmann, R. Wolf, A. Jacobi von Wangelin, *ACS Catal.* **2019**, 9, 7596–7606.
- [48] T. M. Maier, S. Sandl, I. G. Shenderovich, A. Jacobi von Wangelin, J. J. Weigand, R. Wolf, *Chem. Eur. J.* **2019**, 25, 238–245.
- [49] H. Elsen, C. Färber, G. Ballmann, S. Harder, *Angew. Chem. Int. Ed.* **2018**, 57, 7156–7160.
- [50] J. A. Hatnean, J. W. Thomson, P. A. Chase, D. W. Stephan, *Chem. Commun.* **2014**, 50, 301–303.
- [51] A. Biffis, P. Centomo, A. Del Zotto, M. Zecca, *Chem. Rev.* **2018**, 118, 2249–2295.

- [52] R. van Asselt, C. J. Elsevier, *Organometallics* **1992**, *11*, 1999–2001.
- [53] R. van Asselt, C. J. Elsevier, *Tetrahedron* **1994**, *50*, 323–334.
- [54] R. van Asselt, C. J. Elsevier, *Organometallics* **1994**, *13*, 1972–1980.
- [55] R. van Asselt, E. Rijnberg, C. J. Elsevier, *Organometallics* **1994**, *13*, 706–720.
- [56] C. J. Elsevier, *Coord. Chem. Rev.* **1999**, *185-186*, 809–822.
- [57] R. van Asselt, K. Vrieze, C. J. Elsevier, *J. Organomet. Chem.* **1994**, *480*, 27–40.
- [58] R. van Belzen, H. Hoffmann, C. J. Elsevier, *Angew. Chem. Int. Ed. Engl.* **1997**, *36*, 1743–1745.
- [59] M. Gholinejad, V. Karimkhani, I. Kim, *Appl. Organometal. Chem.* **2014**, *28*, 221–224.
- [60] A. L. Gottumukkala, J. F. Teichert, D. Heijnen, N. Eisink, S. van Dijk, C. Ferrer, A. van den Hoogenband, A. J. Minnaard, *J. Org. Chem.* **2011**, *76*, 3498–3501.
- [61] H. D. Magurudeniya, P. Sista, J. K. Westbrook, T. E. Ourso, K. Nguyen, M. C. Maher, M. G. Alemseghed, M. C. Biewer, M. C. Stefan, *Macromol. Rapid Commun.* **2011**, *32*, 1748–1752.
- [62] C. R. Bridges, T. M. McCormick, G. L. Gibson, J. Hollinger, D. S. Seferos, *J. Am. Chem. Soc.* **2013**, *135*, 13212–13219.
- [63] C. R. Bridges, H. Yan, A. A. Pollit, D. S. Seferos, *ACS Macro Lett.* **2014**, *3*, 671–674.
- [64] F. Ragaini, S. Cenini, E. Gallo, A. Caselli, S. Fantauzzi, *Curr. Org. Chem.* **2006**, *10*, 1479–1510.
- [65] F. Ferretti, D. Formenti, F. Ragaini, *Rend. Fis. Acc. Lincei* **2017**, *28*, 97–115.
- [66] F. Ferretti, D. R. Ramadan, F. Ragaini, *ChemCatChem* **2019**, *11*, 4450–4488.
- [67] F. Ragaini, S. Cenini, S. Tollari, *J. Mol. Catal.* **1993**, *85*, L1-L5.
- [68] F. Ragaini, S. Cenini, M. Gasperini, *J. Mol. Catal. A: Chem.* **2001**, *174*, 51–57.
- [69] M. Viganò, F. Ragaini, M. G. Buonomenna, R. Lariccia, A. Caselli, E. Gallo, S. Cenini, J. C. Jansen, E. Drioli, *ChemCatChem* **2010**, *2*, 1150–1164.
- [70] S. Cenini, F. Ragaini, S. Tollari, D. Paone, *J. Am. Chem. Soc.* **1996**, *118*, 11964–11965.
- [71] F. Ragaini, S. Cenini, S. Tollari, G. Tummolillo, R. Beltrami, *Organometallics* **1999**, *18*, 928–942.
- [72] F. Ragaini, S. Cenini, E. Borsani, M. Dompé, E. Gallo, M. Moret, *Organometallics* **2001**, *20*, 3390–3398.
- [73] M. Arrowsmith, M. S. Hill, G. Kociok-Köhn, *Organometallics* **2011**, *30*, 1291–1294.
- [74] A. Cimino, F. Moscatelli, F. Ferretti, F. Ragaini, S. Germain, J. Hannedouche, E. Schulz, L. Luconi, A. Rossin, G. Giambastiani, *New J. Chem.* **2016**, *40*, 10285–10293.
- [75] A. M. Yakub, M. V. Moskalev, N. L. Bazyakina, I. L. Fedushkin, *Russ. Chem. Bull.* **2018**, *67*, 473–478.
- [76] L. Li, P. S. Lopes, C. A. Figueira, C. S. B. Gomes, M. T. Duarte, V. Rosa, C. Fliedel, T. Avilés, P. T. Gomes, *Eur. J. Inorg. Chem.* **2013**, *2013*, 1404–1417.
- [77] L. Li, P. S. Lopes, V. Rosa, C. A. Figueira, M. A. N. D. A. Lemos, M. T. Duarte, T. Avilés, P. T. Gomes, *Dalton Trans.* **2012**, *41*, 5144–5154.
- [78] C. D. Nunes, P. D. Vaz, V. Félix, L. F. Veiros, T. Moniz, M. Rangel, S. Realista, A. C. Mourato, M. J. Calhorda, *Dalton Trans.* **2015**, *44*, 5125–5138.



- [79] I. S. Fomenko, A. L. Gushchin, L. S. Shul'pina, N. S. Ikonnikov, P. A. Abramov, N. F. Romashev, A. S. Poryvaev, A. M. Sheveleva, A. S. Bogomyakov, N. Y. Shmelev, M. V. Fedin, G. B. Shul'pin, M. N. Sokolov, *New J. Chem.* **2018**, 42, 16200–16210.

## 2 Application of Reduced BIAN Aluminium Hydride Complexes in Catalysis



**Abstract:** Aluminium hydride complexes with a reduced ArBIAN backbone have been prepared and characterized. Varying temperature NMR suggests a highly fluxional complex, that was shown to catalyze various hydroboration reactions and the hydrogenation of imines. Compared to previous reports regarding the aluminium-catalyzed hydrogenation of imines, the investigated complex shows improved catalytic activity with an extended range of substrates.

Unpublished results.

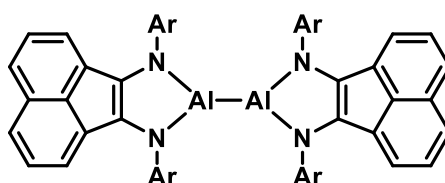
Author contribution: Dieter Schaarschmidt performed initial complex syntheses and characterizations.

## 2.1 Introduction

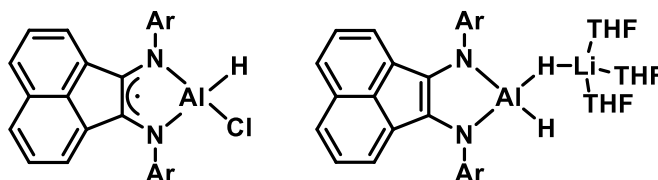
Due to the increasing demand for sustainable chemical processes, researchers' urge to develop more environmentally benign alternatives to established transition metal catalysts intensified drastically in the last decades. Aluminium is the most abundant metal in the earth's crust, it is inexpensive and much less toxic than heavy metals. Besides its well-established application as Lewis acid, recent reports reveal the hidden potential of Aluminium hydrides in catalysis, e.g. hydroboration, hydrosilylation and hydrogenation reactions.<sup>[1,2]</sup>

Whereas the interaction between substrate and catalyst in transition metal catalysis is determined by redox interactions and orbital overlap, the influence of main group metals is mostly determined by their properties in Lewis acidity. Consequently, the application of cooperative ligands, which can provide both sterical and electronical adjustments, is a vibrant and promising field in current research. In this process the syntheses of a wide variety of aluminium complexes were published in recent years.<sup>[3–6]</sup> These feature mostly bulky ligands, since it has been shown on several instances that aluminium organyls easily undergo cluster formation, when ligands of low steric demand were employed. For the synthesis of a practicable catalyst, this is especially important, as many of the reported clusters arrange around potential substrates (e.g. alkenes, alkynes, nitriles).<sup>[7–10]</sup>

*Fedushkin 2012*



*Fedushkin 2017*

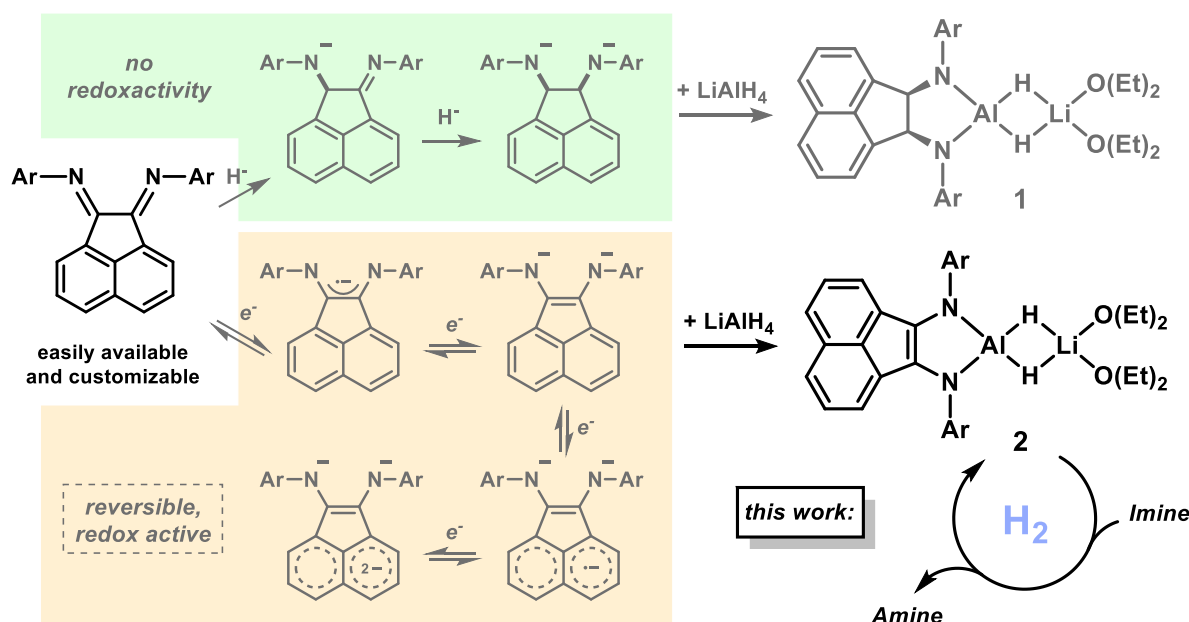


**Figure 2.1** Excerpt of BIAN-Al complexes reported by Fedushkin *et al.*<sup>[6,11]</sup>

Thanks to the accessibility of sterically and electronically adaptable bis(imino)acenaphthenes (BIAN) we decided to dive into these types of ligands for developing our aluminium hydride catalyst. Even though their  $\sigma$ -donor properties can

be increased by reduction, such compounds are still largely underutilized in complex synthesis and catalysis. That being said, the group of Fedushkin has made tremendous efforts in the last years synthesizing numerous complexes to unveil the opportunities we encounter with BIAN ligands in its feasible oxidation states.<sup>[12–15]</sup> In 2017 they also displayed a selection of aluminium hydrides, which covered some of the complexes we synthesized and characterized for this catalytical investigation.<sup>[11,16]</sup> Figure 2.1 shows an abstract of literature-known Al-BIAN complexes, which cover aluminium in the oxidation states +2 and +3, and the BIAN ligand in the radical monoanionic and dianionic state. However, there are no reported catalytic applications for these types of complexes.

In the early two thousands, it was also Fedushkin who revealed that BIANs were capable of accepting up to four electrons by treatment with alkali or alkaline earth metals.<sup>[17,18]</sup> Since then various BIANs could be isolated and were heavily investigated in their corresponding reduced forms.<sup>[19]</sup> On that work we built up our efforts to synthesize aluminium hydrides with a reduced BIAN backbone (Scheme 2.1).

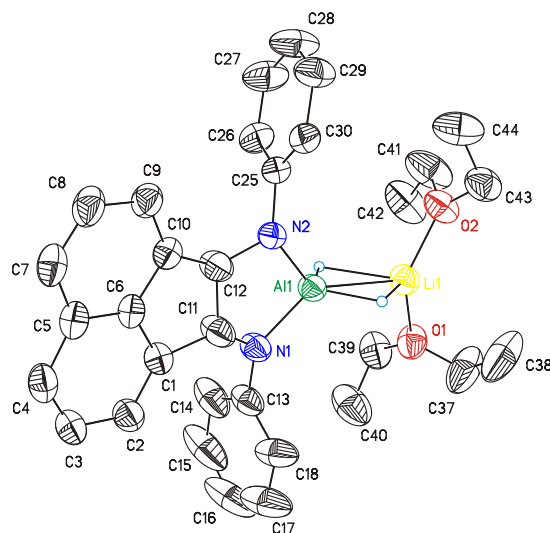


**Scheme 2.1** Synthesis of BIAN Aluminium hydrides **1** and **2**, Ar = 2,6-diisopropylphenyl (dipp).

## 2.2 Results and Discussion

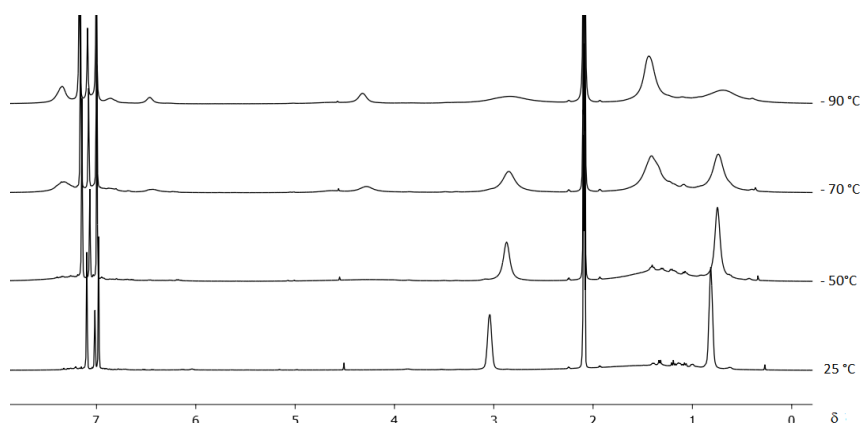
DippBIAN was converted to dippBIAN-H<sub>4</sub> with LiAlH<sub>4</sub> and to dippBIAN-H<sub>2</sub> with the aid of Potassium (2 equiv.), and both were isolated after protonation. The reaction of the

reduced BIAN ligands with  $\text{LiAlH}_4$  proceeds in  $\text{Et}_2\text{O}$  within 12 h, resulting in **1** (fully characterized by Fedushkin *et. al.*<sup>[11]</sup> and us) and **2**. Structurally **2** does not differ substantially from other BIAN aluminium hydrides discussed in Fedushkins work (Figure 2.2).



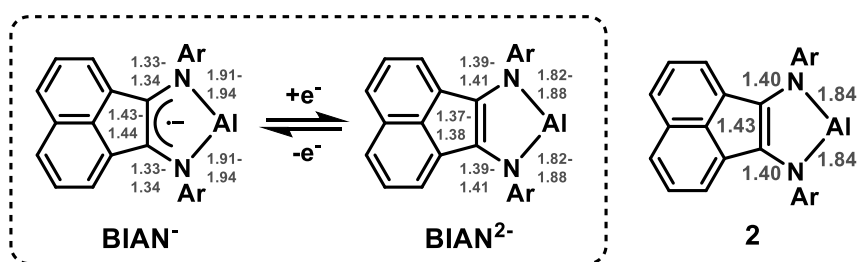
**Figure 2.2** ORTEP diagram (50% probability level) of the molecular structure of **2** with the atom-numbering scheme. Isopropyl substituents, H atoms of the ligand backbone and of diethylether omitted for clarity. Selected bond lengths (Å): C(11)-C(12) 1.429(4), C(11)-N(1) 1.397(3), C(13)-N(1) 1.418(3) N(1)-Al(1) 1.842(2), Al(1)-H(1AL) 1.56(3), Li(1)-H(1AL) 2.01(3), Li(1)-Al(1) 2.608(5), O(1)-Li(1) 1.898(5).

Nevertheless, we ran into some unexpected analytical results with our specific complex during the characterization. In proton NMR we were faced with severe peak broadening. By lowering the temperature we could see a slight sharpening of the aromatic and aliphatic signals of the ligand, whilst the signals of the coordinated ether molecules were significantly broadened and shifted upfield (expected non-coordinated ether signals at 1.10 and 3.25 ppm, Scheme 2.2)<sup>[20]</sup>. These findings suggest a highly fluxional complex.



**Scheme 2.2**  $^1\text{H}$ -NMR spectra of compound **2** (400 MHz, toluene- $d_8$ ) at varying temperatures.

It is worth noting that the observed bond lengths do not fully support the presence of the ligand in the dianion state. This would imply that Al(III) would be reduced nominally to Al(II) by the ligand, which seems rather unlikely due to the reluctance of Al(III) to change its preferred oxidation state.<sup>[21]</sup> There are only a few Al(II) complexes known to this day and these are commonly represented by dialanes.<sup>[22,23]</sup> Nevertheless, we compared the bond lengths of known Al(III)-BIAN complexes with **2** (Scheme 2.3).<sup>[11]</sup> The length of the double bond of **2** would actually indicate the ligand being in the BIAN<sup>-</sup>-state, but on the other hand the remaining bond lengths do not support this proposal either. Even though this matter could not be completely solved as of today, we still propose Al(III) due to the lack of accessibility of Al(II).



**Scheme 2.3** Reported bond lengths of Al(III)-BIAN complexes.<sup>[11]</sup>

In our attempt to find an application for **2**, we were looking into recent developments of catalytic reactions featuring aluminium hydrides as (pre)catalysts. Generally, aluminium hydrides are employed as catalysts in the reduction of organic compounds such as hydroboration, hydrosilylation, hydrogenation and hydrodefluorination reactions.<sup>[1,2]</sup> In case of hydroboration, a variety of substrate groups could be converted successfully with support of aluminium hydride catalysts,<sup>[24–26]</sup> delivering products that are highly valuable for further synthetic applications. In addition to that we looked into the hydrogenation reactions, as these represent a major pillar in the synthetic chemical

industry. Table 2.1 presents the results of hydroborations of triple bonds, ketones and nitriles and of imine hydrogenations with **2** as running catalyst under the conditions of recent publications. However, the acting catalytic systems in these reports were rarely commercially available. In order to make these initial attempts significant anyhow, we compared the catalytic activity with commercial DiBAL-H to see whether further investigations would be justified.

**Table 2.1** Initial attempts setting **2** against commercial diisobutylaluminium hydride.

$$\text{R}-\text{C}(=\text{X})-\text{Y} + \text{H}-\text{Y} \xrightarrow{10 \text{ mol\% } [\text{Al}]} \text{R}-\text{CH}_2-\text{CH}_2-\text{OH}$$

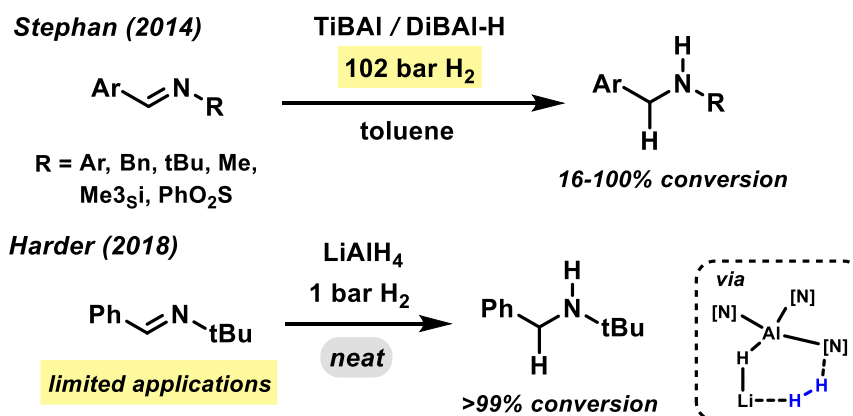
Entry	Substrate	Product	Yield [%] <sup>[a]</sup>		
			DiBAL-H	<b>2</b>	reported
1	$\text{C}_5\text{H}_{11}-\text{C}\equiv\text{C}-\text{H}$	$\text{C}_5\text{H}_{11}-\text{CH}=\text{CH}-\text{BPin}$	70	72	40 – 89 <sup>[b]</sup>
2	$\text{Ph}-\text{C}\equiv\text{C}-\text{H}$	$\text{Ph}-\text{CH}=\text{CH}-\text{BPin}$	84	73	12 ex. <sup>[24]</sup>
3	$\text{C}_4\text{H}_9-\text{CH}(\text{C}_2\text{H}_5)-\text{CHO}$	$\text{C}_4\text{H}_9-\text{CH}(\text{C}_2\text{H}_5)-\text{CH}_2-\text{OBPin}$	93	63	43 – 99 <sup>[c]</sup>
4	$\text{Ph}-\text{CHO}$	$\text{Ph}-\text{CH}_2-\text{OBPin}$	77	88	14 ex. <sup>[25]</sup>
5	$\text{C}_4\text{H}_9-\text{CN}$	$\text{C}_4\text{H}_9-\text{CH}_2-\text{N}(\text{BPin})_2$	0	27	60 – 99 <sup>[d]</sup>
6	$\text{Ph}-\text{CN}$	$\text{Ph}-\text{CH}_2-\text{N}(\text{BPin})_2$	61	70	18 ex. <sup>[26]</sup>
7	$\text{Ph}-\text{CH}=\text{N}-\text{tBu}$	$\text{Ph}-\text{CH}_2-\text{NH}-\text{tBu}$	(43)	(>95)	16 – 100 <sup>[e]</sup>
8	$\text{Ph}-\text{CH}=\text{N}-\text{Ph}$	$\text{Ph}-\text{CH}_2-\text{NH}-\text{Ph}$	(94)	(>95)	15 ex. <sup>[27]</sup>

<sup>[a]</sup> Yields were determined by quantitative <sup>1</sup>H-NMR vs. internal 1,3,5-trimethoxybenzene, GC conversions in brackets; <sup>[b]</sup> 1.2 equiv. HBPIn, toluene, 110 °C, 2 h, cat: DiBAL-H, Et<sub>3</sub>Al-DABCO; <sup>[c]</sup> 1 equiv. HBPIn, benzene, r.t., 0.5-8 h, cat: (HMDS)<sub>2</sub>AlH(μ-H)Li(THF)<sub>3</sub>; <sup>[d]</sup> 2.2 equiv. HBPIn, neat, 60 °C, 3-10 h, cat: {2-F-C<sub>6</sub>H<sub>4</sub>NP(Se)Ph<sub>2</sub>}<sub>2</sub>Al(Me); <sup>[e]</sup> 102 atm. H<sub>2</sub>, toluene, 100 °C, 24 h, cat: DiBAL-H, TiBAL.

For the hydroborations of triple bonds we saw only little to no difference by using **2** instead of DiBAL-H. However, this changed when we used aldehydes as substrates. Even though we could not find the aspired rise in catalytic activity, we could still see a noticeable influence of the catalytic system on the reaction outcome. More promising were the results of the hydroboration of nitriles. Under these conditions we saw a clear boost in catalytic activity by using **2** over DiBAL-H. However, the reported catalytic system for the hydroboration of nitriles published by Harinath *et. al.* easily outperformed **2**.<sup>[26]</sup> The hydrogenation of imines shows high conversions with our

catalyst, surpassing not only DiBAI-H in our tests but also in the reported conditions. Following these results, we focused our efforts on the examination of Al-catalyzed imine hydrogenation.

To this date, there are only two publications covering this type of catalysis (Scheme 2.4).<sup>[27,28]</sup> The group of Stephan showed in 2014 that DiBAI-H could catalyze the reduction at 100 °C and 102 bar of hydrogen. They were able to isolate an inactive dimer that would form during the reaction below 100 °C, leading to the inhibition of the reaction.<sup>[27]</sup> In 2018 Harder *et al.* could show that this type of catalytic reactions can also run at more gentle conditions, namely 85 °C and 1 bar of hydrogen by using simple lithium aluminium hydride as precatalyst. These conditions, however, could only be shown to work by using *N*-Benzylidene-*tert*-butylamine as a substrate. For the application with other imines or in cases in which solvents are necessary, the operating hydrogen pressure has to be raised significantly, just to receive mediocre conversions at best. With aid of DFT calculations they came to the conclusion that the active catalyst may include two inserted imines resulting in a  $\text{LiAlH}_2\text{-[N]}_2$  intermediate, a configuration they were also able to isolate. Their proposed catalytic cycle involved an important effect of the  $\text{Li}^+$  during the  $\text{H}_2$ -activation, which is indicated due to the fact that the Al center is sterically congested with three amide ligands.<sup>[28]</sup> This work has been extended recently by the same group with the application of alkaline earth metal aluminates as catalysts. This work verified the crucial influence of the bimetallic system and the application of alkaline earth metals instead of lithium led to an increase in catalytic activity in some cases. However, the substrate scope remained fairly limited.<sup>[29]</sup>

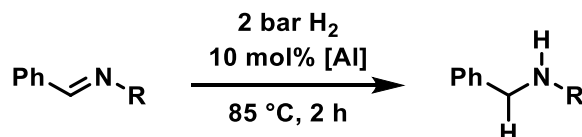


**Scheme 2.4** Aluminium-catalyzed hydrogenation of imines.<sup>[27,28]</sup>



Considering the similarities of **2** and the proposed active catalyst in Harders work, we were eager to apply and compare our catalytic system under similar conditions.

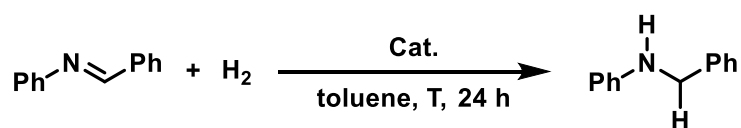
**Table 2.2** Imine hydrogenation at low pressure.



Entry	R	Conditions	[Al]	Conv. [%] <sup>[a]</sup>
1	tBu	neat	LiAlH <sub>4</sub>	>95
2			<b>2</b>	10
5	Bn	neat	LiAlH <sub>4</sub>	82
6			<b>2</b>	45
7		in toluene	LiAlH <sub>4</sub>	19
8			<b>2</b>	11

<sup>[a]</sup> Conversions were determined by quantitative GC-FID vs. internal *n*-C<sub>15</sub>H<sub>32</sub>.

We tested two different liquid imines under neat conditions, of which the *N*-benzylidene-tert-butylamine did not show a catalytic hydrogenation with **2**. Changing the substituent to benzyl made a catalytic hydrogenation possible, yet simple LiAlH<sub>4</sub> easily outperformed our complex. However, the addition of solvent ruins the catalytic activity in both cases and therefore sorely restricts its field of application. That is why we started our optimization experiments with the procedure developed by Stephan *et al.* (Scheme 2.4).

**Table 2.3** Imine hydrogenation optimization experiments.

Entry	Cat. (mol%)	T [°C]	H <sub>2</sub> [bar]	Yield [%] <sup>[a]</sup>
1	<b>2</b> (10)	100	100	>95
2	<b>2</b> (5)	100	100	73
3	<b>2</b> (3)	100	100	50
4	<b>2</b> (1)	100	100	9
<b>5</b>	<b>2</b> (10)	<b>100</b>	<b>50</b>	<b>&gt;95</b> (65 <sup>[b]</sup> , 39 <sup>[c]</sup> )
6	<b>2</b> (10)	100	2	20 <sup>[c]</sup>
7	<b>2</b> (10)	70	50	38
8	<b>2</b> (10)	100	30	55
9	DiBAI-H (10)	100	100	94
10	DiBAI-H (10)	100	50	36
11	TiBAI (10)	100	50	19
12	Et <sub>3</sub> Al (10)	100	50	12
13	TrioctylAl (10)	100	50	21
14	Li[(tBuO) <sub>3</sub> AlH] (10)	100	50	9
15	LiAlH <sub>4</sub> (10)	100	50	22
16	LiAlH <sub>4</sub> (10) + dippBIANH <sub>2</sub> (10)	100	50	29
17	LiAlH <sub>4</sub> (10) + Et <sub>2</sub> O (30)	100	50	56
18	LiAlH <sub>4</sub> (10) + dippBIANH <sub>2</sub> (10) + Et <sub>2</sub> O (30)	100	50	>95

<sup>[a]</sup> Yields were determined by quantitative GC-FID vs. internal *n*-C<sub>15</sub>H<sub>32</sub>, <sup>[b]</sup> fivefold of solvent was used,

<sup>[c]</sup> solvent-free.

We began our optimization experiments at 100 °C and 100 bar of hydrogen to see whether we could replicate the catalyst performance published by Stephan *et al.* Both **2** and DiBAI-H give good results (see entries 1 and 9), with **2** showing complete conversion. By examining the limits of the reaction conditions, we could see that lowering the catalyst loading and temperature severely decreased the yield but lowering the operating pressure to 50 bar delivered yet the same catalytic performance (entry 5). From there we tested other commercial aluminium hydride sources and interestingly **2** exceeded all of them by quite a margin at 50 bar. This includes the (pre)catalysts of our predecessors DiBAI-H and LiAlH<sub>4</sub> (entries 10 and 15). Full hydrogenation could also be reached by in situ preparation of our catalyst, of which the addition of ether seems not only to be necessary for the catalyst formation but also has a strong impact of its own (see entries 15-18). Another noteworthy requirement for this reaction to operate accordingly, is to run the reaction with the least possible amount of solvent. By slightly diluting the reaction mixture, the yield was cut significantly (entry

5). This is in accordance with the previous results, which indicated a negative effect of the solvent. Running the hydrogenation of the chosen imine (melting point 54 °C) under neat conditions did not allow a smooth reaction though (entries 5 and 6).

**Table 2.4** Hydrogenation substrate scope.

$\text{Imine} \xrightarrow[\text{toluene, 100 } ^\circ\text{C, 24 h}]{10 \text{ mol\% } 2, \text{H}_2 (50 \text{ bar})} \text{Amine}$					
Entry	Substrate	Product	X	Conv. [%] <sup>[a]</sup>	Yield [%] <sup>[b]</sup>
1			H	>95	79 (>95)
2			Cl	50	39
3			tBu	51	35
4			CN	84	0
5				57	41
6			CO <sub>2</sub> Me	45	0
7			OCF <sub>3</sub>	41	23
8				>95	72
9				>95	79
10				>95	71
11			H	95	73
12			OMe	47	40
13			Br	82	63
14			CF <sub>3</sub>	74	52
15				82	66
16				42	35
17				43	38
18 <sup>[c]</sup>				>95	72

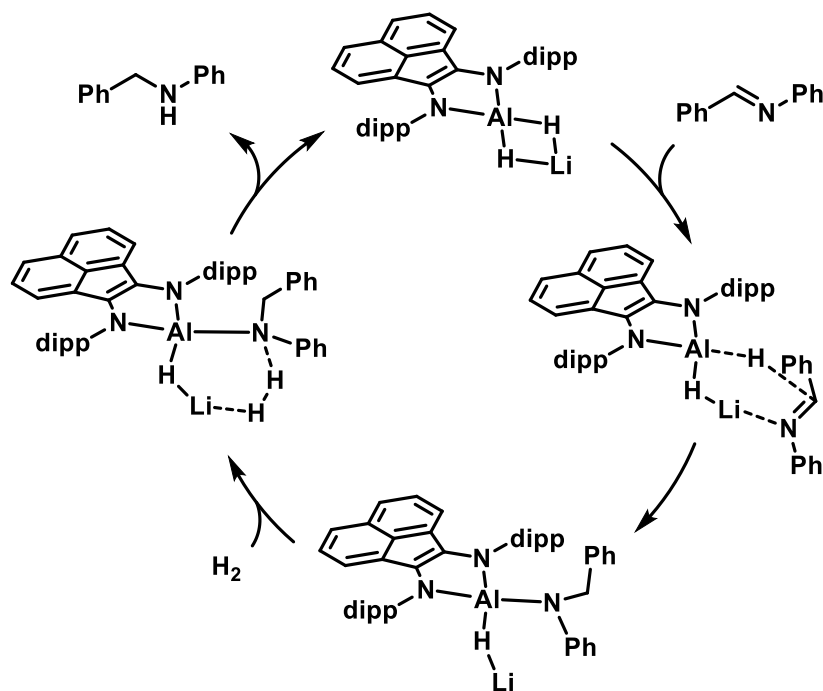
<sup>[a]</sup> Conversions were determined by quantitative GC-FID vs. internal *n*-C<sub>15</sub>H<sub>32</sub>, <sup>[b]</sup> Isolated yield, GC-yield in brackets, <sup>[c]</sup> 20 mol% catalyst was used.

The reaction proceeds with high conversions in half of the performed hydrogenations, mostly the substrates carrying no functional groups. Nevertheless, bromide and

trifluoromethyl substituents were tolerated, whereas chloride and ether substituents dropped the conversion in half. Not tolerated, however, were cyano and ester groups. A broad mixture of products was obtained in these cases, which correlates most likely to their oxidative nature. Ket-imines turned out to be more demanding substrates altogether (entries 16, 17) and the oxime hydrogenation gave the corresponding primary amine after aqueous workup (entry 10). Compared to our predecessors, we could lower the reaction conditions of Stephans work significantly and still extend the scope of the reaction: aliphatic imines could be hydrogenated successfully (entries 15 and 18) and also *N-tert*-Butyl- and *N*-Benzylimines were transformed in higher yields under our conditions (entries 8, 11-14). Harders work on the other hand, showed the full potential of aluminium hydride catalysts by using  $\text{LiAlH}_4$  to form active catalysts *in situ*. We could lower the limitations of their procedure by using a pre synthesized catalyst under harsher reaction conditions, in which simple  $\text{LiAlH}_4$  shows no catalytic activity (see table 2.3, entry 10). Lastly, both publications observe similar effects regarding functional groups as we do under our conditions.

To the best of our knowledge, the discrepancy between the observed conversions and isolated yields is a consequence of product purification. No other side reactions were captured.

Due to the fact that our catalytic system shares structural similarities with those reported by Harder, <sup>[28,29]</sup> we propose an analogical mechanism (Scheme 2.5). After the insertion of an imine, the activation of molecular hydrogen is facilitated by  $\text{Li}^+$  of the bimetallic complex. This leads to the recovery of the catalyst and formation of the amine product. We assume that catalyst deactivation via dimerization, as observed by Stephan,<sup>[27]</sup> is prevented by steric crowding of the dippBIAN ligand. These special properties make complex **2** a highly active aluminium catalyst for the hydrogenation of a variety of imines.



**Scheme 2.5** Proposed catalytic cycle for the hydrogenation of imines.

## 2.3 Conclusion

In summary, synthetic procedures and crystal structures for aluminium hydride complexes with reduced dippBIAN ligands have been presented. Complex **2** shows severe peak broadening in the proton NMR, presumably due to high fluxionality of the complex.

Complex **2** was shown to be an active catalyst for the hydrogenation of imines and hydroboration reactions with alkynes, aldehydes, and nitriles. However, the results did not justify a closer examination of the latter. In comparison to earlier reports regarding aluminium-catalyzed hydrogenation of imines, the investigated complex shows high catalytic activity and an extended substrate scope. In accordance with the results of our predecessors, we assume a promotion of the hydrogen activation through the bimetallic system and prevention of catalyst dimerization by the sterically demanding ligand substituents.

## 2.4 Experimental

Chemicals and Solvents. If not indicated, commercial reagents were used without purification. For catalytic reactions, exclusively dried solvents were used. Liquid substrates were distilled prior to use. All catalyzed reactions were performed under an atmosphere of dry argon using standard Schlenk and glovebox techniques.

Gas chromatography with mass-selective detector. *Agilent* 6890N Network GC-System, mass detector 5975 MS. Column: BPX5 (30m x 0.25 mm x 0.25 $\mu$ m) from *SGE*, carrier gas: H<sub>2</sub>.

Gas chromatography with FID. *Agilent* 7820A GC-Systems. Column: HP 5 19091J 413 (30 m x 0.32 mm x 0.25  $\mu$ m) from *Agilent*, carrier gas: N<sub>2</sub>. GC-FID was used for catalyst screening (calibration with internal standard *n*-pentadecane and analytically pure samples).

NMR. <sup>1</sup>H and <sup>13</sup>C nuclear magnetic resonance spectra were recorded on a *Bruker* FourierHD 300 (300 MHz <sup>1</sup>H; 75 MHz <sup>13</sup>C). Chemical shifts are reported in ppm ( $\delta$ ) relative to internal tetramethylsilane (TMS). Coupling constants (*J*) are reported in Hertz (Hz).

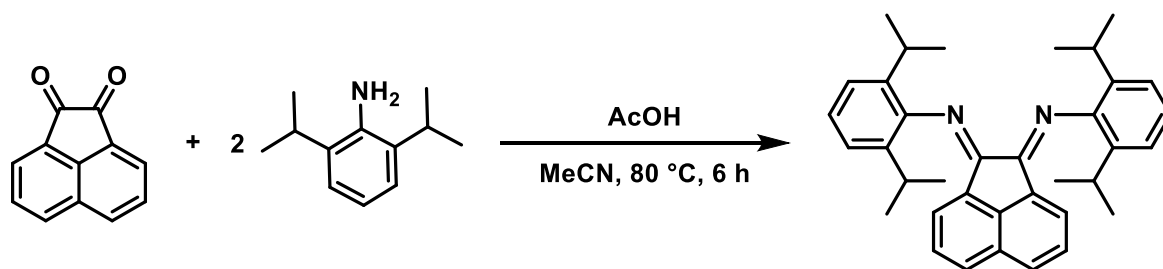
Elemental Analyses (CHN): Elemental Analyses (EA) were performed with a Vario micro cube elemental analyzer.

High resolution mass spectrometry (HRMS). The spectra were recorded by the MS Department at the Department of Chemistry, University of Hamburg.

Liquid injection field desorption ionization (LIFDI) mass spectrometry: Mass spectra were recorded on a Joel AccuTOF GCX in LIFDI mode.

### 2.4.1 Complex Synthesis

Synthesis of *N, N'*-bis(2,6-diisopropylphenyl)acenaphthylene-1,2-diimine (*dipp<sub>2</sub>BIAN*)



The reaction was performed following the procedure of Dastgir *et al.*<sup>[30]</sup>

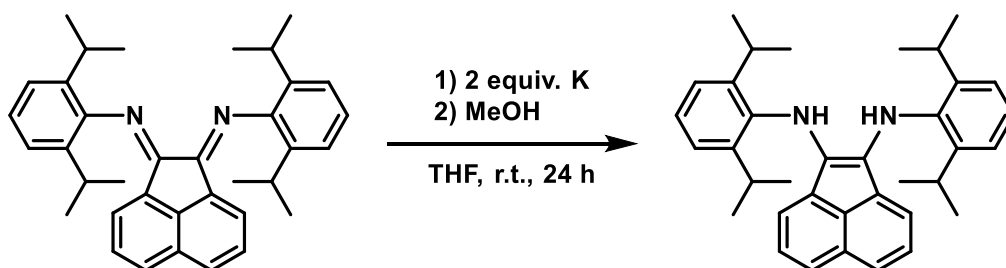
Acenaphthenequinone (95%, 7.05 g, 38.7 mmol) was suspended in acetonitrile (150 mL) and heated under reflux (80 °C) for 60 min. Acetic acid (100 mL) was then added and heating was continued until most of the acenaphthenequinone had dissolved. To this hot suspension 2,6-diisopropylphenylaniline (90%, 16.0 g, 17.0 mL, 89.9 mmol) was added over a period of 30 min and the mixture was heated under reflux for another 5 h and then cooled to room temperature. The resulting orange solid was then filtered, washed with pentane (3 x) and dried in air.

**<sup>1</sup>H-NMR** (300 MHz, CDCl<sub>3</sub>)  $\delta_H$  [ppm] = 7.87 (d,  $J$  = 8.3 Hz, 2H), 7.36 (t,  $J$  = 7.7 Hz, 2H), 7.31 – 7.21 (m, 6H), 6.63 (d,  $J$  = 7.2 Hz, 2H), 3.03 (m, 4H), 1.24 (d,  $J$  = 6.8 Hz, 12H), 0.97 (d,  $J$  = 6.8 Hz, 12H).

**GC-MS** (EI, 70 eV,  $m/z$ ): 500 [M]<sup>+</sup>, 485, 457, 427, 341, 324, 310, 282, 254, 174, 132, 91, 65.

The data corresponds to the literature values.<sup>[31]</sup>

Synthesis of *N,N'*-bis(2,6-diisopropylphenyl)acenaphthylene-1,2-diamine (*dipp*<sub>2</sub>BIANH<sub>2</sub>)

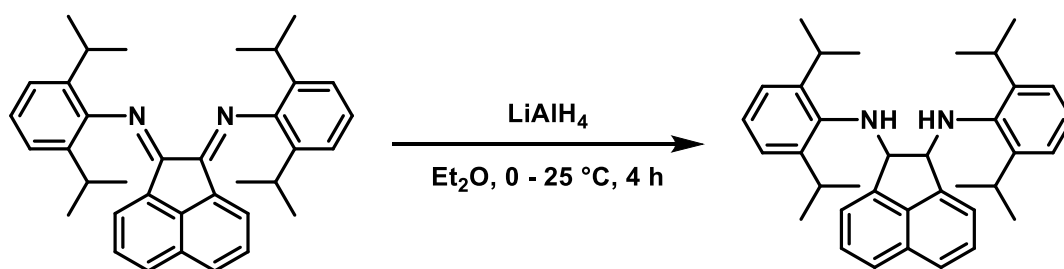


Under argon atmosphere *dipp*<sub>2</sub>BIAN (1.00 g, 2.00 mmol) was suspended in absolute THF (15 mL) and to this suspension was then added potassium (157 mg, 4.02 mmol). After stirring for 24 h at room temperature MeOH (1 mL) was added, the reaction mixture was filtered, and the filtrate was evaporated to dryness. The solid residue was extracted with hexane (20 mL) and the solvent was removed in vacuo to give a violet solid.

**<sup>1</sup>H-NMR** (300 MHz, C<sub>6</sub>D<sub>6</sub>)  $\delta_{\text{H}}$  [ppm] = 7.25 – 7.16 (m, 8H), 6.92 (dd,  $J$  = 8.3, 7.0 Hz, 2H), 6.50 (d,  $J$  = 7.0 Hz, 2H), 4.99 (s, 2H), 3.55 (m, 4H), 1.19 (d,  $J$  = 6.8 Hz, 12H), 1.09 (d,  $J$  = 6.8 Hz, 12H).

The data corresponds to the literature values.<sup>[32]</sup>

Synthesis of *N,N'*-bis(2,6-diisopropylphenyl)-1,2-dihydroacenaphthylene-1,2-diamine (*dipp*<sub>2</sub>BIANH<sub>4</sub>)



The reaction was performed following the procedure of Dastgir *et al.*<sup>[30]</sup>

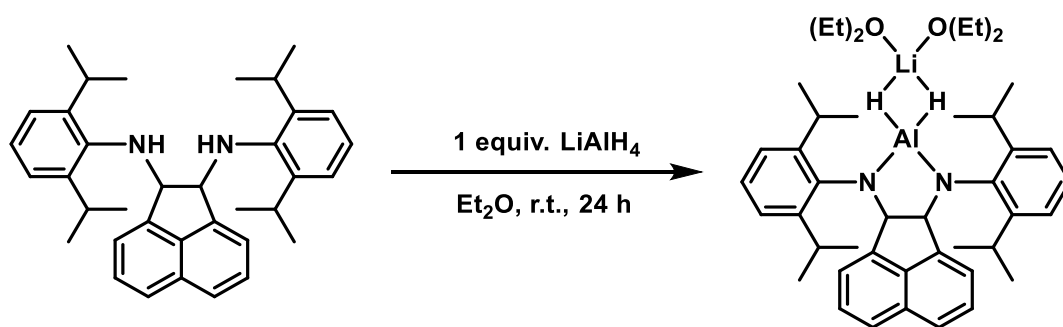
A diethyl ether suspension (50 mL) of *dipp*<sub>2</sub>BIAN (3.60 g, 7.19 mmol) was added dropwise to a suspension of LiAlH<sub>4</sub> (0.412 g, 10.9 mmol) in diethyl ether (60 mL) at 0 °C and the reaction mixture was stirred for 1 h. The mixture was warmed to room temperature, stirred for additional 3 h and then quenched with 10% aqueous HCl



solution. The mixture was extracted with  $\text{CH}_2\text{Cl}_2$  (3 x 40 mL) and the combined organic layers were dried over  $\text{Na}_2\text{SO}_4$ , filtered and the solvent was removed in vacuo. The residue was purified by flash chromatography using  $\text{CH}_2\text{Cl}_2$ /pentane 3:1 ( $R_f$ -value: 0.40) to give  $\text{dipp}_2\text{BIANH}_4$  as colourless solid.

**$^1\text{H-NMR}$**  (300 MHz,  $\text{CDCl}_3$ ):  $\delta_{\text{H}}$  [ppm] = 7.65 (d,  $J$  = 8.3 Hz, 2H), 7.31 (dd,  $J$  = 8.3, 6.9 Hz, 2H), 7.21 – 7.07 (m, 6H), 6.66 (d,  $J$  = 6.9 Hz, 2H), 5.29 (s, 2H), 4.22 (s, 2H), 3.23 (m, 4H), 1.16 (dd,  $J$  = 15.5, 6.8 Hz, 24H).

### Synthesis of aluminium complex 1



To the solution of  $\text{dipp}_2\text{BIANH}_4$  (0.38 g, 0.75 mmol) in diethyl ether (15 mL) was added  $\text{LiAlH}_4$  (29 mg, 0.75 mmol). The reaction mixture was stirred at room temperature for 12 h. Evaporation of the solvent gave the title compound as a colourless solid material (475 mg, 0.69 mmol, 92%). Single crystals of the title compound were obtained by recrystallization from diethyl ether at  $-20^\circ\text{C}$ .

**$^1\text{H-NMR}$**  (400 MHz,  $\text{C}_6\text{D}_6$ )  $\delta_{\text{H}}$  [ppm] = 7.51 (d,  $J$  = 8.1 Hz, 2H), 7.33 (dd,  $J$  = 7.1, 2.0 Hz, 2H), 7.18–7.29 (m, 6H), 6.98 (d,  $J$  = 6.8 Hz, 2H), 5.70 (s, 2H; N–CH), 4.26–4.38 (m, 2H;  $\text{CH}(\text{CH}_3)_2$ ), 3.89 (br, 2H; Al–H), 3.77–3.89 (m, 2H;  $\text{CH}(\text{CH}_3)_2$ ), 2.81 (q,  $J$  = 7.1 Hz, 8H;  $\text{O}(\text{CH}_2\text{CH}_3)_2$ ), 1.61 (d,  $J$  = 6.9 Hz, 6H;  $\text{CH}(\text{CH}_3)_2$ ), 1.50 (d,  $J$  = 6.7 Hz, 6H;  $\text{CH}(\text{CH}_3)_2$ ), 1.08 (d,  $J$  = 6.9 Hz, 6H;  $\text{CH}(\text{CH}_3)_2$ ), 1.04 (d,  $J$  = 6.8 Hz, 6H;  $\text{CH}(\text{CH}_3)_2$ ), 0.59 (t,  $J$  = 7.1 Hz, 12H;  $\text{O}(\text{CH}_2\text{CH}_3)_2$ );

**$^{13}\text{C-NMR}$**  (101 MHz,  $\text{C}_6\text{D}_6$ )  $\delta_{\text{C}}$  [ppm] = 148.9 (quart. C), 148.8 (quart. C), 148.3 (quart. C), 148.0 (quart. C), 136.8 (quart. C), 132.5 (quart. C).

C), 127.8, 124.6, 123.6, 123.3, 123.1, 120.5, 71.1 (N–CH), 65.6 (O(CH<sub>2</sub>CH<sub>3</sub>)<sub>2</sub>), 28.8 (CH(CH<sub>3</sub>)<sub>2</sub>), 27.7 (CH(CH<sub>3</sub>)<sub>2</sub>), 27.3 (CH(CH<sub>3</sub>)<sub>2</sub>), 26.3 (CH(CH<sub>3</sub>)<sub>2</sub>), 25.4 (CH(CH<sub>3</sub>)<sub>2</sub>), 23.3 (CH(CH<sub>3</sub>)<sub>2</sub>), 14.2 (O(CH<sub>2</sub>CH<sub>3</sub>)<sub>2</sub>).

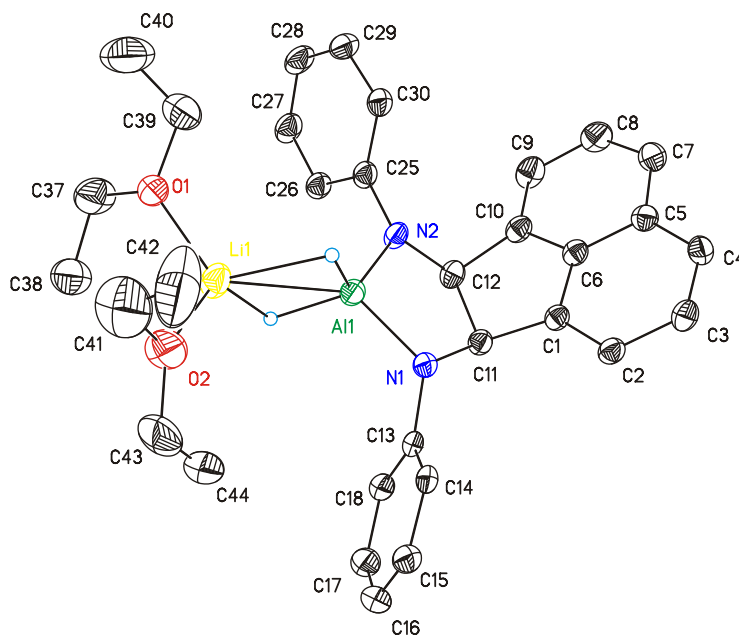
**EA**

Anal. calcd (%) for C<sub>44</sub>H<sub>64</sub>AlLiN<sub>2</sub>O<sub>2</sub>: C, 76.93; H, 9.39; N, 4.08.  
Found: C, 77.76; H, 9.17; N, 4.10.

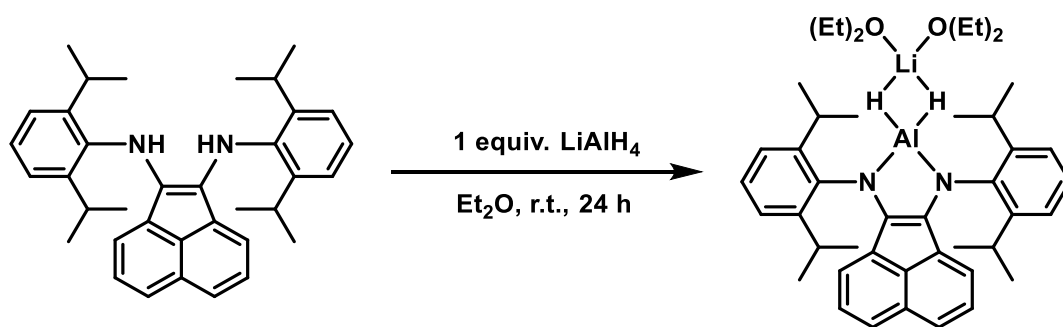
**LIFDI-MS**

(*m/z*) calculated for C<sub>72</sub>H<sub>88</sub>Al<sub>2</sub>Li<sub>4</sub>N<sub>4</sub> [(**1**)<sub>2</sub> - (OEt<sub>2</sub>)<sub>4</sub> + 2Li]: 1090.73,  
found: 1090.84 [*M*]<sup>+</sup>.

**ORTEP diagram** (50% probability level) of the molecular structure of **1** with the atom-numbering scheme. Isopropyl substituents, H atoms of the ligand backbone and of diethylether omitted for clarity:



Selected bond lengths (Å), angles (°): C(11)–C(12) 1.590(3), C(11)–N(1) 1.469(3), C(13)–N(1) 1.425(3), N(1)–Al(1) 1.827(2), Al(1)–H(1AL) 1.57(2), Li(1)–Al(1) 2.649(4), Li(1)–H(1AL) 2.04(2), Li(1)–O(1) 1.940(5); C(13)–N(1)–C(11) 118.27(18), C(11)–N(1)–Al(1) 111.51(14), N(2)–Al(1)–N(1) 92.38(9), N(1)–Al(1)–H(1AL) 120.8(9), N(1)–Al(1)–Li(1) 135.33(12), H(1AL)–Al(1)–H(2AL) 93.7(12), O(1)–Li(1)–H(1AL) 113.4(7), O(2)–Li(1)–O(1) 113.0(2).

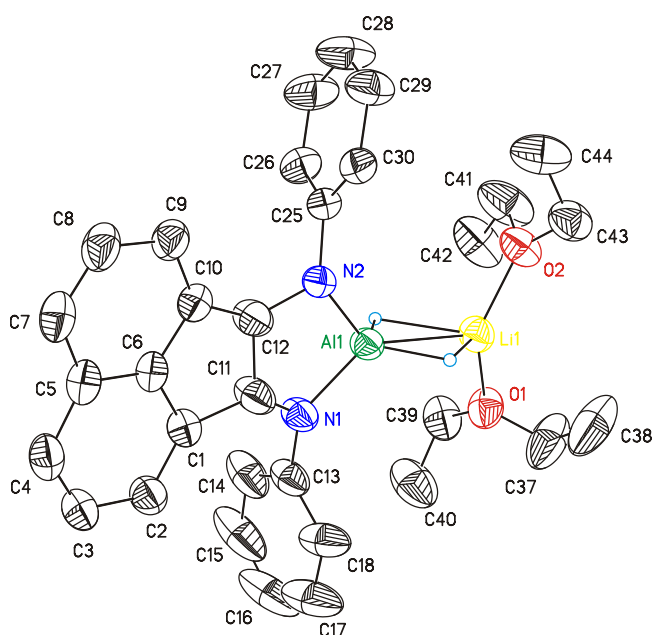
*Synthesis of aluminium complex 2*

To the solution of  $\text{dipp}_2\text{BIANH}_2$  (0.50 g, 0.99 mmol) in diethyl ether (15 mL) was added  $\text{LiAlH}_4$  (38 mg, 1.00 mmol). The reaction mixture was stirred at room temperature for 12 h. All volatiles were removed under reduced pressure and the solid residue was washed with heptane (20 mL). The title compound was obtained as a green solid material (555 mg, 0.81 mmol, 81%). Single crystals of the title compound were obtained by recrystallization from diethyl ether at  $-20^\circ\text{C}$ .

**EA**                      Anal. calcd (%) for  $\text{C}_{44}\text{H}_{62}\text{AlLiN}_2\text{O}_2$ : C, 77.16; H, 9.12; N, 4.09.  
                              Found: C, 77.13; H, 8.75; N, 4.06

**LIFDI-MS**        (m/z) calculated for  $\text{C}_{36}\text{H}_{42}\text{AlLiN}_2$  [**2** -  $(\text{OEt}_2)_2$ ]: 536.33, found: 536.41 [ $M$ ] $^+$ .

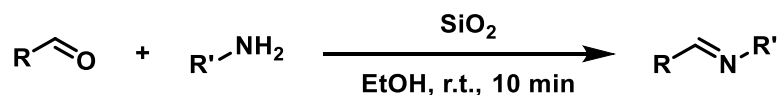
**ORTEP diagram** (50% probability level) of the molecular structure of **2** with the atom-numbering scheme. Isopropyl substituents, H atoms of the ligand backbone and of diethylether omitted for clarity:



Selected bond lengths (Å), angles (°): C(11)-C(12) 1.429(4), C(11)-N(1) 1.397(3), C(13)-N(1) 1.418(3) N(1)-Al(1) 1.842(2), Al(1)-H(1AL) 1.56(3), Li(1)-H(1AL) 2.01(3), Li(1)-Al(1) 2.608(5), O(1)-Li(1) 1.898(5); C(11)-N(1)-C(13) 122.3(2), C(11)-N(1)-Al(1) 105.73(16), N(1)-Al(1)-N(2) 92.61(9), N(1)-Al(1)-H(1AL) 113.7(10), N(1)-Al(1)-Li(1) 132.70(12), H(1AL)-Al(1)-H(2AL) 98.7(14), O(1)-Li(1)-H(1AL) 104.4(8), O(1)-Li(1)-O(2) 129.3(3).

Crystal and intensity collection data for	<b>2</b>	<b>1</b>
Chemical formula	C <sub>44</sub> H <sub>62</sub> AlLiN <sub>2</sub> O <sub>2</sub>	C <sub>44</sub> H <sub>64</sub> AlLiN <sub>2</sub> O <sub>2</sub>
Formula weight	684.87	686.89
Temperature / K	123.00	122.99
Wavelength / Å	1.54184	0.71073
Crystal system, space group	monoclinic, P2 <sub>1/n</sub>	monoclinic, P2 <sub>1/n</sub>
<i>a</i> / Å	11.0627(5)	12.0961(4)
<i>b</i> / Å	17.8984(11)	20.0272(7)
<i>c</i> / Å	21.6065(10)	18.2501(7)
$\alpha$ / Å	90	90
$\beta$ / Å	95.684(4)	106.957(4)
$\gamma$ / Å	90	90
<i>V</i> / Å <sup>3</sup>	4257.2(4)	4228.9(3)
$\rho_{\text{calcd}}$ / g·cm <sup>-3</sup>	1.069	1.079
<i>F</i> (000)	1488	1496
Crystal size / mm	0.24 x 0.19 x 0.05	0.26 x 0.16 x 0.04
<i>Z</i>	4	4
Max. and min. transmission	0.994, 0.970	0.997, 0.988
$\mu$ / mm <sup>-1</sup>	0.674	0.083
$\theta$ / °	4.112-73.599	3.267-27.996
Index ranges	-13 ≤ <i>h</i> ≤ 13 -22 ≤ <i>k</i> ≤ 19 -26 ≤ <i>l</i> ≤ 18	-15 ≤ <i>h</i> ≤ 14 -23 ≤ <i>k</i> ≤ 24 -23 ≤ <i>l</i> ≤ 21
Total / unique reflections	22786 / 8357	25660 / 9049
Data / restraints / parameters	8357 / 84 / 477	9049 / 0 / 468
<i>R</i> <sub>int</sub>	0.0409	0.0575
<i>R</i> <sub>1</sub> , <i>wR</i> <sub>2</sub> [≥2σ( <i>I</i> )]	0.0659, 0.1645	0.0663, 0.1563
<i>R</i> <sub>1</sub> , <i>wR</i> <sub>2</sub> (all data)	0.1023, 0.1928	0.1067, 0.1810
Goodness-of-fit <i>S</i> on <i>F</i> <sup>2</sup>	1.018	1.035
Largest diff. peak and hole / eÅ <sup>-3</sup>	0.413, -0.276	0.636, -0.482

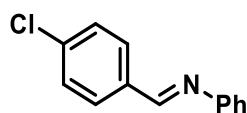
### 2.4.2 Preparation of Imines



The reaction was performed following the procedure of Guzen *et al.*<sup>[33]</sup>

Aldehyde (5 mmol), Aniline (5 mmol) and Silica (1.0 g) were mixed in ethanol (5 mL) and irradiated in the water bath of an ultrasonic cleaner at room temperature for a period of 10 minutes. After completion of the reaction, the mixture was filtered, and the filtrate was evaporated under reduced pressure.

#### 1-(4-chlorophenyl)-*N*-phenylmethanimine



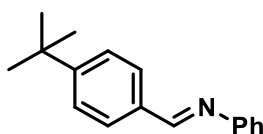
$\text{C}_{13}\text{H}_{10}\text{ClN}$  215.68 g/mol

**$^1\text{H}$  NMR** (300 MHz, Chloroform-*d*)  $\delta$  8.44 (s, 1H), 8.05 – 7.76 (m, 2H), 7.54 – 7.35 (m, 4H), 7.34 – 7.16 (m, 3H).

**GC-MS** (EI, 70 eV, *m/z*): 215 [ $\text{M}$ ]<sup>+</sup>, 180, 152, 125, 104, 91, 77, 51.

The data corresponds to the literature values.<sup>[34]</sup>

#### 1-(4-(*tert*-butyl)phenyl)-*N*-phenylmethanimine

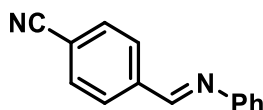


$\text{C}_{17}\text{H}_{19}\text{N}$  237.35 g/mol

**$^1\text{H}$  NMR** (300 MHz, Chloroform-*d*)  $\delta$  8.35 (s, 1H), 7.82 – 7.69 (m, 2H), 7.47 – 7.37 (m, 2H), 7.38 – 7.25 (m, 2H), 7.21 – 7.06 (m, 3H), 1.28 (s, 9H).

**GC-MS** (EI, 70 eV, *m/z*): 237 [ $\text{M}$ ]<sup>+</sup>, 222, 206, 180, 147, 133, 119, 104, 91, 77.

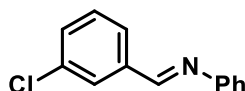
The data corresponds to the literature values.<sup>[35]</sup>

**4-((phenylimino)methyl)benzonitrile**C<sub>14</sub>H<sub>10</sub>N<sub>2</sub> 206.25 g/mol

**<sup>1</sup>H NMR** (300 MHz, Chloroform-*d*) δ 8.52 (s, 1H), 8.03 (d, *J* = 8.3 Hz, 2H), 7.78 (d, *J* = 8.4 Hz, 2H), 7.50 – 7.36 (m, 2H), 7.36 – 7.18 (m, 3H).

**GC-MS** (EI, 70 eV, *m/z*): 206 [M]<sup>+</sup>, 178, 153, 117, 104, 77, 65, 51.

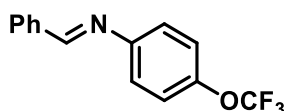
The data corresponds to the literature values.<sup>[36]</sup>

**1-(3-chlorophenyl)-*N*-phenylmethanimine**C<sub>13</sub>H<sub>10</sub>ClN 215.68 g/mol

**<sup>1</sup>H NMR** (300 MHz, Chloroform-*d*) δ 8.33 (s, 1H), 7.86 (t, *J* = 1.8 Hz, 1H), 7.66 (dt, *J* = 7.1, 1.6 Hz, 1H), 7.44 – 7.26 (m, 4H), 7.24 – 7.07 (m, 3H).

**GC-MS** (EI, 70 eV, *m/z*): 215 [M]<sup>+</sup>, 180, 152, 125, 91, 77, 65, 51.

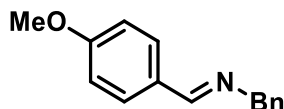
The data corresponds to the literature values.<sup>[36]</sup>

**1-phenyl-*N*-(4-(trifluoromethoxy)phenyl)methanimine**C<sub>14</sub>H<sub>10</sub>F<sub>3</sub>NO 265.24 g/mol

**<sup>1</sup>H NMR** (300 MHz, Chloroform-*d*) δ 8.33 (s, 1H), 7.86 (t, *J* = 1.8 Hz, 1H), 7.66 (dt, *J* = 7.1, 1.6 Hz, 1H), 7.44 – 7.26 (m, 4H), 7.24 – 7.07 (m, 3H).

**GC-MS** (EI, 70 eV, m/z): 265 [M]<sup>+</sup>, 196, 167, 141, 115, 91, 69, 51.

***N*-benzyl-1-(4-methoxyphenyl)methanimine**



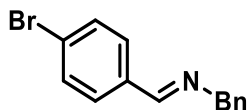
C<sub>15</sub>H<sub>15</sub>NO 225.29 g/mol

**<sup>1</sup>H NMR** (300 MHz, Chloroform-*d*) δ 8.25 (t, *J* = 1.4 Hz, 1H), 7.68 – 7.63 (m, 2H), 7.26 (d, *J* = 4.1 Hz, 4H), 7.21 – 7.16 (m, 1H), 6.88 – 6.83 (m, 2H), 4.72 (d, *J* = 1.4 Hz, 2 H), 3.77 (s, 3H).

**GC-MS** (EI, 70 eV, m/z): 225 [M]<sup>+</sup>, 194, 134, 117, 91.

The data corresponds to the literature values.<sup>[37]</sup>

***N*-benzyl-1-(4-bromophenyl)methanimine**

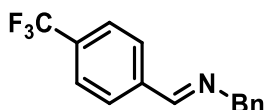


C<sub>14</sub>H<sub>12</sub>BrN 274.16 g/mol

**<sup>1</sup>H NMR** (300 MHz, Chloroform-*d*) δ 8.27 (t, *J* = 1.5 Hz, 1H), 7.61 – 7.55 (m, 2H), 7.51 – 7.45 (m, 2H), 7.32 – 7.19 (m, 5H), 4.74 (d, *J* = 1.4 Hz, 2H).

**<sup>13</sup>C NMR** (75 MHz, CDCl<sub>3</sub>) δ 160.6, 139.0, 135.1, 131.8, 129.7, 128.6, 128.0, 127.1, 125.2, 65.04.

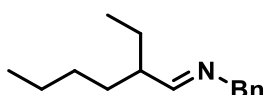
**GC-MS** (EI, 70 eV, m/z): 274 [M]<sup>+</sup>, 155, 117, 105, 91, 79, 77.

***N*-benzyl-1-(4-(trifluoromethyl)phenyl)methanimine**C<sub>15</sub>H<sub>12</sub>F<sub>3</sub>N 263.26 g/mol

**<sup>1</sup>H NMR** (300 MHz, Chloroform-*d*) δ 8.37 (t, *J* = 1.5 Hz, 1H), 7.83 (d, *J* = 8.1 Hz, 2H), 7.60 (d, *J* = 8.2 Hz, 2H), 7.33 – 7.20 (m, 5H), 4.79 (d, *J* = 1.4 Hz, 2H).

**GC-MS** (EI, 70 eV, *m/z*): 263 [M]<sup>+</sup>, 195, 172, 159, 104, 91, 77.

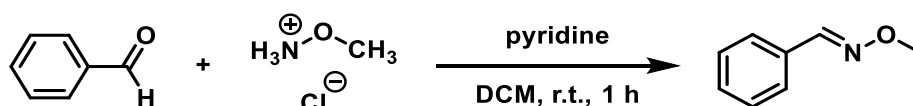
The data corresponds to the literature values.<sup>[38]</sup>

***N*-benzyl-2-ethylhexan-1-imine**C<sub>15</sub>H<sub>23</sub>N 217.36 g/mol

**<sup>1</sup>H NMR** (300 MHz, Chloroform-*d*) δ 7.47 (dt, *J* = 6.8, 1.4 Hz, 1H), 7.29 – 7.13 (m, 5H), 4.51 (d, *J* = 1.3 Hz, 2H), 2.20 – 2.04 (m, 1H), 1.50 – 1.14 (m, 8H), 0.91 – 0.74 (m, 6H).

**<sup>13</sup>C NMR** (75 MHz, CDCl<sub>3</sub>) δ 170.4, 139.5, 128.4, 127.8, 126.8, 66.1, 46.7, 31.9, 29.4, 25.4, 22.8, 14.0, 11.7.

**GC-MS** (EI, 70 eV, *m/z*): 217 [M]<sup>+</sup>, 188, 174, 160, 146, 118, 91.

**Benzaldehyde *O*-methyl oxime**

The reaction was performed following the procedure of Dubost *et al.*<sup>[39]</sup>

Benzaldehyde (1.06 g, 10.0 mmol) was added to a mixture of *O*-methylhydroxylamine-hydrochloride (1.00 g, 12.0 mmol) and pyridine (0.98 g, 40 mmol) in 30 mL



dichloromethane (DCM). After stirring for 1 hour at room temperature, the solvent was removed in vacuo. The residue was dissolved in a small amount of DCM and filtered over silica. DCM was distilled off to give a colorless liquid.

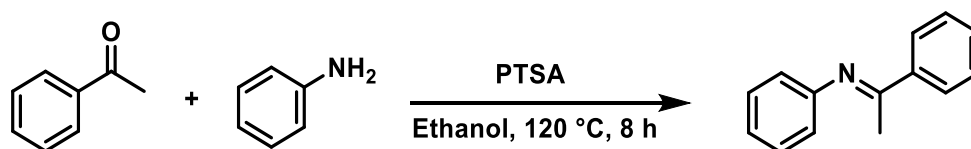
**<sup>1</sup>H NMR** (300 MHz, Chloroform-*d*) δ 7.98 (s, 1H), 7.52 – 7.45 (m, 2H), 7.31 – 7.24 (m, 3H), 3.89 (s, 3H).

**<sup>13</sup>C NMR** (75 MHz, CDCl<sub>3</sub>) δ 148.6, 132.2, 129.8, 128.7, 123.7, 62.0.

**GC-MS** (EI, 70 eV, *m/z*): 135 [M]<sup>+</sup>, 104, 77.

The data corresponds to the literature values.<sup>[39]</sup>

### ***N*,1-diphenylethan-1-imine**



The reaction was performed following the procedure of Barluenga *et al.*<sup>[40]</sup>

Acetophenone (3.60 g, 30 mmol) was dissolved in 20 mL dry Toluene. Aniline (2.79 g, 30 mmol) and *p*-toluenesulfonic acid monohydrate (57.0 mg, 0.3 mmol) were added. The mixture was refluxing for 8 hours in a dean stark apparatus. When no more water was evolving, the reaction was allowed to cool to room temperature and the solvent was distilled off. The residue was mixed with pentane and cooled to 8 °C. The product crystallized as yellow solid.

**<sup>1</sup>H NMR** (300 MHz, Chloroform-*d*) δ 7.94 – 7.86 (m, 2H), 7.42 – 7.33 (m, 3H), 7.31 – 7.23 (m, 2H), 7.05 – 6.97 (m, 1H), 6.75 – 6.70 (m, 2H), 2.16 (s, 3H).

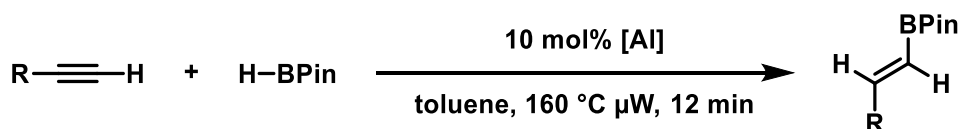
**<sup>13</sup>C NMR** (75 MHz, CDCl<sub>3</sub>) δ 165.5, 151.7, 139.5, 129.0, 128.4, 127.2, 123.2, 119.4, 17.4.

**GC-MS** (EI, 70 eV, *m/z*): 195 [M]<sup>+</sup>, 180, 118, 103, 77.

The data corresponds to the literature values.<sup>[40]</sup>

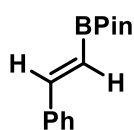
### 2.4.3 Catalytic Reactions

#### Hydroboration reactions

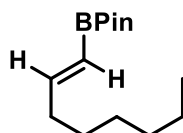


The reaction was performed following a modified procedure of Bismuto *et al.*<sup>[24]</sup>

Under argon atmosphere the aluminium catalyst (10 mol%) and 1,3,5-trimethoxybenzene standard for quantitative NMR (0.25 mg, 0.15 mmol) were weighed in a microwave glass vial and dissolved in toluene (2.0 mL). To this was added pinacolborane (0.6 mmol) and the alkyne (0.5 mmol). The reaction was performed in the microwave at 160 °C for 12 minutes. The solvent was removed in vacuo and NMR samples were measured in C<sub>6</sub>D<sub>6</sub> to determine the yield by quantitative <sup>1</sup>H-NMR spectroscopy.

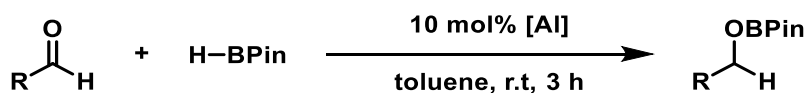


**<sup>1</sup>H-NMR** (300 MHz, C<sub>6</sub>D<sub>6</sub>):  $\delta$  [ppm] = 7.77 (d,  $J$  = 18.4 Hz, 1H), 7.35 – 7.30 (m, 2H), 7.06 – 6.97 (m, 3H), 6.46 (d,  $J$  = 18.4 Hz, 1H), 1.13 (s, 12H).



**<sup>1</sup>H-NMR** (300 MHz, CDCl<sub>3</sub>):  $\delta$  [ppm] = 6.63 (dt,  $J$  = 18.0, 6.4 Hz, 1H), 5.42 (dt,  $J$  = 18.0, 1.6 Hz, 1H), 2.20 – 2.08 (m, 2H), 1.50 – 1.39 (m, 2H), 1.39 – 1.28 (m, 4H), 1.26 (s, 12H), 1.24 (d,  $J$  = 1.6 Hz, 2H), 0.90-0.85 (m, 3H).

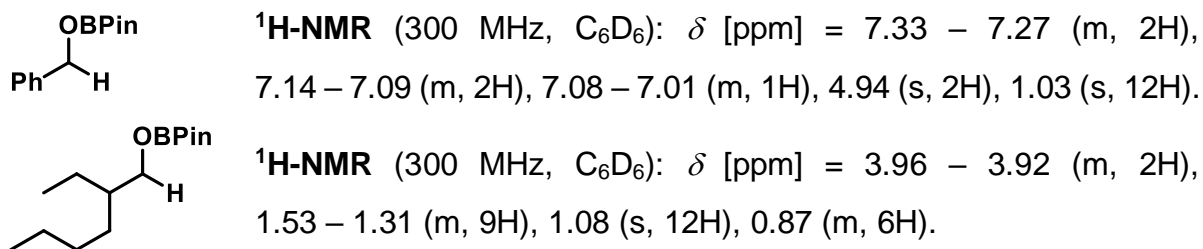
The data corresponds to the literature values.<sup>[24]</sup>



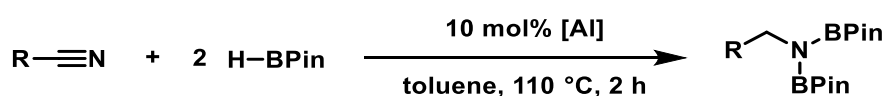
The reaction was performed following a modified procedure of Pollard *et al.*<sup>[25]</sup>

Under argon atmosphere the aluminium catalyst (10 mol%) and 1,3,5-trimethoxybenzene standard for quantitative NMR (0.25 mg, 0.15 mmol) were weighed in a flask and dissolved in toluene (2.0 mL). To this was added pinacolborane (0.6 mmol) and the aldehyde (0.5 mmol). The reaction was stirred at room temperature for

3 hours. The solvent was removed in vacuo and NMR samples were measured in C<sub>6</sub>D<sub>6</sub> to determine the yield by quantitative <sup>1</sup>H-NMR spectroscopy.

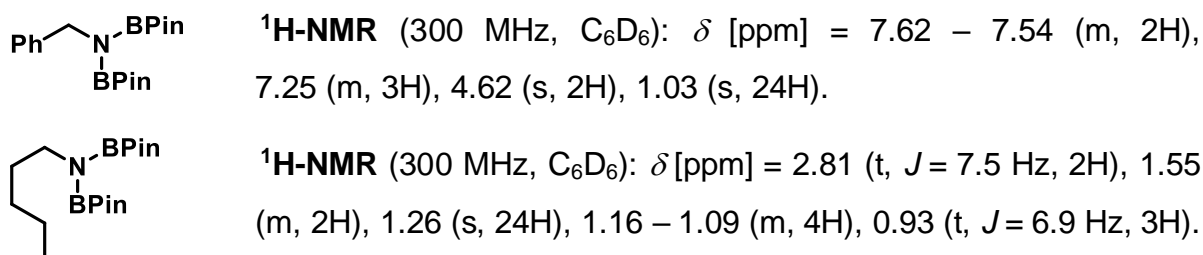


The data corresponds to the literature values.<sup>[25]</sup>

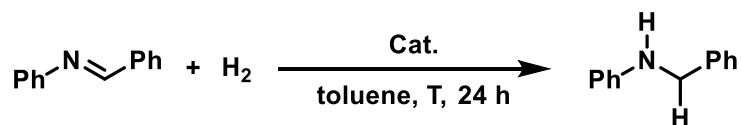


The reaction was performed following a modified procedure of Harinath *et al.*<sup>[26]</sup>

Under argon atmosphere the aluminium catalyst (10 mol%) and 1,3,5-trimethoxybenzene standard for quantitative NMR (0.25 mg, 0.15 mmol) were weighed in a microwave glass vial and dissolved in toluene (2.0 mL). To this was added pinacolborane (1.2 mmol) and the nitrile (0.5 mmol). The reaction was performed in the microwave at 110° C for 2 hours. The solvent was removed in vacuo and NMR samples were measured in C<sub>6</sub>D<sub>6</sub> to determine the yield by quantitative <sup>1</sup>H-NMR spectroscopy.



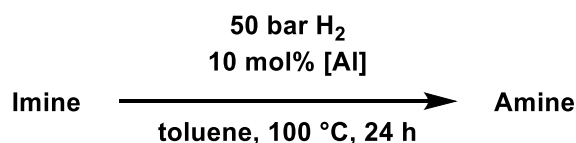
The data corresponds to the literature values.<sup>[26]</sup>

*Imine Hydrogenations*

**Optimization procedure:** Under argon atmosphere imine (0.250 mmol) and the aluminium catalyst (10 mol%) was weighed in an autoclave vial and dissolved in toluene (0.15 mL). The imine/catalyst solution was thoroughly mixed, the septum of the vial was penetrated with a needle and the vial was put into an autoclave. The reactor was sealed and attached to a thoroughly purged hydrogen gas line. The reactor was put under 47 atm. H<sub>2</sub>, and heated to 100 °C (final pressure 50 atm. H<sub>2</sub>) for 24 h while the solution is rigorously stirred. The reaction was quenched with water (1 mL), extracted with EtOAc and the organic phase was dried over NaSO<sub>4</sub>. Conversions and yields were determined by quantitative GC-FID vs. *n*-pentadecane as internal standard.

Entry	Cat. (mol%)	T [°C]	H <sub>2</sub> [bar]	Yield [%] <sup>[a]</sup>
1	<b>2</b> (10)	100	100	>95
2	<b>2</b> (5)	100	100	73
3	<b>2</b> (3)	100	100	50
4	<b>2</b> (1)	100	100	9
<b>5</b>	<b>2</b> ( <b>10</b> )	<b>100</b>	<b>50</b>	<b>&gt;95</b> (65 <sup>[b]</sup> )
6	<b>2</b> (10)	70	50	38
7	<b>2</b> (10)	100	30	55
8	DiBAI-H (10)	100	100	94
9	DiBAI-H (10)	100	50	36
10	TiBAI (10)	100	50	19
11	Et <sub>3</sub> Al (10)	100	50	12
12	TrioctylAl (10)	100	50	21
13	Li[(tBuO) <sub>3</sub> AlH] (10)	100	50	9
14	LiAlH <sub>4</sub> (10)	100	50	22
15	LiAlH <sub>4</sub> (10) + dippBIANH <sub>2</sub> (10)	100	50	29
16	LiAlH <sub>4</sub> (10) + Et <sub>2</sub> O (30)	100	50	56
17	LiAlH <sub>4</sub> (10) + dippBIANH <sub>2</sub> (10) + Et <sub>2</sub> O (30)	100	50	>95

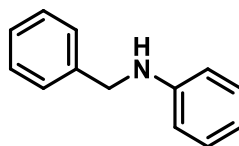
<sup>[a]</sup> Yields were determined by quantitative GC-FID vs. internal *n*-C<sub>15</sub>H<sub>32</sub>. <sup>[b]</sup> 0.75 mL of solvent were used.



**General procedure:** Under argon atmosphere imine (0.250 mmol) and the aluminium catalyst **2** (10 mol%, 17 mg) was weighed in an autoclave vial and dissolved in toluene (0.15 mL). The imine/catalyst solution was thoroughly mixed, the septum of the vial was penetrated with a needle and the vial was put into an autoclave. The reactor was sealed and attached to a thoroughly purged hydrogen gas line. The reactor was put under 47 atm. H<sub>2</sub>, and heated to 100 °C (final pressure 50 atm. H<sub>2</sub>) for 24 h while the solution is rigorously stirred. The reaction was quenched with water (1 mL), extracted with Et<sub>2</sub>O (3 x 1 mL) and the combined organic phases were dried over NaSO<sub>4</sub>. The drying agent was filtered off and the clear solution was treated with HCl (1 mL, 1.0 M in Et<sub>2</sub>O) and the protonated amine was collected via filtration.

### ***N*-benzylaniline**

Treated with 1.0 M HCl in Et<sub>2</sub>O for isolation. NMR measured of protonated form.



C<sub>13</sub>H<sub>13</sub>N 183.25 g/mol

**<sup>1</sup>H NMR** (300 MHz, Methanol-*d*<sub>4</sub>) δ 7.40 – 7.18 (m, 5H), 7.13 – 7.02 (m, 2H), 6.71 – 6.51 (m, 3H), 4.31 (s, 2H).

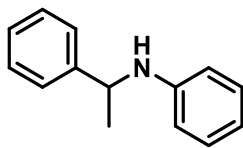
**<sup>13</sup>C NMR** (75 MHz, MeOD) δ 150.08, 141.51, 129.90, 129.38, 128.34, 127.77, 117.93, 114.11, 48.76.

**GC-MS** (EI, 70 eV, *m/z*): 183 [M]<sup>+</sup>, 106, 91, 65, 51.

The data is identical to a commercially available sample and corresponds to the literature values.<sup>[41]</sup>

***N*-(1-phenylethyl)aniline**

Treated with 1.0 M HCl in Et<sub>2</sub>O for isolation. NMR measured of protonated form.



C<sub>14</sub>H<sub>15</sub>N 197.28 g/mol

**<sup>1</sup>H NMR** (300 MHz, Methanol-*d*<sub>4</sub>) δ 7.53 – 7.46 (m, 3H), 7.41 (d, *J* = 1.1 Hz, 5H), 7.33 – 7.26 (m, 2H), 4.81 (q, *J* = 6.9 Hz, 1H), 1.79 (d, *J* = 6.9 Hz, 3H).

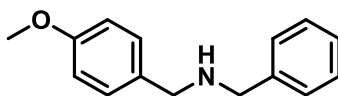
**<sup>13</sup>C NMR** (75 MHz, MeOD) δ 136.87, 131.18, 130.84, 130.24, 129.15, 124.68, 64.63, 18.84.

**GC-MS** (EI, 70 eV, *m/z*): 197 [M]<sup>+</sup>, 182, 152, 120, 105, 93, 77, 66, 51.

The data corresponds to the literature values.<sup>[42]</sup>

***N*-benzyl-1-(4-methoxyphenyl)methanamine**

Treated with 1.0 M HCl in Et<sub>2</sub>O for isolation. NMR measured of protonated form.



C<sub>15</sub>H<sub>17</sub>NO 227.31 g/mol

**<sup>1</sup>H-NMR** (300 MHz, Methanol-*d*<sub>4</sub>) δ 7.55 – 7.38 (m, 7H), 7.09 – 6.97 (m, 2H), 4.21 (d, *J* = 10.2 Hz, 4H), 3.84 (s, 3H).

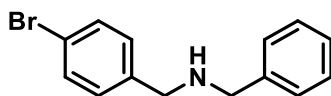
**<sup>13</sup>C-NMR** (75 MHz, MeOD) δ 162.19, 132.67, 132.50, 131.05, 130.67, 130.30, 124.09, 115.57, 55.84, 51.77, 51.62.

**GC-MS** (EI, 70 eV, *m/z*): 227 [M]<sup>+</sup>, 226, 196, 136, 121, 106, 91, 77, 67, 52.

The data corresponds to the literature values.<sup>[43]</sup>

***N*-benzyl-1-(4-bromophenyl)methanamine**

Treated with 1.0 M HCl in Et<sub>2</sub>O for isolation. NMR measured of protonated form.



C<sub>14</sub>H<sub>14</sub>BrN 276.18 g/mol

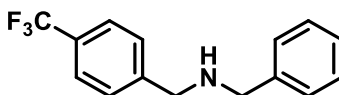
**<sup>1</sup>H-NMR** (300 MHz, Methanol-*d*<sub>4</sub>) δ 7.68 – 7.62 (m, 1H), 7.54 – 7.40 (m, 8H), 4.30 – 4.21 (m, 4H).

**<sup>13</sup>C-NMR** (75 MHz, MeOD) δ 133.44, 133.06, 132.41, 131.69, 131.08, 130.74, 130.33, 52.24, 52.08, 51.38.

**GC-HRMS** (CI, *m/z*): found 276.0388 [M+H]<sup>+</sup> (calculated 276.0382).

***N*-benzyl-1-(4-(trifluoromethyl)phenyl)methanamine**

Treated with 1.0 M HCl in Et<sub>2</sub>O for isolation. NMR measured of protonated form.



C<sub>15</sub>H<sub>14</sub>F<sub>3</sub>N 265.28 g/mol

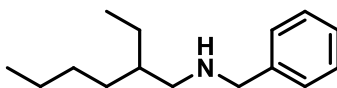
**<sup>1</sup>H-NMR** (300 MHz, Methanol-*d*<sub>4</sub>) δ 7.85 – 7.67 (m, 4H), 7.59 – 7.45 (m, 5H), 4.37 (s, 2H), 4.31 (s, 2H).

**<sup>13</sup>C-NMR** (75 MHz, MeOD) δ 132.30, 131.85, 131.14, 130.82, 130.35, 127.14, 127.09, 52.46, 51.40.

**GC-HRMS** (CI, *m/z*): found 266.1149 [M+H]<sup>+</sup> (calculated 266.1151).

***N*-benzyl-2-ethylhexan-1-amine**

Treated with 1.0 M HCl in Et<sub>2</sub>O for isolation. NMR measured of protonated form.

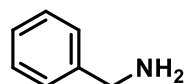


C<sub>15</sub>H<sub>25</sub>N 219.37 g/mol

<b><math>^1\text{H-NMR}</math></b>	(300 MHz, Methanol- $d_4$ ) $\delta$ 7.48 – 7.33 (m, 6H), 4.14 (d, $J$ = 5.1 Hz, 2H), 2.84 (d, $J$ = 6.7 Hz, 2H), 1.61 (h, $J$ = 6.4 Hz, 1H), 1.45 – 1.06 (m, 8H), 0.81 (q, $J$ = 7.4, 6.9 Hz, 6H).
<b><math>^{13}\text{C-NMR}</math></b>	(75 MHz, MeOD) $\delta$ 132.29, 131.24, 130.73, 130.27, 52.74, 51.64, 37.95, 31.35, 29.41, 24.52, 23.87, 14.33, 10.46.
<b>GC-HRMS</b>	(CI, m/z): found 220.2150 $[\text{M}+\text{H}]^+$ (calculated 220.2060).

### Phenylmethanamine

Treated with 1.0 M HCl in Et<sub>2</sub>O for isolation. NMR measured of protonated form.



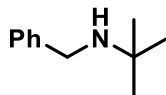
C<sub>7</sub>H<sub>9</sub>N 107.16 g/mol

<b><math>^1\text{H-NMR}</math></b>	(300 MHz, Methanol- $d_4$ ) $\delta$ 7.52 – 7.39 (m, 5H), 4.13 (s, 2H).
<b><math>^{13}\text{C-NMR}</math></b>	(75 MHz, MeOD) $\delta$ 134.47, 130.24, 129.98, 44.37.

The data is identical to a commercially available sample and corresponds to the literature values.<sup>[44]</sup>

### N-benzyl-2-methylpropan-2-amine

Treated with 1.0 M HCl in Et<sub>2</sub>O for isolation. NMR measured of protonated form.



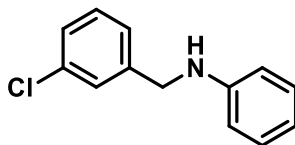
C<sub>11</sub>H<sub>17</sub>N 163.26 g/mol

<b><math>^1\text{H-NMR}</math></b>	(300 MHz, Methanol- $d_4$ ) $\delta$ 7.50 (m, 5H), 4.20 (s, 2H), 1.49 (s, 9H).
<b><math>^{13}\text{C-NMR}</math></b>	(75 MHz, MeOD) $\delta$ 133.09, 131.04, 130.56, 130.31, 58.67, 46.65, 27.66, 25.85.
<b>GC-HRMS</b>	(CI, m/z): found 164.1409 $[\text{M}+\text{H}]^+$ (calculated 164.1434).



***N*-(3-chlorobenzyl)aniline**

Treated with 1.0 M HCl in Et<sub>2</sub>O for isolation. NMR measured of protonated form.

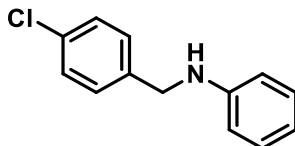


C<sub>13</sub>H<sub>12</sub>ClN 217.70 g/mol

<b><sup>1</sup>H-NMR</b>	(300 MHz, Methanol- <i>d</i> <sub>4</sub> ) δ 7.62 – 7.34 (m, 9H), 4.63 (s, 2H).
<b><sup>13</sup>C-NMR</b>	(75 MHz, MeOD) δ 135.90, 134.32, 131.74, 131.44, 131.33, 130.91, 130.85, 130.32, 129.81, 126.25, 124.08, 123.95, 55.86.
<b>GC-HRMS</b>	(CI, <i>m/z</i> ): found 218.0729 [M+H] <sup>+</sup> (calculated 218.0731).

***N*-(4-chlorobenzyl)aniline**

Treated with 1.0 M HCl in Et<sub>2</sub>O for isolation. NMR measured of protonated form.



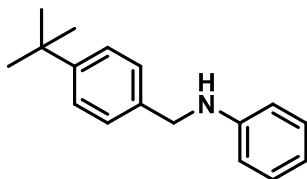
C<sub>13</sub>H<sub>12</sub>ClN 217.70 g/mol

<b><sup>1</sup>H-NMR</b>	(300 MHz, Methanol- <i>d</i> <sub>4</sub> ) δ 7.64 – 7.34 (m, 9H), 4.63 (s, 2H).
<b><sup>13</sup>C-NMR</b>	(75 MHz, MeOD) δ 136.94, 133.16, 131.43, 131.33, 130.87, 130.28, 124.05, 55.86.
<b>GC-MS</b>	(EI, 70 eV, <i>m/z</i> ): 217 [M] <sup>+</sup> , 182, 125, 90, 77, 65, 51.

The data corresponds to the literature values.<sup>[41]</sup>

***N*-(4-(tert-butyl)benzyl)aniline**

Treated with 1.0 M HCl in Et<sub>2</sub>O for isolation. NMR measured of protonated form.



C<sub>17</sub>H<sub>21</sub>N 239.36 g/mol

**<sup>1</sup>H-NMR** (300 MHz, Methanol-*d*<sub>4</sub>) δ 7.61 – 7.52 (m, 3H), 7.52 – 7.46 (m, 2H), 7.46 – 7.40 (m, 2H), 7.40 – 7.35 (m, 2H), 4.58 (s, 2H), 1.34 (s, 9H).

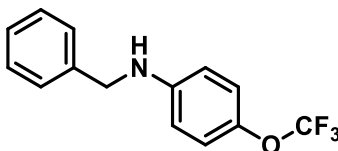
**<sup>13</sup>C-NMR** (75 MHz, MeOD) δ 152.85, 135.17, 129.95, 129.78, 129.36, 127.68, 125.68, 122.65, 55.29, 34.20, 30.21.

**GC-MS** (EI, 70 eV, *m/z*): 239 [M]<sup>+</sup>, 222, 182, 147, 132, 117, 91, 77, 51.

The data corresponds to the literature values.<sup>[45]</sup>

***N*-benzyl-4-(trifluoromethoxy)aniline**

Treated with 1.0 M HCl in Et<sub>2</sub>O for isolation. NMR measured of protonated form.



C<sub>14</sub>H<sub>12</sub>F<sub>3</sub>NO 267.25 g/mol

**<sup>1</sup>H-NMR** (300 MHz, Methanol-*d*<sub>4</sub>) δ 7.44 (m, 9H), 4.61 (s, 2H).

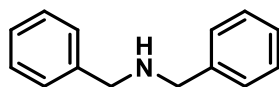
**<sup>13</sup>C-NMR** (75 MHz, MeOD) δ 135.99, 132.42, 131.21, 130.80, 130.23, 125.57, 123.83, 56.39.

**GC-MS** (EI, 70 eV, *m/z*): 267 [M]<sup>+</sup>, 190, 176, 161, 139, 115, 91, 81, 68, 63.

The data corresponds to the literature values.<sup>[46]</sup>

**Dibenzylamine**

Treated with 1.0 M HCl in Et<sub>2</sub>O for isolation. NMR measured of protonated form.



C<sub>14</sub>H<sub>15</sub>N 197.28 g/mol

**<sup>1</sup>H-NMR** (300 MHz, Methanol-*d*<sub>4</sub>) δ 7.56 – 7.43 (m, 10H), 4.26 (s, 4H).

**<sup>13</sup>C-NMR** (75 MHz, MeOD) δ 132.40, 131.09, 130.73, 130.32, 52.06.

**GC-HRMS** (CI, *m/z*): found 198.1288 [M+H]<sup>+</sup> (calculated 198.1277).

***N*-methyl-1-phenylmethanamine**

Treated with 1.0 M HCl in Et<sub>2</sub>O for isolation. NMR measured of protonated form.



C<sub>8</sub>H<sub>11</sub>N 121.18 g/mol

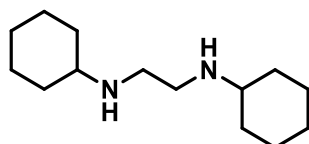
**<sup>1</sup>H-NMR** (300 MHz, Methanol-*d*<sub>4</sub>) δ 7.57 – 7.41 (m, 5H), 4.21 (s, 2H), 2.74 (s, 3H).

**<sup>13</sup>C-NMR** (75 MHz, MeOD) δ 132.55, 130.89, 130.73, 130.32, 53.62, 33.12.

**GC-HRMS** (CI, *m/z*): found 122.0966 [M+H]<sup>+</sup> (calculated 122.0964).

***N*<sup>1</sup>,*N*<sup>2</sup>-dicyclohexylethane-1,2-diamine**

Treated with 1.0 M HCl in Et<sub>2</sub>O for isolation. NMR measured of protonated form.

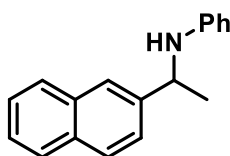


C<sub>14</sub>H<sub>28</sub>N<sub>2</sub> 224.39 g/mol

<b><sup>1</sup>H-NMR</b>	(300 MHz, Methanol- <i>d</i> <sub>4</sub> ) δ 3.42 (s, 4H), 3.28 – 3.11 (m, 2H), 2.18 (m, 4H), 2.01 – 1.85 (m, 4H), 1.75 (d, <i>J</i> = 12.5 Hz, 2H), 1.44 (m, 10H).
<b><sup>13</sup>C-NMR</b>	(75 MHz, D <sub>2</sub> O) δ 57.94, 40.02, 28.70, 24.33, 23.78.
<b>GC-HRMS</b>	(CI, <i>m/z</i> ): found 225.2357 [M+H] <sup>+</sup> (calculated 225.2325).

### ***N*-(1-(naphthalen-2-yl)ethyl)aniline**

Treated with 1.0 M HCl in Et<sub>2</sub>O for isolation. NMR measured of protonated form.



C<sub>18</sub>H<sub>17</sub>N 247.34 g/mol

<b><sup>1</sup>H-NMR</b>	(300 MHz, Methanol- <i>d</i> <sub>4</sub> ) δ 8.02 – 7.80 (m, 4H), 7.64 – 7.26 (m, 8H), 5.01 (q, <i>J</i> = 6.9 Hz, 1H), 1.90 (d, <i>J</i> = 6.9 Hz, 3H).
<b><sup>13</sup>C-NMR</b>	(75 MHz, MeOD) δ 135.22, 135.10, 134.48, 133.93, 131.20, 131.02, 130.22, 129.39, 129.18, 128.80, 128.28, 127.96, 125.49, 124.83, 64.94, 18.85.
<b>GC-MS</b>	(EI, 70 eV, <i>m/z</i> ): 247 [M] <sup>+</sup> , 232, 155, 127, 93, 77.

The data correspond to the literature values.<sup>[47]</sup>

## 2.5 References

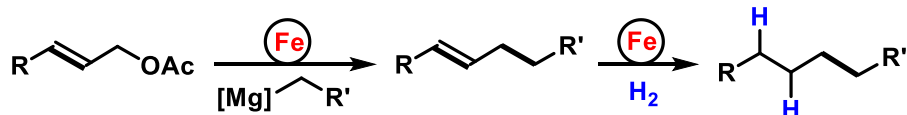
- [1] G. I. Nikonov, *ACS Catal.* **2017**, *7*, 7257–7266.
- [2] W. Li, X. Ma, M. G. Walawalkar, Z. Yang, H. W. Roesky, *Coord. Chem. Rev.* **2017**, *350*, 14–29.
- [3] G. Szigethy, A. F. Heyduk, *Dalton Trans.* **2012**, *41*, 8144–8152.
- [4] B. E. Cole, J. P. Wolbach, W. G. Dougherty, N. A. Piro, W. S. Kassel, C. R. Graves, *Inorg. Chem.* **2014**, *53*, 3899–3906.
- [5] L. A. Berben, *Chem. Eur. J.* **2015**, *21*, 2734–2742.
- [6] I. L. Fedushkin, M. V. Moskalev, A. N. Lukoyanov, A. N. Tishkina, E. V. Baranov, G. A. Abakumov, *Chem. Eur. J.* **2012**, *18*, 11264–11276.
- [7] W. Uhl, F. Breher, A. Mbonimana, J. Gauss, D. Haase, A. Lützen, W. Saak, *Eur. J. Inorg. Chem.* **2001**, *2001*, 3059–3066.
- [8] A. Stasch, M. Ferbinteanu, J. Prust, W. Zheng, F. Cimpoesu, H. W. Roesky, J. Magull, H.-G. Schmidt, M. Noltemeyer, *J. Am. Chem. Soc.* **2002**, *124*, 5441–5448.
- [9] N. D. Reddy, H. W. Roesky, M. Noltemeyer, H.-G. Schmidt, *Inorg. Chem.* **2002**, *41*, 2374–2378.
- [10] S. S. Kumar, J. Rong, S. Singh, H. W. Roesky, D. Vidovic, J. Magull, D. Neculai, V. Chandrasekhar, M. Baldus, *Organometallics* **2004**, *23*, 3496–3500.
- [11] V. G. Sokolov, T. S. Koptseva, M. V. Moskalev, A. V. Piskunov, M. A. Samsonov, I. L. Fedushkin, *Russ. Chem. Bull.* **2017**, *66*, 1569–1579.
- [12] I. L. Fedushkin, V. M. Makarov, V. G. Sokolov, G. K. Fukin, M. O. Maslov, S. Y. Ketkov, *Russ. Chem. Bull.* **2014**, *63*, 870–882.
- [13] D. A. Razborov, A. N. Lukoyanov, V. M. Makarov, M. A. Samsonov, I. L. Fedushkin, *Russ. Chem. Bull.* **2015**, *64*, 2377–2385.
- [14] V. G. Sokolov, T. S. Koptseva, M. V. Moskalev, N. L. Bazyakina, A. V. Piskunov, A. V. Cherkasov, I. L. Fedushkin, *Inorg. Chem.* **2017**, *56*, 13401–13410.
- [15] I. L. Fedushkin, A. A. Skatova, N. L. Bazyakina, V. A. Chudakova, N. M. Khvoinova, A. S. Nikipelov, O. V. Eremenko, A. V. Piskunov, G. K. Fukin, K. A. Lyssenko, *Russ. Chem. Bull.* **2013**, *62*, 1815–1828.
- [16] V. G. Sokolov, T. S. Koptseva, V. A. Dodonov, R. V. Rummyantsev, I. L. Fedushkin, *Russ. Chem. Bull.* **2018**, *67*, 2164–2171.
- [17] I. L. Fedushkin, A. A. Skatova, V. A. Chudakova, G. K. Fukin, *Angew. Chem. Int. Ed.* **2003**, *42*, 3294–3298.
- [18] I. L. Fedushkin, A. A. Skatova, V. A. Chudakova, G. K. Fukin, S. Dechert, H. Schumann, *Eur. J. Inorg. Chem.* **2003**, *2003*, 3336–3346.
- [19] M. Viganò, F. Ferretti, A. Caselli, F. Ragaini, M. Rossi, P. Mussini, P. Macchi, *Chem. Eur. J.* **2014**, *20*, 14451–14464.
- [20] G. R. Fulmer, A. J. M. Miller, N. H. Sherden, H. E. Gottlieb, A. Nudelman, B. M. Stoltz, J. E. Bercaw, K. I. Goldberg, *Organometallics* **2010**, *29*, 2176–2179.
- [21] S. Nagendran, H. W. Roesky, *Organometallics* **2008**, *27*, 457–492.
- [22] O. V. Kazarina, C. Gourlaouen, L. Karmazin, A. G. Morozov, I. L. Fedushkin, S. Dagorne, *Dalton Trans.* **2018**, *47*, 13800–13808.

- [23] E. Wiberg, N. Wiberg, *Lehrbuch der anorganischen Chemie*, 102. Auflage, Walter de Gruyter, Berlin, New York **2007**.
- [24] A. Bismuto, S. P. Thomas, M. J. Cowley, *Angew. Chem. Int. Ed.* **2016**, *55*, 15356–15359.
- [25] V. A. Pollard, S. A. Orr, R. McLellan, A. R. Kennedy, E. Hevia, R. E. Mulvey, *Chem. Commun.* **2018**, *54*, 1233–1236.
- [26] A. Harinath, J. Bhattacharjee, T. K. Panda, *Adv. Synth. Catal.* **2019**, *361*, 850–857.
- [27] J. A. Hatnean, J. W. Thomson, P. A. Chase, D. W. Stephan, *Chem. Commun.* **2014**, *50*, 301–303.
- [28] H. Elsen, C. Färber, G. Ballmann, S. Harder, *Angew. Chem. Int. Ed.* **2018**, *57*, 7156–7160.
- [29] H. Elsen, J. Langer, M. Wiesinger, S. Harder, *Organometallics* **2020**.
- [30] S. Dastgir, K. S. Coleman, A. R. Cowley, M. L. H. Green, *Organometallics* **2010**, *29*, 4858–4870.
- [31] A. Paulovicova, U. El-Ayaan, K. Shibayama, T. Morita, Y. Fukuda, *Eur. J. Inorg. Chem.* **2001**, *2001*, 2641–2646.
- [32] I. L. Fedushkin, V. A. Chudakova, G. K. Fukin, S. Dechert, M. Hummert, H. Schumann, *Russ. Chem. Bull.* **2004**, *53*, 2744–2750.
- [33] K. P. Guzen, A. S. Guarezemini, A. T.G. Órfão, R. Cella, C. M.P. Pereira, H. A. Stefani, *Tetrahedron Lett.* **2007**, *48*, 1845–1848.
- [34] R. Torregrosa, I. M. Pastor, M. Yus, *Tetrahedron* **2005**, *61*, 11148–11155.
- [35] R. Fertig, T. Irrgang, F. Freitag, J. Zander, R. Kempe, *ACS Catal.* **2018**, *8*, 8525–8530.
- [36] D. Yadav, B. Bhanage, *Synlett* **2014**, *25*, 1611–1615.
- [37] O.-Y. Lee, K.-L. Law, D. Yang, *Org. Lett.* **2009**, *11*, 3302–3305.
- [38] E. C. Volpe, P. T. Wolczanski, E. B. Lobkovsky, *Organometallics* **2010**, *29*, 364–377.
- [39] E. Dubost, C. Fossey, T. Cailly, S. Rault, F. Fabis, *J. Org. Chem.* **2011**, *76*, 6414–6420.
- [40] J. Barluenga, A. Jiménez-Aquino, F. Aznar, C. Valdés, *J. Am. Chem. Soc.* **2009**, *131*, 4031–4041.
- [41] D. B. Bagal, R. A. Watile, M. V. Khedkar, K. P. Dhake, B. M. Bhanage, *Catal. Sci. Technol.* **2012**, *2*, 354–358.
- [42] H. Kato, I. Shibata, Y. Yasaka, S. Tsunoi, M. Yasuda, A. Baba, *Chem. Commun.* **2006**, 4189–4191.
- [43] C. J. Smith, C. D. Smith, N. Nikbin, S. V. Ley, I. R. Baxendale, *Org. Biomol. Chem.* **2011**, *9*, 1927–1937.
- [44] T. D. Nixon, M. K. Whittlesey, J. M.J. Williams, *Tetrahedron Lett.* **2011**, *52*, 6652–6654.
- [45] A. Afanasenko, S. Elangovan, M. C. A. Stuart, G. Bonura, F. Frusteri, K. Barta, *Catal. Sci. Technol.* **2018**, *8*, 5498–5505.
- [46] J. P. Patel, A.-H. Li, H. Dong, V. L. Korlipara, M. J. Mulvihill, *Tetrahedron Lett.* **2009**, *50*, 5975–5977.
- [47] Z. Wang, X. Ye, S. Wei, P. Wu, A. Zhang, J. Sun, *Org. Lett.* **2006**, *8*, 999–1001.

### 3 Iron-Catalyzed Allylation-Hydrogenation Sequences as Masked Alkyl-Alkyl Cross-Couplings

*Fe-catalyzed allylation-hydrogenation:*

= formal *alkyl-alkyl cross-coupling*



**Abstract:** An iron-catalyzed allylation of organomagnesium reagents (alkyl, aryl) with simple allyl acetates proceeds under mild conditions (Fe(OAc)<sub>2</sub> or Fe(acac)<sub>2</sub>, Et<sub>2</sub>O, r.t.) to furnish various alkene and styrene derivatives. Mechanistic studies indicate the operation of a homotopic catalyst. The sequential combination of such iron-catalyzed allylation with an iron-catalyzed hydrogenation results in an overall C(sp<sup>3</sup>)-C(sp<sup>3</sup>)-bond formation that constitutes an attractive alternative to challenging direct cross-coupling protocols with alkyl halides.

50% of the optimization experiments (see Chapter 3.4.2) were part of the Master Thesis “Eisen-katalysierte Kreuzkupplung allylischer Acetate” (“Iron-catalyzed Cross-Coupling of allylic Acetates”) by Josef Bernauer

Reproduced from Josef Bernauer, Guojiao Wu, Axel Jacobi von Wangelin; *RSC Adv.* **2019**, 9, 31217-31223, DOI: 10.1039/c9ra07604b, with permission from The Royal Society of Chemistry. Schemes, tables and text may differ from the published article.

Author contribution: radical clock experiments (see Scheme 3.5) were performed in collaboration with Dr. Guojiao Wu.

### 3.1 Introduction

The development of transition metal-catalyzed cross-coupling reactions has propelled the art of C-C bond formation like no other new methodology in the past decades.<sup>[1,2]</sup> Among them, Pd and Ni catalysts have clearly dominated the field by virtue of their high versatility and chemoselectivity.<sup>[3]</sup> However, noble and toxic metal catalysts (e.g. Pd, Rh, Ir, Ni and Co) exhibit high costs and/or significant levels of toxicity which limit their general applicability under modern sustainability criteria.

Iron-catalyzed cross-coupling reactions have recently been developed to great maturity and now constitute a powerful alternative to the established noble metal systems.<sup>[4–10]</sup> Most protocols utilize organic halides as electrophiles (mostly I, Br); only very few reactions involve activated ester derivatives (triflates, tosylates, phosphonates).<sup>[11–14]</sup> Iron-catalyzed cross-couplings reactions at alkenyl acetates were only recently reported.<sup>[15–17]</sup>

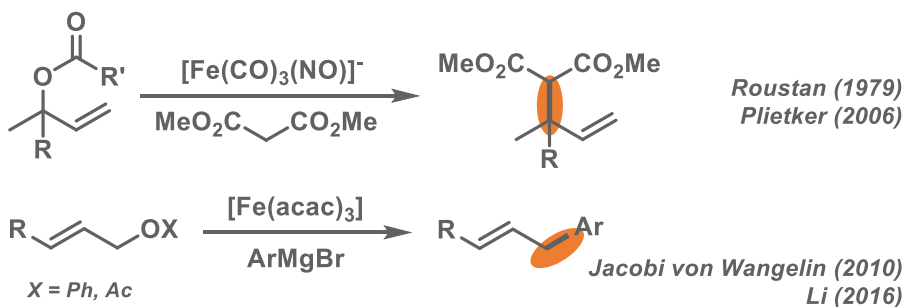
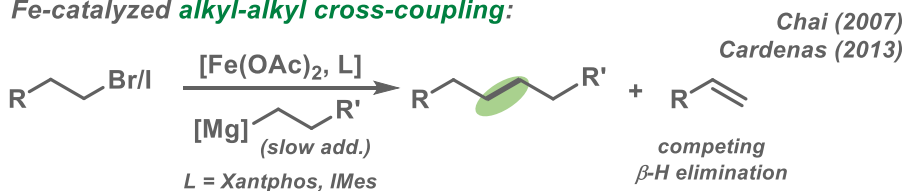
Allyl alcohols constitute one of the most easily accessible class of electrophiles by numerous substitution or reduction methods from abundant starting materials (allyl halides,  $\alpha,\beta$ -unsaturated carbonyls). However, there is no concise report of iron-catalyzed reactions of simple allyl alcohol derivatives with organo-metallic reagents. A handful of iron-catalyzed allylations have been reported.<sup>[18–20]</sup> The Hieber-type salt  $\text{Na}[\text{Fe}(\text{CO})_3(\text{NO})]$  (which is iso-electronic to  $\text{Pd}^0$ ) was especially competent in the catalytic allylation of malonates (Scheme 3.1, top).<sup>[21]</sup> Xu and Zhou later reported similar reactions with the stable tetrabutylammonium salt in a CO atmosphere.<sup>[22]</sup> Plietker *et al.* performed similar reactions in the presence of phosphine ligands that prevented the formation of inactive catalyst derivatives.<sup>[18]</sup> Substitutions of allyl carbonates with *N*-, *O*-, *S*-nucleophiles and stereoselective reactions were reported under such conditions.<sup>[23–26]</sup> Arylations of selected allyl alcohol derivatives with aryl-Grignard reagents have been reported by Li and coworkers and us.<sup>[15,27]</sup>

We envisioned the development of an Fe-catalyzed cross-coupling between alkylmagnesium reagents and diverse allyl acetates that benefits from the intrinsic properties of allyl acetates as activated C-electrophiles and the utility of the pendant alkene moiety for further manipulation. While being a formal  $\text{sp}^3$ -electrophile, allyl-X substrates exhibit strikingly different reactivity patterns than alkyl-electrophiles due to the vicinal alkenyl moiety, the absence of  $\beta$ -hydrogen atoms, and the ability to engage

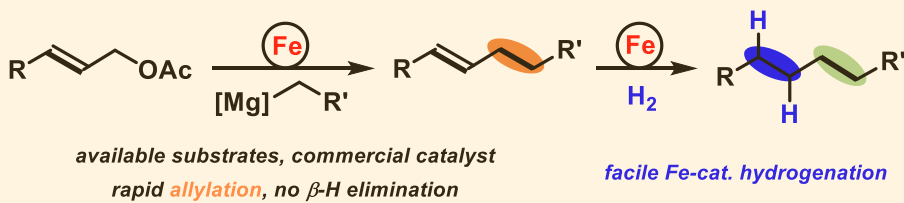


in  $\eta^3$ -coordination to transition metals. In comparison with allyl-X electrophiles, alkyl-X electrophiles exhibit a low propensity to undergo oxidative addition to transition metal complexes, engage in rapid side reactions ( $\beta$ -H elimination, rearrangement), and undergo slow reductive elimination. Consequently, there are very few literature reports on iron-catalyzed alkyl-alkyl cross-couplings which exhibit only moderate yields, limited substrate scope (few examples, alkyl-Br/I), and require special conditions (slow addition over 7 h) and/or expensive ligands (Xantphos, IMes; Scheme 3.1, center).<sup>[28–30]</sup>

We surmised that the combination of an effective allylation reaction with a subsequent hydrogenation reaction would constitute an attractive alternative to the challenging alkyl-alkyl cross-coupling reactions (Scheme 3.1, bottom).<sup>[15]</sup> Such method utilizes the wide availability and easy preparation of alkyl-Grignard reagents. The success of the cross-coupling with substituted allyl acetates relies on the strict control of chemoselectivity as the nucleophilic Grignard reagent may readily undergo direct attack at the carboxyl function under thermodynamic control. Iron-catalyzed hydrogenations have been reported for a variety of olefins.<sup>[31]</sup> There are a handful of powerful homogeneous iron catalysts based on pincer-type ligands<sup>[32,33]</sup> and heterogeneous catalysts derived from the reduction of iron salts with organometallic or hydride reagents.<sup>[34–37]</sup> With regard to the latter catalyst class, we surmised that the iron catalyst that formed under the conditions of the cross-coupling reaction with the organomagnesium halide might also be competent in the subsequent alkene hydrogenation (Scheme 3.1, bottom right).<sup>[15]</sup>

**Fe-catalyzed allylation:****Fe-catalyzed alkyl-alkyl cross-coupling:****Fe-catalyzed allylation-hydrogenation:**

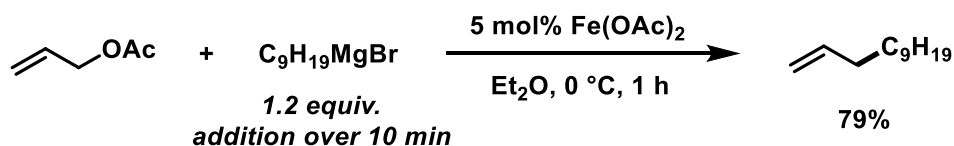
= formal alkyl-alkyl cross-coupling

Scheme 3.1 Iron-catalyzed allylic substitutions.<sup>[15,18,21,27–29,31]</sup>

## 3.2 Results and Discussion

**Initial optimizations.** The envisaged sequence of an iron-catalyzed allylation of organomagnesium halides and an iron-catalyzed hydrogenation required the development of a robust allylation reaction with alkylmagnesium halides. From a rapid survey of various catalyst precursors, additives, solvents, and conditions, reactions between allyl acetate and a very low excess of the *n*-alkylmagnesium bromide (1.2 equiv., addition over 10 min) with the commercial pre-catalyst iron(II) acetate (5 mol%  $\text{Fe}(\text{OAc})_2$ ) in diethylether were identified as being most effective (Scheme 3.2, see Chapter 3.4.2 for optimization experiments). Importantly,  $\text{Fe}(\text{OAc})_2$  effectively inhibited the competing formal  $\beta$ -H elimination of the Grignard reagent. Other solvents like THF, toluene, *N*-methyl-2-pyrrolidinone (NMP), and 1,2-dimethoxyethane (DME) afforded much lower yields. Toluene/ $\text{Et}_2\text{O}$  mixtures and ethyl acetate gave similar results. The addition of ligands (amines, *N*-heterocyclic carbenes) showed no

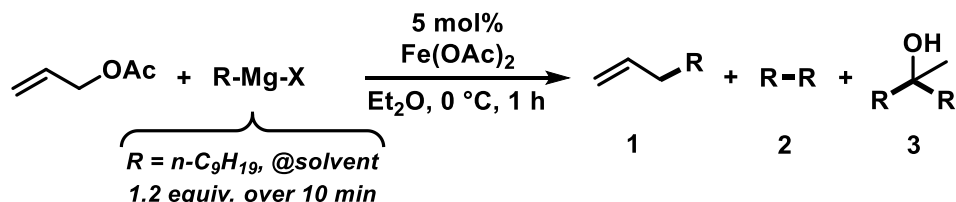
significant effect on the reaction outcome, whereas phosphines led to complete catalyst inhibition.



**Scheme 3.2** Optimized conditions for iron-catalyzed alkylation of allyl acetate.

The major side reactions observed were the formation of homocoupling products from the Grignard reagent<sup>[29]</sup> and the nucleophilic attack at the carbonyl group. The composition of the Grignard reagent (RMgX, X = Cl, Br, I; RMgX vs. R<sub>2</sub>Mg) and the choice of solvent exerted a strong influence on the reaction selectivities, most likely as a direct consequence of the Schlenk equilibrium (Table 3.1).<sup>[38]</sup> The alkyl-magnesium chloride and the dialkylmagnesium in Et<sub>2</sub>O predominantly afforded the carboxylate substitution product from the uncatalyzed background reaction (entries 1 and 8). The alkyl-magnesium bromide (in Et<sub>2</sub>O) and its LiCl-adduct (in THF) gave highest conversions (entries 4-6).

**Table 3.1** Variation of Grignard reagents.

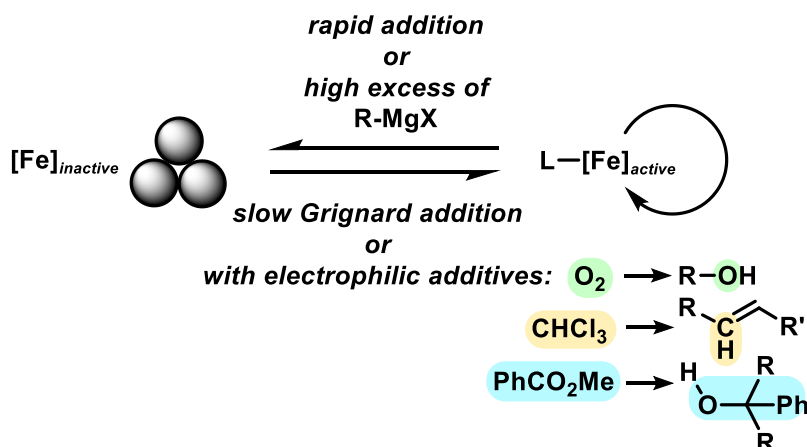


Entry	X	Solvent (RMgX)	1 [%]	2 [%]	3 [%]
1	Cl	Et <sub>2</sub> O	0	<1	52
2	Cl	THF	37	12	11
3	Cl·LiCl	THF	54	5	2
4	Br	Et <sub>2</sub> O	76	11	<1
5	Br	THF	69	6	2
6	Br·LiCl	THF	77	5	2
7	I	Et <sub>2</sub> O	32	35	0
8 <sup>[a]</sup>	<i>n</i> -C <sub>9</sub> H <sub>19</sub>	Dioxane	1	<1	48

Yields were determined by quantitative GC-FID vs. internal *n*-pentadecane. <sup>[a]</sup>MgBr<sub>2</sub> was filtered off prior to Grignard reagent addition.

With substituted allyl acetates bearing alkyl groups, the iron-catalyzed allylation was slowed and the formation of the tertiary alcohol was observed as main product. High cross-coupling yields were re-established by slow addition of the Grignard reagent

(over 1-6 h). An alternative procedure involved addition of 50 mol% chloroform to the reaction which allowed Grignard addition over only 45 min. A similar protocol was reported but the role of chloroform remained unclear.<sup>[12]</sup> We speculate that chloroform buffers high concentrations of Grignard reagent and thereby prevents over-reduction of the catalyst to naked Fe(0) species which would rapidly aggregate to inactive particles.<sup>[39,40]</sup> A similar effect should be observed with electrophilic additives that react with the Grignard reagent in slower rates than the desired cross-coupling but sufficiently rapid to prohibit catalyst reduction. Consistent with this hypothesis, a brief evaluation of electrophiles revealed beneficial effects of the presence of esters, organochlorides, and air under the reaction conditions (Scheme 3.3; see also Scheme 3.6).



**Scheme 3.3** Catalyst activity and effect of reaction additives.

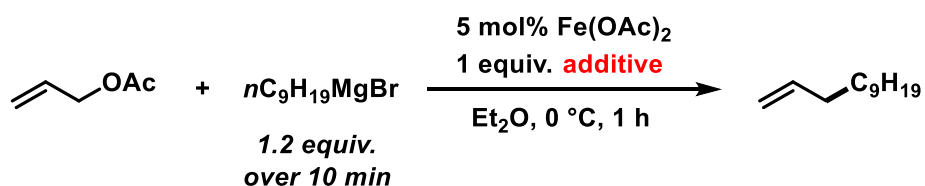
**Substrate scope.** We then explored the substrate scope of the iron-catalyzed allylation of alkylmagnesium bromides under the optimized conditions (condition A, see Table 3.2). The reaction proceeds with very high regiocontrol most likely through a  $\pi$ -allyliron intermediate as alkylation selectively occurred at the less hindered allyl termini. This is exemplified by the identical product (and yield) that was obtained from prenyl acetate and 2-methylbut-3-en-2-yl acetate, respectively (entries 4 and 5). Bulky allyl acetate derivatives required slow Grignard addition and higher catalyst loading to give moderate yields. Primary, secondary, and tertiary allyl acetates underwent alkylation under the same conditions. The (*E*)-alkene isomers were formed in all cases with *E/Z* stereoselectivities of >50/1. Halide substituents were not tolerated in the 2-allyl position (entries 7, 8).

**Table 3.2** Iron-catalyzed alkylations of allyl acetates (**Condition A**).

$  \begin{array}{c}  \text{R}'\text{-CH=CH-CH}_2\text{-OAc} + \text{R-MgBr} \xrightarrow[\text{Et}_2\text{O, 0 }^\circ\text{C, 1 h}]{\begin{array}{c} 5 \text{ mol\% Fe(OAc)}_2 \\ 50 \text{ mol\% CHCl}_3 \end{array}} \text{R}'\text{-CH=CH-CH}_2\text{-CH}_2\text{-R} \\  \text{1.4 equiv.} \\  \text{over 45 min}  \end{array}  $				
Entry	Allyl acetate	Product	R'	Yield [%] <sup>[a]</sup>
1			H	85
2			Me	72
3			<i>n</i> C <sub>6</sub> H <sub>13</sub>	67
4				61 (<5 <sup>[b]</sup> )
5				59
6			Me	80
7			Cl	0
8			Br	0
9				37 <sup>[c]</sup>
10				53 <sup>[c]</sup>
11				16 <sup>[c]</sup>
12				64

<sup>[a]</sup> Isolated yields; *E/Z* product ratios >50/1. <sup>[b]</sup> C<sub>9</sub>H<sub>19</sub>MgCl·LiCl was used. <sup>[c]</sup> 10 mol% Fe(OAc)<sub>2</sub>, RMgBr addition over 1 h.

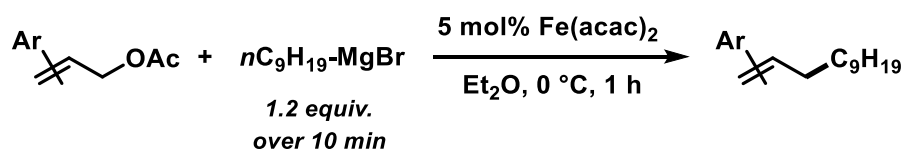
A screening of functional additives documented moderate compatibility with nitriles and good tolerance of esters and amines (Table 3.3). Alcohols required the addition of an extra equivalent Grignard reagent.

**Table 3.3** External functional group test.

Entry	Additive	Additive conversion [%] <sup>[a]</sup>	Yield [%] <sup>[a]</sup>
1	-	-	77
2	PhCN	0	21
3	<i>n</i> -C <sub>3</sub> H <sub>7</sub> CN	9	49
4	PhNO <sub>2</sub>	90	<1
5	EtNO <sub>2</sub>	87	8
6	PhNH <sub>2</sub>	77	9
7	<i>n</i> -C <sub>6</sub> H <sub>13</sub> NH <sub>2</sub>	0	80
8	PhCHO	100	16
9	PhCO <sub>2</sub> Me	0	82
10	<i>n</i> -C <sub>3</sub> H <sub>7</sub> CO <sub>2</sub> Me	4	72
11	PhOH	0	75 <sup>[b]</sup>
12	<i>n</i> -C <sub>5</sub> H <sub>11</sub> OH	6	79 <sup>[b]</sup>

<sup>[a]</sup> Yields were determined by quantitative GC-FID vs. internal *n*-pentadecane. <sup>[b]</sup> 2.2 equiv. *n*-C<sub>9</sub>H<sub>19</sub>MgBr.

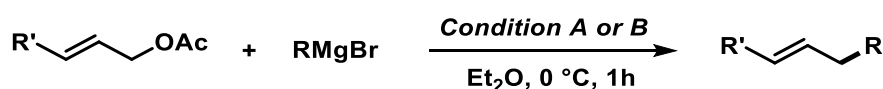
In an effort to further expand the scope of this allylation reaction, we employed aryl-substituted allyl acetates (Table 3.4). Enhanced selectivities were obtained from the use of Fe(acac)<sub>2</sub> as pre-catalyst (acac = acetylacetonato). The presence of CHCl<sub>3</sub> or slow addition of the Grignard reagent did not show any improvements (condition B). Again, increased steric hindrance of the substrates led to lower reactivities.

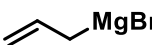
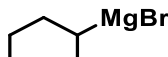
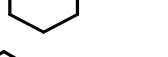
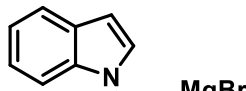
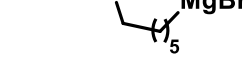
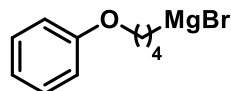

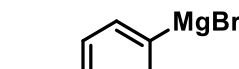
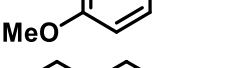
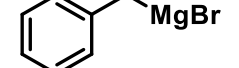
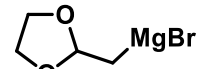
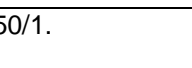
**Table 3.4** Iron-catalyzed alkylations of aryl-substituted allyl acetates (**Condition B**).

Entry	Acetate	Product	X	Yield [%] <sup>[a]</sup>
1			H	72 (39 <sup>[b]</sup> )
2			OMe	65
3			Cl	44
4			Me	57
5				17
6				68
7				51
8				56 <sup>[c]</sup>

<sup>[a]</sup> Isolated yields; *E/Z* of products >50/1. <sup>[b]</sup> with C<sub>9</sub>H<sub>19</sub>MgCl·LiCl. <sup>[c]</sup> *E/Z* 25/1

Finally, we employed different Grignard reagents in reactions with various allyl acetate derivatives (Table 3.5). Higher yields were obtained with catalytic Fe(acac)<sub>2</sub> when aryl groups were present in the allyl acetate or Grignard reagents. Primary and secondary alkyl-magnesium bromides and arylmagnesium bromides afforded good to very good yields of the cross-coupling products. It is important to note that the conditions A and B exhibited distinct reactivities: Condition A, in the presence of CHCl<sub>3</sub> and with catalytic Fe(OAc)<sub>2</sub>, facilitated reactions with sterically demanding allyl acetate derivatives. Condition B (no CHCl<sub>3</sub>, with Fe(acac)<sub>2</sub>) gave higher selectivities for aryl-containing substrates. Allylmagnesium bromide underwent carboxylate substitution (entry 2). 1,3-Dioxolane-2-methylmagnesium bromide was unreactive (entry 15).

**Table 3.5** Variation of the Grignard reagents (**Condition A and B**).

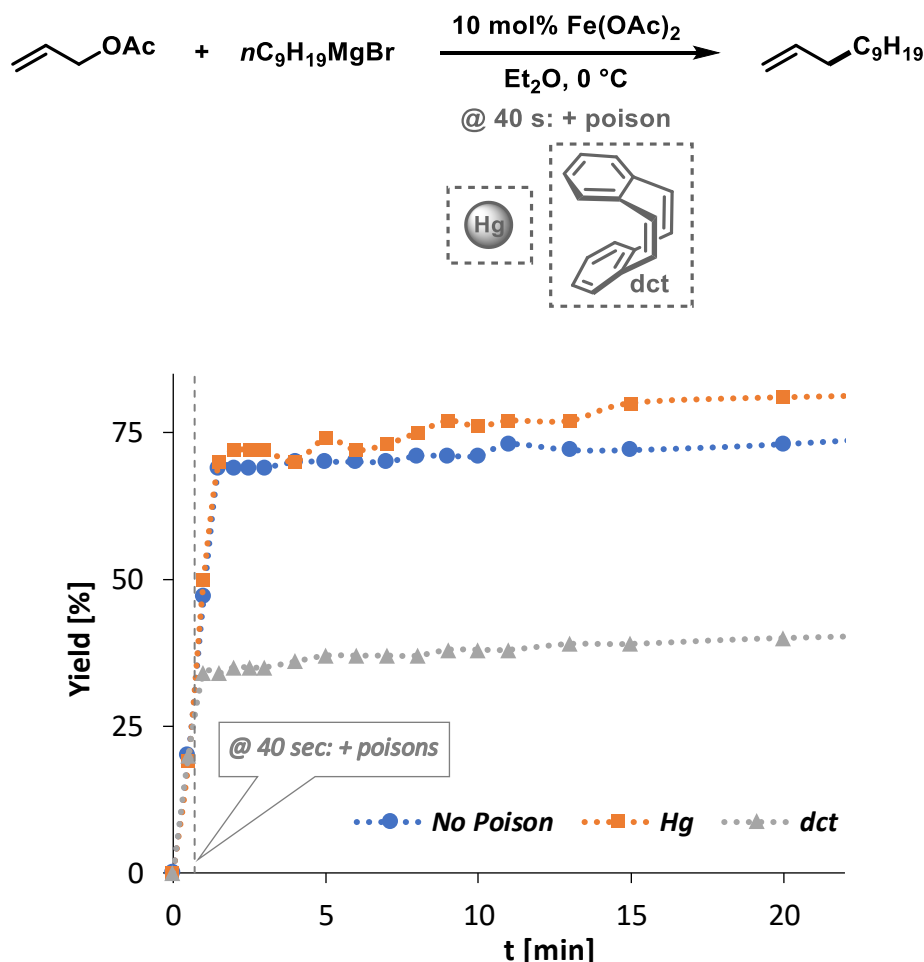
Entry	RMgBr	R'	Yield [%] <sup>[a]</sup>	
			A	B
1	MeMgBr	Ph	-	68
2	 MgBr	Ph	0	0
3	 MgBr	Ph	-	68
4	 MgBr	H	76	-
5	 MgBr	Ph	-	65
6	 MgBr	H	-	64
7	 MgBr	Ph	-	75
8	 MgBr	H	-	71
9	PhMgBr	Ph	11	64
10	PhMgBr	H	17	65
11	 MgBr	Ph	-	77
12	 MgBr	H	22	82
13	 MgBr	<i>n</i> C <sub>6</sub> H <sub>13</sub>	<5	<5
14	 MgBr	Ph	-	42
15	 MgBr	Ph	0	0

<sup>a</sup> Isolated yields; *E/Z* of products >50/1.

**Mechanistic studies.** The clear distinction whether homogeneous or heterogeneous catalysis is operating can be intricate, as the catalysts can be part of an equilibrium between several species and the spectroscopic tools often perturb the system under investigation. We performed Maitlis' hot filtration test which showed comparable catalytic activity in both the filtrate and filter phases.<sup>[41]</sup> The most reliable insight can be derived from kinetic experiments that are conducted *in operando* under the catalytic reaction conditions.<sup>[41,42]</sup> Reaction progress analyses showed no sigmoidal curvature that would have been indicative of an initial catalyst nucleation and particle growth. On the contrary, the highest catalyst activity was recorded at the onset of conversion within the first 30 s of the reaction. Furthermore, kinetic poisoning experiments were conducted (Scheme 3.4). Amalgamation of a potential Fe(0) catalyst was not observed upon addition of 100 equiv. Hg per Fe.<sup>[43,44]</sup> The addition of dibenzo[*a,e*]cyclo-



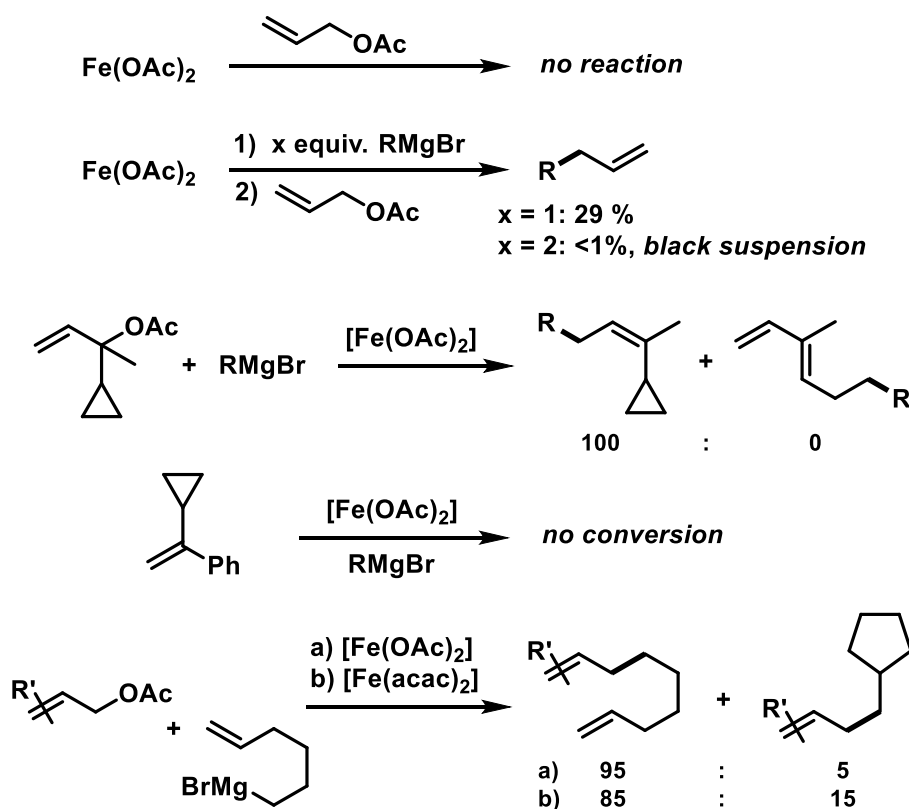
octatetraene (dct, 2 equiv. per Fe),<sup>[16,45,46]</sup> a selective homotopic poison of low-valent late transition metals, resulted in immediate and complete inhibition of catalytic activity. This observation constitutes a strong indication of a homogeneous catalysis mechanism.



**Scheme 3.4** Poisoning experiments with Hg (100 equiv. per Fe) and dct (2 equiv. per Fe).

We have collected further mechanistic insight from a set of key experiments: The strongly reducing conditions in the presence of a large excess of Grignard reagent led to rapid deactivation of the catalyst,<sup>[39]</sup> an effect that already became apparent from the adaptation of slow-addition protocols (*vide supra*). Stoichiometric reactions between all components of this allylation protocol provided further insight (Scheme 3.5). No direct reaction between allyl acetate and  $\text{Fe(OAc)}_2$  occurred so that an allyliron or reduced iron species (both form in the presence of the Grignard reagent) may act as active catalyst in the formal oxidative addition of allyl acetate. Reaction with equimolar substrates and pre-catalyst gave 29% product yield, whereas the presence of 2 equiv. nonylmagnesium bromide effectively suppressed product formation

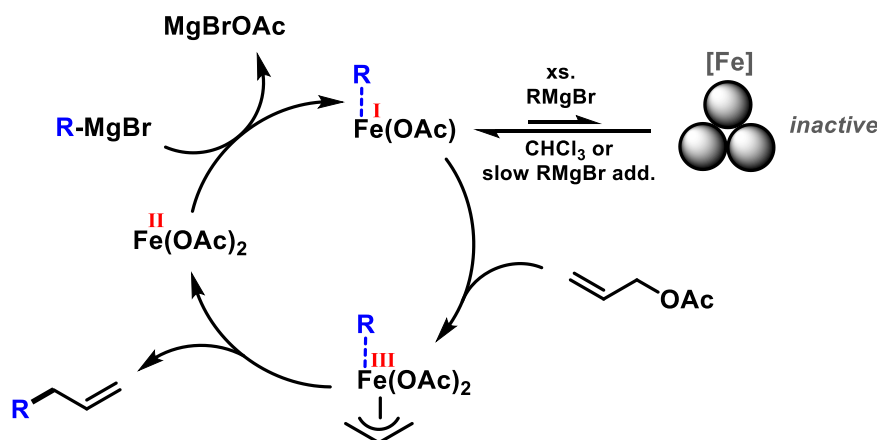
(Scheme 3.5). It is well known that reactions of ferrous salts with 2 equiv. alkyl-Grignard reagents form iron(0) species which rapidly nucleate and grow to particles if no suitable ligands are available. The formation of catalytically inactive Fe(0) particles in the presence of excess Grignard reagent may indicate that higher oxidation state catalysts are operating, presumably Fe(I) which is in accord with recent literature reports under very similar conditions.<sup>[29,47,48]</sup> However, we cannot exclude the formation of soluble ferrate(0) complexes.<sup>[49]</sup> Radical clock experiments did not fully support the potential intermediacy of organic radicals.<sup>[50]</sup> No ring-opening was observed with the 1-cyclopropyl-bearing allyl acetate under the standard conditions. The operation of radical addition of an open-shell Fe catalyst to the alkene group was excluded by the absence of any reactivity with  $\alpha$ -cyclopropyl styrene. 5-Hexenylmagnesium bromide underwent only minor ring-closure.



**Scheme 3.5** Key mechanistic experiments.

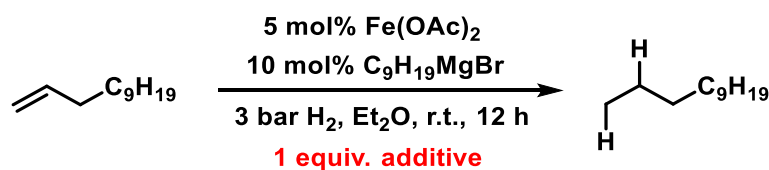
Based on the collected data from these key experiments, we postulate a mechanism that commences with reduction of the Fe(II) pre-catalyst to an active Fe(I) species. Over-reduction to inactive Fe(0) particles in the presence of high concentrations of the Grignard reagent can be healed by addition of suitable (buffering) electrophiles such as chloroform, esters, or allyl acetate itself. Addition of allyl acetate leads to an  $\eta^3$ -

allyliron complex that undergoes reductive elimination of the C-C coupling product (Scheme 3.6).



Scheme 3.6 Proposed mechanism.

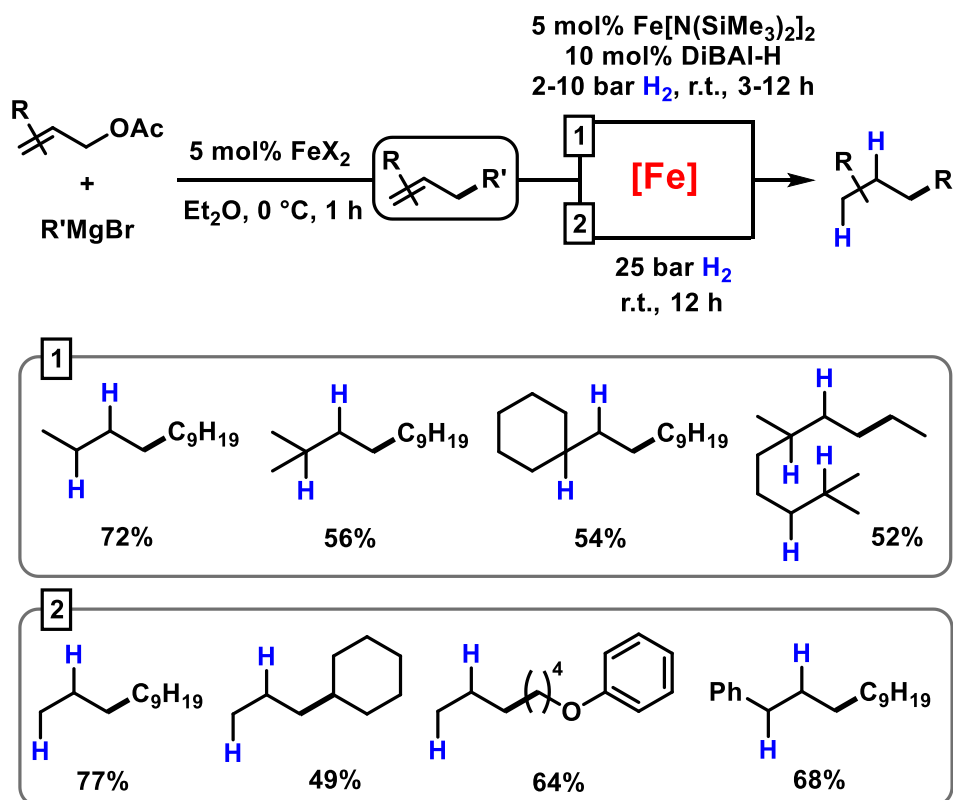
**Sequential allylation-hydrogenation.** Having established reaction conditions for the allylation of alkylmagnesium halides, the development of a conceptually distinct alternative to the rather challenging alkyl-alkyl cross-coupling reactions still requires an effective Fe-catalyzed alkene hydrogenation<sup>[31–37]</sup>. Several hydrogenation protocols with a variety of homogeneous and heterogeneous iron catalysts have been reported in the past decade.<sup>[31,34,51–56]</sup> Interestingly, hydrogenation catalysts have also been reported to form from ferrous salts and alkylmagnesium halides, which may enable sequential allylation-hydrogenation reactions with the same catalyst mixture. However, there is very little knowledge on the conversion of *in situ* prepared product mixtures (without workup) and the potential cross-contamination of iron catalysts by residual byproducts from the preceding steps. We therefore performed hydrogenation reactions in the presence of all possible byproducts from the allylation step under conditions A and B (Table 3.6). While residual allyl acetate showed no detrimental effect on the activity of the Fe catalyst, the presence of inorganic bromide salts (MgBr<sub>2</sub> or LiBr) inhibited the hydrogenation step (entries 2 and 4).

**Table 3.6** Halide-containing additives as poisons of iron-catalyzed alkene hydrogenations.

Entry	Additive	Conversion [%] <sup>[a]</sup>	Yield [%] <sup>[a]</sup>
1	-	100	77
2	MgBr <sub>2</sub>	19	<1
3	MgCl <sub>2</sub>	100	72
4	LiBr	3	<1
5	CHCl <sub>3</sub>	0	0

<sup>[a]</sup> Yields determined by quantitative GC-FID vs. internal *n*-pentadecane.

An alternative method of hydrogenation can be applied if the crude mixture of the allylation reaction is worked up (by aqueous extraction of MgBr<sub>2</sub>) prior to the hydrogenation. This strategy has enabled the hydrogenation of allylation products in good yields with a Fe[N(SiMe<sub>3</sub>)<sub>2</sub>]<sub>2</sub>/DiBAL-H (diisobutylaluminium hydride) catalyst under mild conditions (method 1 in Scheme 3.7).<sup>[31]</sup> When not making the effort to work up the crude allylation reactions, sequential hydrogenations can be performed at elevated pressure (25 bar H<sub>2</sub>) to afford the alkanes with very similar yields (method 2 in Scheme 3.7).

**Scheme 3.7** Sequential iron-catalyzed allylation and hydrogenation.

### 3.3 Conclusions

The iron-catalyzed allylation of alkyl and aryl Grignard reagents with allyl acetate derivatives operates under very mild conditions with a commercial catalyst. Kinetic experiments suggest a highly active homotopic catalyst. Slow Grignard addition protocols or the presence of electrophilic additives (e.g. chloroform) enhanced catalyst activity and lifetime. The sequential combination of the iron-catalyzed allylation of alkyl-magnesium halides with an iron-catalyzed hydrogenation of the resultant alkenes results in a formal  $sp^3$ - $sp^3$ -cross-coupling that proved otherwise challenging. The presence of high bromide concentrations inhibited the hydrogenation step.

### 3.4 Experimental

Chemicals and Solvents. If not indicated, commercial reagents were used without purification. For catalytic reactions, exclusively dried solvents were used. Liquid substrates were distilled prior to use. THF was dried over sodium/benzophenone and distilled. All Fe-catalyzed reactions were performed under an atmosphere of dry argon using standard Schlenk and glovebox techniques.

Analytical thin-layer chromatography. TLC was performed using aluminium plates with silica gel and fluorescent indicator (Merck, 60F<sub>254</sub>). Thin-layer chromatography plates were visualized by exposure to UV light and/or by immersion in an aqueous staining solution of KMnO<sub>4</sub>.

Column chromatography. Flash column chromatography with silica gel 60 Å (220-240 mesh) from *Acros*. Mixtures of pentane with ethyl acetate were used as eluents.

Gas chromatography with mass-selective detector. *Agilent* 6890N Network GC-System, mass detector 5975 MS. Column BPX5 (30m x 0.25 mm x 0.25µm) from *SGE*, carrier gas: H<sub>2</sub>. Standard heating procedure: 50°C (2 min), 25°C/min -> 300°C (5 min).

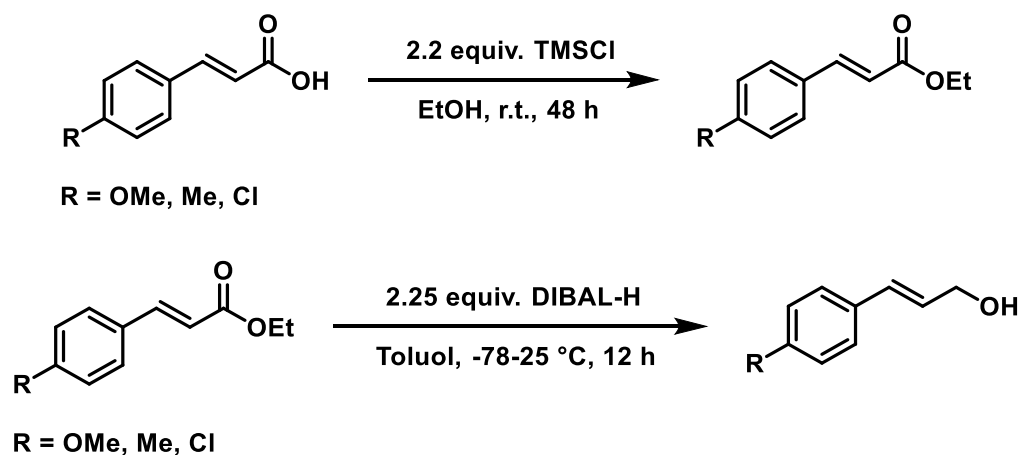
Gas chromatography with FID. *Agilent* 7820A GC-Systems. Column: HP 5 19091J 413 (30 m x 0.32 mm x 0.25 µm) from *Agilent*, carrier gas: N<sub>2</sub>. GC-FID was used for catalyst screening (calibration with analytically pure samples vs. internal *n*-pentadecane).

NMR. <sup>1</sup>H and <sup>13</sup>C nuclear magnetic resonance spectra were recorded on a *Bruker* Avance 300 (300 MHz <sup>1</sup>H; 75 MHz <sup>13</sup>C) and *Bruker* Avance 400 (400 MHz <sup>1</sup>H, 101 MHz <sup>13</sup>C) spectrometers. Chemical shifts are reported in ppm (δ) relative to internal tetramethylsilane (TMS). Coupling constants (*J*) are reported in Hertz (Hz).

High resolution mass spectrometry (HRMS). The spectra were recorded by the Central Analytics Lab at the Department of Chemistry, University of Regensburg.

### 3.4.1 Preparation of Starting Materials

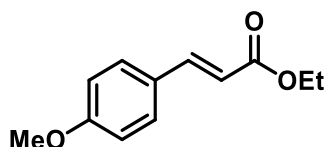
#### Preparation of Allylic Alcohols - Procedure 1



#### Representative procedure on the example of 4-methoxy cinnamyl alcohol:

- 1) Chlorotrimethylsilane (TMSCl, 33 mmol, 4.2 mL) was added to a solution of 4-methoxycinnamic acid (15 mmol, 2.67 g) in 75 ml of ethanol. The solution was stirred at room temperature for 48 hours. The solvent was then removed under reduced pressure.
- 2) 13.5 ml of a 1.0 M diisobutylaluminum hydride (DIBAL-H) solution in toluene was added dropwise at -78 °C to a solution of 4-methoxy ethyl cinnamate (6 mmol, 1.24 g) in toluene (18 mL) over 45 minutes. The reaction was stirred at room temperature for 12 hours before gently hydrolyzing with ice-cooled 1.0 M aqueous HCl solution (15 mL). The aqueous phase was extracted with Et<sub>2</sub>O and the combined organic phases were then dried over NaSO<sub>4</sub>. After filtering off the drying agent, the solvent was distilled off under reduced pressure. No further purification was required.<sup>[57]</sup>

#### 4-methoxyethyl cinnamate



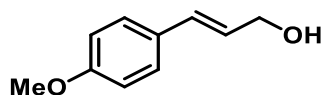
C<sub>12</sub>H<sub>14</sub>O<sub>3</sub> 206.24 g/mol

**Yield** 3.07 g, 14.9 mmol, 99%

<b><math>^1\text{H-NMR}</math></b>	(300 MHz, $\text{CDCl}_3$ ) $\delta_{\text{H}}$ [ppm] = 7.64 (d, $J$ = 16.0 Hz, 1H), 7.54 - 7.43 (m, 2H), 6.96 - 6.82 (m, 2H), 6.31 (d, $J$ = 16.0 Hz, 1H), 4.25 (q, $J$ = 7.1 Hz, 2H), 3.84 (s, 3H), 1.33 (t, $J$ = 7.1 Hz, 3H).
<b><math>^{13}\text{C-NMR}</math></b>	(75 MHz, $\text{CDCl}_3$ ) $\delta_{\text{C}}$ [ppm] = 167.4, 161.3, 144.3, 129.7, 127.2, 115.7, 114.3, 60.4, 55.4, 14.4.
<b>GC-MS</b>	(EI, 70 eV, $m/z$ ): 206 $[\text{M}]^+$ , 194, 181, 161, 149, 136, 121, 110, 78, 69, 51.

The data corresponds to the literature values.<sup>[58]</sup>

#### 4-methoxy cinnamyl alcohol

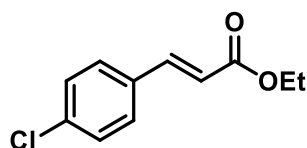


$\text{C}_{10}\text{H}_{12}\text{O}_2$  164.20 g/mol

<b>Yield</b>	879 mg, 5.4 mmol, 89%
<b><math>^1\text{H-NMR}</math></b>	(400 MHz, $\text{CDCl}_3$ ) $\delta_{\text{H}}$ [ppm] = 7.36 - 7.29 (m, 2H), 6.90 - 6.81 (m, 2H), 6.56 (d, $J$ = 15.9 Hz, 1H), 6.24 (dt, $J$ = 15.9, 6.0 Hz, 1H), 4.30 (d, $J$ = 5.6 Hz, 2H), 3.81 (s, 3H).
<b><math>^{13}\text{C-NMR}</math></b>	(101 MHz, $\text{CDCl}_3$ ) $\delta_{\text{C}}$ [ppm] = 159.4, 131.0, 129.4, 127.7, 126.3, 114.0, 64.0, 55.3.
<b>GC-MS</b>	(EI, 70 eV, $m/z$ ): 164 $[\text{M}]^+$ , 147, 136, 121, 110, 78, 50.

The data corresponds to the literature values.<sup>[59]</sup>

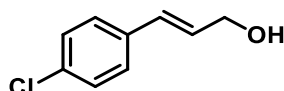
#### 4-chloroethyl cinnamate



$\text{C}_{11}\text{H}_{11}\text{ClO}_2$  210.66 g/mol

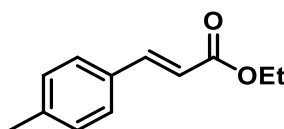


<b>Yield</b>	3.15 g, 15 mmol, 100%
<b><sup>1</sup>H-NMR</b>	(300 MHz, CDCl <sub>3</sub> ) δ <sub>H</sub> [ppm] = 7.63 (d, <i>J</i> = 16.0 Hz, 1H), 7.51 - 7.29 (m, 4H), 6.40 (d, <i>J</i> = 16.0 Hz, 1H), 4.26 (q, <i>J</i> = 7.1 Hz, 2H), 1.33 (t, <i>J</i> = 7.1 Hz, 3H).
<b><sup>13</sup>C-NMR</b>	(75 MHz, CDCl <sub>3</sub> ) δ <sub>C</sub> [ppm] = 166.8, 143.2, 136.1, 133.0, 129.2, 129.2, 118.9, 60.7, 14.3.
<b>GC-MS</b>	(EI, 70 eV, <i>m/z</i> ): 210 [M] <sup>+</sup> , 182, 165, 138, 102, 75, 63, 50. The data corresponds to the literature values. <sup>[58]</sup>

**4-chloro cinnamyl alcohol**

C<sub>9</sub>H<sub>9</sub>ClO 168.62 g/mol

<b>Yield</b>	877 mg, 5.2 mmol, 87%
<b><sup>1</sup>H-NMR</b>	(400 MHz, CDCl <sub>3</sub> ) δ <sub>H</sub> [ppm] = 7.39-7.26 (m, 4H), 6.58 (d, <i>J</i> = 15.9 Hz, 1H), 6.34 (dt, <i>J</i> = 15.9, 5.6 Hz, 1H), 4.33 (dd, <i>J</i> = 5.6, 1.5 Hz, 2H).
<b><sup>13</sup>C-NMR</b>	(101 MHz, CDCl <sub>3</sub> ) δ <sub>C</sub> [ppm] = 135.2, 133.3, 129.8, 129.2, 128.8, 127.7, 63.6.
<b>GC-MS</b>	(EI, 70 eV, <i>m/z</i> ): 168 [M] <sup>+</sup> , 151, 122, 115, 91, 61. The data corresponds to the literature values. <sup>[59]</sup>

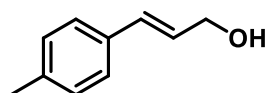
**4-methyl ethyl cinnamate**

C<sub>12</sub>H<sub>14</sub>O<sub>2</sub> 190.24 g/mol

<b>Yield</b>	2.86 g, 15 mmol, 100%
<b><sup>1</sup>H-NMR</b>	(300 MHz, CDCl <sub>3</sub> ) δ <sub>H</sub> [ppm] = 7.66 (d, <i>J</i> = 16.0 Hz, 1H), 7.42 (d, <i>J</i> = 8.2 Hz, 2H), 7.19 (d, <i>J</i> = 8.0 Hz, 2H), 6.39 (d, <i>J</i> = 16.0 Hz, 1H), 4.26 (q, <i>J</i> = 7.1 Hz, 2H), 2.37 (s, 3H), 1.34 (t, <i>J</i> = 7.1 Hz, 3H).
<b><sup>13</sup>C-NMR</b>	(75 MHz, CDCl <sub>3</sub> ) δ <sub>C</sub> [ppm] = 167.3, 144.6, 140.7, 131.7, 129.6, 128.1, 117.2, 60.4, 21.5, 14.4.
<b>GC-MS</b>	(EI, 70 eV, <i>m/z</i> ): 190 [M] <sup>+</sup> , 172, 162, 145, 132, 115, 103, 91, 76, 63, 51.

The data corresponds to the literature values.<sup>[58]</sup>

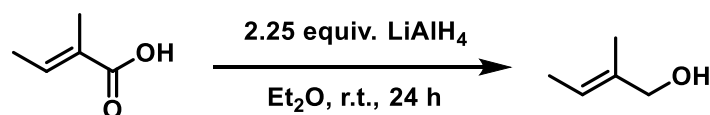
#### 4-methyl cinnamyl alcohol



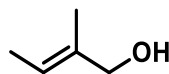
C<sub>10</sub>H<sub>12</sub>O 148.21 g/mol

<b>Yield</b>	629 mg, 4.2 mmol, 71%
<b><sup>1</sup>H-NMR</b>	(400 MHz, CDCl <sub>3</sub> ) δ <sub>H</sub> [ppm] = 7.29 (d, <i>J</i> = 8.1 Hz, 2H), 7.13 (d, <i>J</i> = 7.9 Hz, 2H), 6.59 (d, <i>J</i> = 15.9 Hz, 1H), 6.32 (dt, <i>J</i> = 15.9, 5.9 Hz, 1H), 4.31 (dd, <i>J</i> = 5.8, 1.3 Hz, 2H), 2.34 (s, <i>J</i> = 8.0 Hz, 3H).
<b><sup>13</sup>C-NMR</b>	(101 MHz, CDCl <sub>3</sub> ) δ <sub>C</sub> [ppm] = 137.6, 133.9, 131.3, 129.3, 127.4, 126.4, 63.9, 21.2.
<b>GC-MS</b>	(EI, 70 eV, <i>m/z</i> ): 148 [M] <sup>+</sup> , 131, 105, 71, 55.

The data corresponds to the literature values.<sup>[59]</sup>

*Preparation of Allylic Alcohols - Procedure 2*

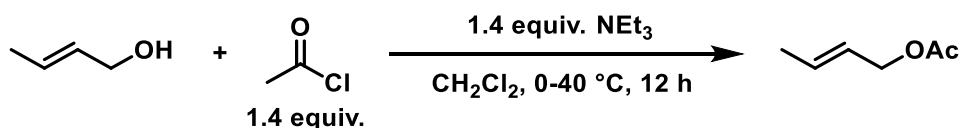
Under inert gas atmosphere ( $N_2$ ), lithiumaluminum hydride (34 mmol, 1.29 g) was charged in 40 mL of absolute  $Et_2O$ . Tiglic acid (15 mmol, 1.5 g) was dissolved in 20 mL of absolute  $Et_2O$  and added dropwise over a period of 2 hours with the aid of a dropping funnel. The suspension was stirred for 24 hours at room temperature and then carefully hydrolyzed with ice water and 15% aqueous NaOH solution (2 mL each). After addition of another 25 mL of ice water, the reaction mixture was filtered and the aqueous phase was extracted with  $Et_2O$ . The collected organic phases were dried over  $NaSO_4$ . The drying agent was filtered off and the solvent was carefully removed at 50 °C at ambient pressure. The product was purified by distillation at 60 °C at 20 mbar.<sup>[60]</sup>

**(E)-2-methylbut-2-en-1-ol**

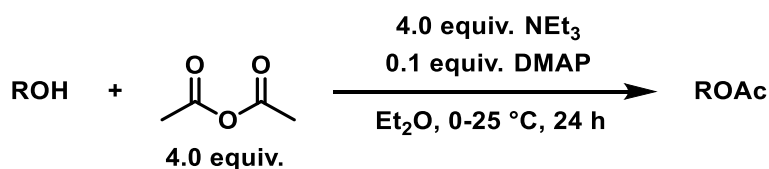
$C_5H_{10}O$  86.13 g/mol

<b>Yield</b>	586 mg, 6.8 mmol, 45%
<b><math>^1H</math>-NMR</b>	(300 MHz, $CDCl_3$ ) $\delta_H$ [ppm] = 5.58 - 5.39 (m, 1H), 3.98 (d, $J$ = 5.9 Hz, 2H), 1.65 (d, $J$ = 1.0 Hz, 3H), 1.61 (ddd, $J$ = 6.7, 2.1, 1.0 Hz, 4H).
<b><math>^{13}C</math>-NMR</b>	(101 MHz, $CDCl_3$ ) $\delta_C$ [ppm] = 135.5, 120.7, 69.1, 13.4, 13.1.
<b>GC-HRMS</b>	(CI, m/z): found 86.07269 $[M]^+$ (calculated 86.07262).

The data corresponds to the literature values.<sup>[60]</sup>

*Acetylation reactions*Procedure A

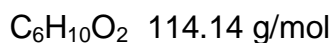
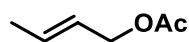
Representative procedure on the example of Crotylacetate: Crotyl alcohol (50 mmol, 3.6 g) and triethylamine (70 mmol, 9.0 mL) were dissolved in dichloromethane (25 mL) in a dry three-necked flask. The solution was cooled to 0 °C and acetyl chloride (70 mmol, 4.6 mL) in 25 mL dichloromethane was slowly added dropwise via a dropping funnel. The mixture was subsequently heated under reflux for 12 hours and, after cooling to room temperature, the precipitate formed was filtered off. The yellow solution was washed with saturated NaHCO<sub>3</sub> solution and with distilled water. The organic phase was dried over NaSO<sub>4</sub>. After filtering off the drying agent, the solvent was carefully distilled off under reduced pressure (500 mbar). Product purification was carried out by distillation at 80 °C under a pressure of 20 mbar.<sup>[61]</sup>

Procedure B

Representative procedure on the example of 4-methoxycinnamylacetate: 4-methoxycinnamyl alcohol (4 mmol, 657 mg), triethylamine (16 mmol, 2.2 mL) and 4-(dimethylamino)-pyridine (DMAP) (0.4 mmol, 49 mg) were dissolved in absolute Et<sub>2</sub>O (20 mL). The solution was cooled to 0 °C. and acetic anhydride (16 mmol, 1.5 mL) was added dropwise. The mixture was stirred at room temperature for 24 hours. The reaction solution was then washed with saturated NaHCO<sub>3</sub> solution, 10% aqueous NaOH solution and saturated NaCl solution, and the organic phase was dried over NaSO<sub>4</sub>. After filtering off the drying agent, the solvent was distilled off under reduced pressure. The crude product was purified by flash chromatography when necessary.<sup>[62]</sup>

**Crotyl acetate**

Synthesized according to procedure A.



**Yield** 1.92 g, 16.8 mmol, 34%

**$^1\text{H-NMR}$**  (300 MHz,  $\text{CDCl}_3$ )  $\delta_{\text{H}}$  [ppm] = 5.80 (dq,  $J$  = 12.8, 6.4 Hz, 1H), 5.59 (dtd,  $J$  = 8.1, 6.5, 1.5 Hz, 1H), 4.49 (d,  $J$  = 6.5 Hz, 2H), 2.06 (s, 3H), 1.72 (dd,  $J$  = 6.4, 1.0 Hz, 3H).

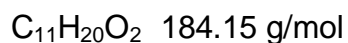
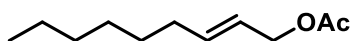
**$^{13}\text{C-NMR}$**  (101 MHz,  $\text{CDCl}_3$ )  $\delta_{\text{C}}$  [ppm] = 170.9, 131.5, 125.1, 65.2, 21.0, 17.8.

**GC-HRMS** (CI,  $m/z$ ): found 114.0667  $[\text{M}]^+$  (calculated 114.0681).

The data corresponds to the literature values.<sup>[63]</sup>

**(E)-non-2-en-1-yl acetate**

Synthesized according to procedure A.



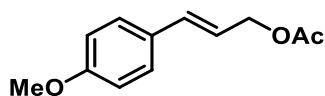
**$^1\text{H-NMR}$**  (300 MHz, Chloroform- $d$ )  $\delta$  5.77 (dtt,  $J$  = 15.5, 6.6, 1.1 Hz, 1H), 5.55 (dtt,  $J$  = 15.5, 6.5, 1.4 Hz, 1H), 4.50 (dt,  $J$  = 6.5, 1.1 Hz, 2H), 2.06 (d,  $J$  = 1.8 Hz, 5H), 1.49 – 1.17 (m, 8H), 0.96 – 0.78 (m, 3H).

**$^{13}\text{C-NMR}$**  (75 MHz,  $\text{CDCl}_3$ )  $\delta$  170.94, 136.82, 123.62, 65.39, 32.28, 31.68, 28.85, 22.61, 21.09, 14.10.

**GC-HRMS** (EI, 70 eV  $m/z$ ): found 184.14653  $[\text{M}]^{+*}$  (calculated 184.14578).

**4-methoxycinnamyl acetate**

Synthesized according to procedure B.

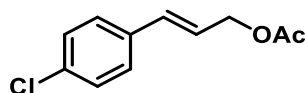


$C_{12}H_{14}O_3$  206.24 g/mol

<b>Yield</b>	644 mg, 3.1 mmol, 78%
<b><math>^1H</math>-NMR</b>	(400 MHz, $CDCl_3$ ) $\delta_H$ [ppm] = 7.39 - 7.30 (m, 2H), 6.92 - 6.79 (m, 2H), 6.60 (d, $J$ = 15.9 Hz, 1H), 6.15 (dt, $J$ = 15.8, 6.6 Hz, 1H), 4.70 (dd, $J$ = 6.6, 1.1 Hz, 2H), 3.81 (s, 3H), 2.09 (s, 3H).
<b><math>^{13}C</math>-NMR</b>	(101 MHz, $CDCl_3$ ) $\delta_C$ [ppm] = 170.9, 159.6, 134.1, 129.0, 127.9, 120.9, 114.0, 65.4, 55.3, 21.1.
<b>GC-MS</b>	(EI, 70 eV, m/z): 206 $[M]^+$ , 163, 147, 135, 115, 103, 91, 78, 63, 51. The data corresponds to the literature values. <sup>[64]</sup>

**4-chlorocinnamyl acetate**

Synthesized according to procedure B.

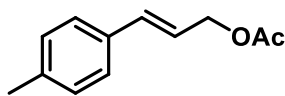


$C_{11}H_{11}ClO_2$  210.66 g/mol

<b>Yield</b>	608 mg, 2.9 mmol, 73%
<b><math>^1H</math>-NMR</b>	(400 MHz, $CDCl_3$ ) $\delta_H$ [ppm] = 7.34 - 7.27 (m, 4H), 6.60 (d, $J$ = 15.9 Hz, 1H), 6.26 (dt, $J$ = 15.9, 6.4 Hz, 1H), 4.72 (dd, $J$ = 6.4, 1.2 Hz, 2H), 2.10 (s, 3H).
<b><math>^{13}C</math>-NMR</b>	(101 MHz, $CDCl_3$ ) $\delta_C$ [ppm] = 170.8, 134.7, 133.8, 132.9, 128.8, 127.8, 123.9, 64.9, 21.0.
<b>GC-MS</b>	(EI, 70 eV, m/z): 210 $[M]^+$ , 168, 151, 133, 115, 103, 89, 77, 63, 51. The data corresponds to the literature values. <sup>[64]</sup>

**4-methylcinnamyl acetate**

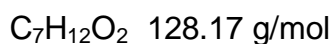
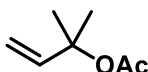
Synthesized according to procedure B.



<b>Yield</b>	613 mg, 3.2 mmol, 81%
<b><math>^1\text{H-NMR}</math></b>	(400 MHz, $\text{CDCl}_3$ ) $\delta_{\text{H}}$ [ppm] = 7.29 (d, $J$ = 8.1 Hz, 2H), 7.13 (d, $J$ = 7.9 Hz, 2H), 6.62 (d, $J$ = 15.9 Hz, 1H), 6.24 (dt, $J$ = 15.8, 6.5 Hz, 1H), 4.72 (dd, $J$ = 6.5, 1.1 Hz, 2H), 2.34 (s, 3H), 2.10 (s, 3H).
<b><math>^{13}\text{C-NMR}</math></b>	(101 MHz, $\text{CDCl}_3$ ) $\delta_{\text{C}}$ [ppm] = 170.9, 138.0, 134.3, 133.4, 129.3, 126.6, 122.1, 65.3, 21.2, 21.0.
<b>GC-MS</b>	(EI, 70 eV, $m/z$ ): 190 $[\text{M}]^+$ , 148, 131, 115, 103, 91, 77, 65, 51. The data corresponds to the literature values. <sup>[64]</sup>

**2-methylbut-3-en-2-yl acetate**

Synthesized according to procedure B.

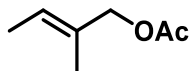


<b>Yield</b>	548 mg, 4.3 mmol, 22%
<b><math>^1\text{H-NMR}</math></b>	(400 MHz, $\text{CDCl}_3$ ) $\delta_{\text{H}}$ [ppm] = 6.07 (dd, $J$ = 17.5, 10.9 Hz, 1H), 5.16 (d, $J$ = 17.5 Hz, 1H), 5.06 (dd, $J$ = 10.9, 0.5 Hz, 1H), 1.98 (s, 3H), 1.51 (s, 6H).
<b><math>^{13}\text{C-NMR}</math></b>	(101 MHz, $\text{CDCl}_3$ ) $\delta_{\text{C}}$ [ppm] = 170.1, 142.6, 112.6, 80.6, 29.4, 26.5, 22.3.
<b>GC-HRMS</b>	(CI, $m/z$ ): found 128.0795 $[\text{M}]^+$ (calculated 128.0788).

The data corresponds to the literature values.<sup>[62]</sup>

**(E)-2-methylbut-2-en-1-ylacetate**

Synthesized according to procedure B.

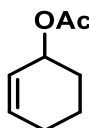


<b>Yield</b>	344 mg, 2.7 mmol, 67%
<b><sup>1</sup>H-NMR</b>	(400 MHz, CDCl <sub>3</sub> ) δ <sub>H</sub> [ppm] = 5.64 - 5.45 (m, 1H), 4.45 (s, 2H), 2.07 (s, 3H), 1.73 - 1.55 (m, 6H).
<b><sup>13</sup>C-NMR</b>	(101 MHz, CDCl <sub>3</sub> ) δ <sub>C</sub> [ppm] = 171.1, 130.8, 124.2, 70.4, 21.0, 13.6, 13.3.
<b>GC-HRMS</b>	R <sub>t</sub> = 4.49 min (CI, m/z): found 129.0909 [M+H] <sup>+</sup> (calculated 129.0910).

The data corresponds to the literature values.<sup>[65]</sup>

**Cyclohex-2-en-1-yl acetate**

Synthesized according to procedure B.



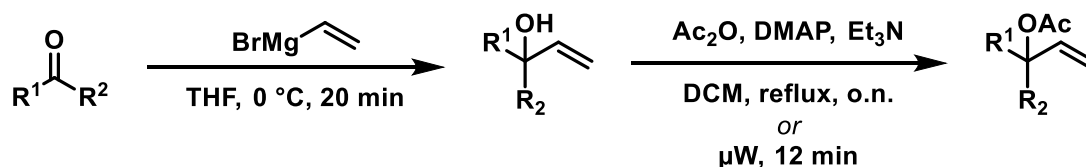
<b>Yield</b>	1.20 g, 8.6 mmol, 57%
--------------	-----------------------



<b><math>^1\text{H-NMR}</math></b>	(300 MHz, Chloroform- $d$ ) $\delta$ 5.95 (dtd, $J = 10.1, 3.7, 1.3$ Hz, 1H), 5.70 (dtd, $J = 10.1, 4.0, 2.2$ Hz, 1H), 5.25 (tdq, $J = 5.6, 3.5, 2.0$ Hz, 1H), 2.22 – 1.75 (m, 6H), 1.75 – 1.53 (m, 3H).
<b><math>^{13}\text{C-NMR}</math></b>	(75 MHz, $\text{CDCl}_3$ ) $\delta$ 170.79, 132.71, 125.66, 68.08, 28.28, 24.86, 21.45, 18.85.
<b>GC-MS</b>	$R_t = 5.22$ min (EI, 70 eV, $m/z$ ): 140 $[\text{M}]^+$ , 98, 79, 77, 70, 65, 53, 51.

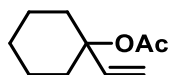
The data corresponds to the literature values.<sup>[63]</sup>

#### Alkenylation-Acetylation Reactions



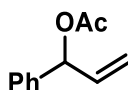
**Alkenylation:** To a solution of the ketone (10 mmol, 1 equiv.) in THF (20 mL) was added vinylmagnesium bromide (1.0 M in THF, 12 mmol, 1.2 equiv.) under nitrogen at 0 °C and the reaction was stirred for 20 minutes. The reaction was then quenched with a saturated aqueous  $\text{NH}_4\text{Cl}$  solution and extracted with diethyl ether. The combined organic layers were washed with brine, dried over sodium sulfate, filtered and evaporated to give the crude allylic alcohol that was engaged in the next step without further purification.

**Acylation:** The acylation of allylic alcohols was carried out using microwaveassisted heating conditions described as follow. The allylic alcohol (10 mmol, 1 equiv.),  $\text{Et}_3\text{N}$  (5.6 mL, 40 mmol, 4 equiv.),  $\text{Ac}_2\text{O}$  (1.8 mL, 20 mmol, 2 equiv.) and DMAP (0.360 g, 3.0 mmol, 0.3 equiv), were added in turn in a microwave-designed vial. The reaction mixture was heated under microwave-assisted heating at 100 °C for 12 min. The reaction was then quenched with a saturated aqueous  $\text{NH}_4\text{Cl}$  solution and extracted with diethyl ether. The combined organic layers were washed with brine, dried over sodium sulfate, filtered and evaporated to give a crude product that was purified by flash chromatography on silica gel.

**1-vinylcyclohexyl acetate**
 $\text{C}_{10}\text{H}_{16}\text{O}_2$  168.24 g/mol

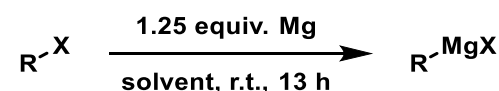
<b>Yield</b>	350 mg, 2.1 mmol, 27%
<b><math>^1\text{H-NMR}</math></b>	(300 MHz, Chloroform- $d$ ) $\delta$ 6.10 (dd, $J$ = 17.7, 11.0 Hz, 1H), 5.22 – 5.07 (m, 2H), 2.17 (q, $J$ = 6.5, 6.1 Hz, 2H), 2.02 (s, 3H), 1.65 – 1.39 (m, 6H), 1.35 – 1.20 (m, 2H).
<b><math>^{13}\text{C-NMR}</math></b>	(75 MHz, $\text{CDCl}_3$ ) $\delta$ 169.94, 141.97, 113.54, 81.78, 34.88, 25.37, 22.17, 21.88.
<b>GC-MS</b>	$R_t$ = 4.70 min (EI, 70 eV, $m/z$ ): 126 $[\text{M-Ac}]^+$ , 111, 108, 93, 91, 83, 79, 77, 55.

The data corresponds to the literature values.<sup>[66]</sup>

**1-phenylallyl acetate**
 $\text{C}_{11}\text{H}_{12}\text{O}_2$  176.22 g/mol

<b>Yield</b>	1.41 g, 8.0 mmol, 89%
<b><math>^1\text{H-NMR}</math></b>	(300 MHz, Chloroform- $d$ ) $\delta$ 7.44 – 7.24 (m, 5H), 6.27 (dt, $J$ = 5.9, 1.4 Hz, 1H), 6.01 (ddd, $J$ = 17.1, 10.4, 5.9 Hz, 1H), 5.37 – 5.20 (m, 2H), 2.12 (s, 3H).
<b>GC-MS</b>	$R_t$ = 6.58 min (EI, 70 eV, $m/z$ ): 176 $[\text{M}]^+$ , 134, 116, 105, 91, 77, 65, 55.

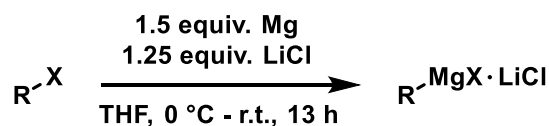
The data corresponds to the literature values.<sup>[66]</sup>

*Synthesis of the Grignard reagents*

R = Alkyl, Aryl

X = Cl, Br, I

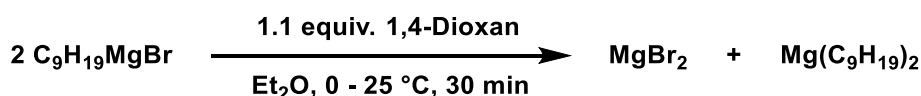
Representative procedure on the example of 1-Bromononane in Et<sub>2</sub>O: All reaction steps were carried out under inert gas atmosphere (N<sub>2</sub>). 1-Bromononane (40 mmol, 7.6 mL) was added dropwise to a suspension of magnesium turnings (50 mmol, 1.22 g) in Et<sub>2</sub>O (30 mL) at room temperature over a period of 1 hour using a syringe pump. The reaction solution was then stirred at room temperature for 12 hours.<sup>[67]</sup>



R = Alkyl, Aryl

X = Cl, Br

Representative procedure on the example of 1-Bromononane: All reaction steps were carried out under inert gas atmosphere (N<sub>2</sub>). 1-Bromononane (20 mmol, 3.8 mL) was added dropwise to a suspension of magnesium turnings (30 mmol, 0.73 g) and LiCl (25 mmol, 1.06 g) in THF (15 mL) at 0 °C over a period of 1 hour using a syringe pump. The reaction solution was then stirred at room temperature for 12 hours.

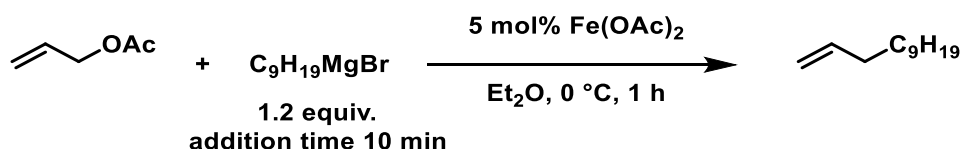


All reaction steps were carried out in an Argon-filled glovebox. A 1.0 M *n*-nonyl-magnesium bromide solution in Et<sub>2</sub>O (3 mmol, 3 mL) was added dropwise over a period of 5 minutes to a solution of dry 1,4-dioxane (3.3 mmol, 291 mg) in absolute Et<sub>2</sub>O (2 mL) at 0 °C. The mixture was then stirred at room temperature for 30 minutes and the precipitate formed was filtered off by means of a syringe filter.

Grignard solutions were titrated with salicylaldehyde phenylhydrazone (0.25 mmol, 53 mg) as indicator in THF (4 mL) to determine their concentration.<sup>[68]</sup>

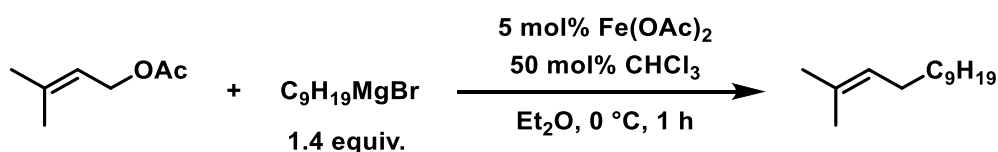
### 3.4.2 Iron-catalyzed cross-coupling reactions

#### *Procedure during optimization*



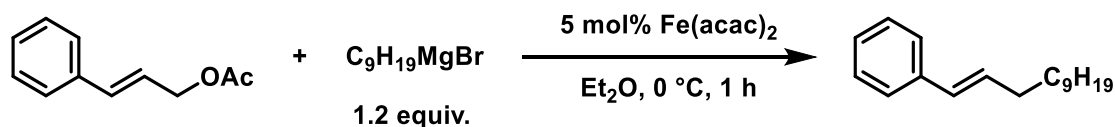
A suspension of  $\text{Fe}(\text{OAc})_2$  (0.025 mmol, 4.3 mg) in absolute  $\text{Et}_2\text{O}$  (2 mL) was cooled to 0 °C under a nitrogen atmosphere in a flame dried reaction tube. After the addition of freshly distilled allyl acetate (0.5 mmol, 54  $\mu\text{L}$ ), a 1.0 M *n*-nonylmagnesium bromide solution (0.6 mmol, 0.6 mL) in  $\text{Et}_2\text{O}$  was added dropwise over a period of 10 minutes and the mixture was stirred at 0 °C for 1 hour. The reaction mixture was then hydrolyzed with a saturated  $\text{NH}_4\text{Cl}$  solution and the aqueous phase was extracted with  $\text{EtOAc}$ . Yields were determined by quantitative GC-FID vs. internal *n*-pentadecane.

#### *Protocol A*



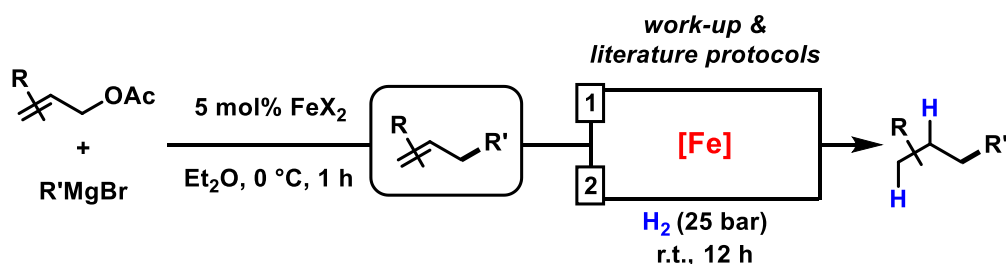
Representative procedure on the example of 2-methyltridec-2-ene: A suspension of  $\text{Fe}(\text{OAc})_2$  (0.025 mmol, 4.3 mg) and dry  $\text{CHCl}_3$  (0.25 mmol, 20  $\mu\text{L}$ ) in absolute  $\text{Et}_2\text{O}$  (2 mL) was cooled to 0 °C under a nitrogen atmosphere in a flame dried reaction tube. After the addition of freshly distilled prenyl acetate (0.5 mmol, 70  $\mu\text{L}$ ), a 1.0 M *n*-nonylmagnesium bromide solution (0.7 mmol, 0.7 mL) in  $\text{Et}_2\text{O}$  was added dropwise over a period of 45 minutes and the mixture was stirred at 0 °C for 1 hour. The reaction mixture was then hydrolyzed with a saturated  $\text{NH}_4\text{Cl}$  solution and the aqueous phase was extracted with  $\text{EtOAc}$ . The solvent was removed under reduced pressure. Product purification was carried out by kugelrohr distillation at 150 °C at 20 mbar.

## Protocol B



Representative procedure on the example of (E)-1-phenyldodec-1-ene: A suspension of  $\text{Fe}(\text{acac})_2$  (0.025 mmol, 6.4 mg) in absolute  $\text{Et}_2\text{O}$  (2 mL) was cooled to  $0\text{ }^\circ\text{C}$  under a nitrogen atmosphere in a flame dried reaction tube. After the addition cinnamyl acetate (0.5 mmol, 84  $\mu\text{L}$ ), a 1.0 M *n*-nonylmagnesium bromide solution (0.7 mmol, 0.7 mL) in  $\text{Et}_2\text{O}$  was added dropwise over a period of 10 minutes and the mixture was stirred at  $0\text{ }^\circ\text{C}$  for 1 hour. The reaction mixture was then hydrolyzed with a saturated  $\text{NH}_4\text{Cl}$  solution and the aqueous phase was extracted with  $\text{EtOAc}$ . The solvent was removed under reduced pressure. The crude product was purified by column chromatography.

## Cross Coupling with subsequent hydrogenation

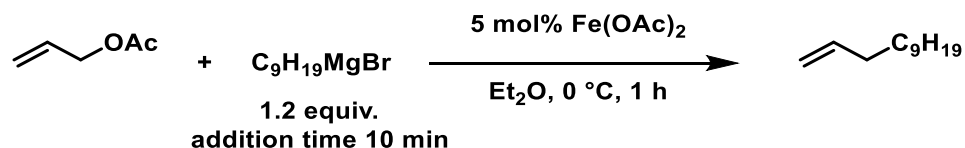


For Route 1, the isolated product of the coupling reaction was hydrogenated according to literature.<sup>[31]</sup> The products were analyzed via GC-MS and GC-FID.

For Route 2, the reaction was carried out according to Condition A (without addition of  $\text{CHCl}_3$ ) or B in an autoclave vial. After completion of the reaction, a small sample was taken out for quantitative GC-FID, and the vial was transferred into an argon-filled glovebox. The septum was penetrated with a cannula and the reaction vial was put into an autoclave, which was set under a pressure of 25 bar of  $\text{H}_2$ . The reaction was stirred overnight and then quenched with aqueous  $\text{NH}_4\text{Cl}$  solution. The organic phase

was extracted with ethyl acetate, dried over sodium sulfate and filtered over a short layer of silica. The products were analyzed via GC-MS and GC-FID.

*Optimization experiments with allyl acetate*

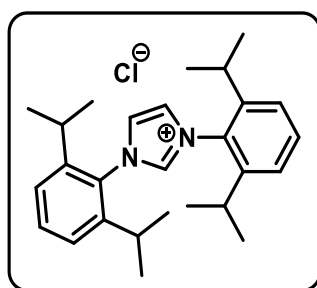


Entry	Change of reaction conditions	Yield [%] <sup>[a]</sup>
1	Fe(OAc) <sub>2</sub> (99.99%)	73
2	Pd(OAc) <sub>2</sub>	Traces
3	Pd(PPh <sub>3</sub> ) <sub>4</sub>	Traces
4	Co(OAc) <sub>2</sub>	Traces
5	NiBr <sub>2</sub>	Traces
6	CuBr	78 (<5 <sup>[b]</sup> )
7	none	0
8	FeCl <sub>2</sub>	58
9	FeCl <sub>3</sub>	61
10	FeBr <sub>2</sub>	66
11	FeI <sub>2</sub> x 2 THF	51
12	<b>Fe(OAc)<sub>2</sub></b>	<b>71</b>
13	Fe(acac) <sub>2</sub>	66
14	Fe(acac) <sub>3</sub>	59
15	Fe(N(TMS) <sub>2</sub> ) <sub>2</sub>	45
16	Fe(OTf) <sub>3</sub>	48
17	1	62
18	3	54
19	5	71
20	8	72
21	<b>10</b>	<b>78</b>
22	12	77
23	15	78
24	Heptane	4
25	<b>Et<sub>2</sub>O</b>	<b>71</b>
26	Et <sub>2</sub> O/NMP (20/1)	20
27	Toluene	41
28	Et <sub>2</sub> O/Toluene (3/1)	70
29	Et <sub>2</sub> O/Toluene (1/1)	71
30	Et <sub>2</sub> O/Toluene (1/3)	70
31	EtOAc	63
32	DME	44
33	MTBE	55
34	0.5	75 <sup>[c]</sup>
35	1.0	78 <sup>[c]</sup>
36	2.0	78 <sup>[c]</sup>

37		-20	30 <sup>[c]</sup>
38		-10	66 <sup>[c]</sup>
<b>39</b>	Temperature [°C]	<b>0</b>	<b>78<sup>[c]</sup></b>
40		25	73 <sup>[c]</sup>
41		12.5 mol% dppp	0 <sup>[c]</sup>
42		25 mol% IPr·HCl	52 <sup>[c]</sup>
43		25 mol% NEt <sub>3</sub>	61 <sup>[c]</sup>
44	Additives	12.5 mol% TMEDA	62 <sup>[c]</sup>
45		12.5 mol% DABCO	62 <sup>[c]</sup>
46		12.5 mol% CH <sub>2</sub> Cl <sub>2</sub>	55 <sup>[c]</sup>
47		12.5 mol% Glucosamin·HCl	70 <sup>[c]</sup>

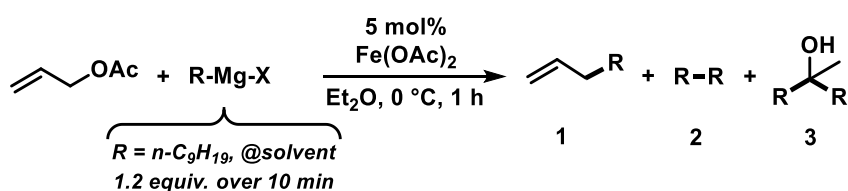
<sup>[a]</sup> Yields were determined by quantitative GC-FID vs. internal *n*-pentadecane. <sup>[b]</sup> 0.01 mol% CuBr

<sup>[c]</sup> 10 mol% Fe(OAc)<sub>2</sub>.



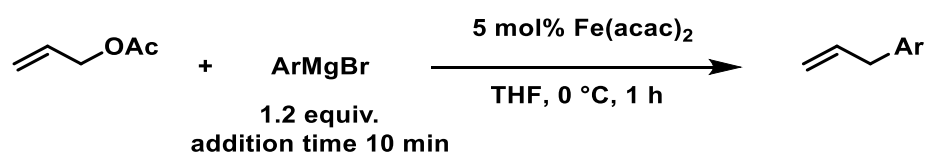
IPr·HCl

### Influence of the Schlenck equilibrium



Entry	X	Solvent (RMgX)	1 [%]	2 [%]	3 [%]
1	Cl	Et <sub>2</sub> O	0	<1	52
2	Cl	THF	37	12	11
3	Cl·LiCl	THF	54	5	2
<b>4</b>	<b>Br</b>	<b>Et<sub>2</sub>O</b>	<b>76</b>	<b>11</b>	<b>&lt;1</b>
5	Br	THF	69	6	2
6	Br·LiCl	THF	77	5	2
7	I	Et <sub>2</sub> O	32	35	0
8	<i>n</i> -C <sub>9</sub> H <sub>19</sub>	Dioxane	1	<1	48

## Application of ArMgBr

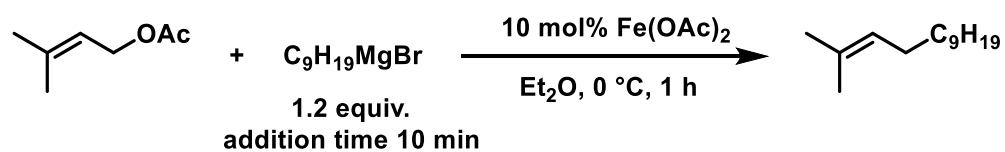


Entry	Change of reaction conditions	ArMgBr	Yield [%] <sup>[a]</sup>
1	None		0
2	FeCl <sub>2</sub>		80
3	FeBr <sub>2</sub>		66
4	Fe(OAc) <sub>2</sub>		52
5	Iron Precursor	in THF	83
6	Fe(OTf) <sub>3</sub>		65
7	FeBr <sub>2</sub>		52 <sup>[b]</sup>
8	Fe(OAc) <sub>2</sub>		17 <sup>[b]</sup>
9	Fe(acac) <sub>2</sub>	in Et <sub>2</sub> O	65 <sup>[b]</sup>
10	THF		83
11	THF/NMP (20/1)		74
12	Et <sub>2</sub> O		81
13	Toluol	in THF	82
14	Benzol	(not soluble in Et <sub>2</sub> O)	68 <sup>[c]</sup>
15	Solvent	Et <sub>2</sub> O	55
16	THF		55
17	Et <sub>2</sub> O		65
18	THF	in Et <sub>2</sub> O	61
19	-10		79
20	Temperature [°C]	0	83
21	25	in THF	44
22	6.25 mol% dppp		62
23	12.5 mol% IPr·HCl		78
24	12.5 mol% NEt <sub>3</sub>		80
25	6.25 mol% TMEDA		77
26	30 mol% CH <sub>2</sub> Cl <sub>2</sub>	in THF	74
27	6.25 mol% Glucosamin·HCl		40

<sup>[a]</sup> Yields were determined by quantitative GC-FID vs. internal *n*-pentadecane. <sup>[b]</sup> Reaction was run in Et<sub>2</sub>O. <sup>[c]</sup> Reaction temperature 25 °C.

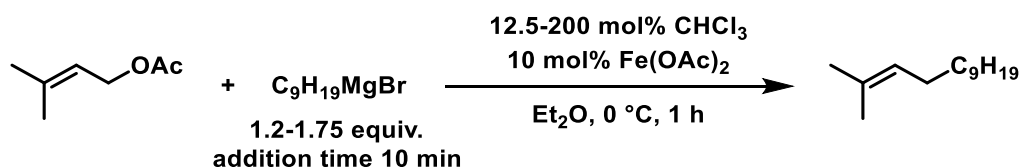


## Optimization experiments with alkyl-substituted acetates



Entry	Change of reaction conditions	Conversion [%] <sup>[a]</sup>	Yield [%] <sup>[a]</sup>
1	<b>Fe(OAc)<sub>2</sub></b>	<b>89</b>	<b>15</b>
2	Fe(acac) <sub>2</sub>	84	3
3	Iron Precursor FeCl <sub>2</sub>	76	9
4	FeBr <sub>2</sub>	76	1
5	Fe(OTf) <sub>3</sub>	76	3
6	25 mol% IPr·HCl	73	3
7	25 mol% NEt <sub>3</sub>	81	14
8	12.5 mol% TMEDA	84	5
9	Additives 12.5 mol% DABCO	82	7
10	12.5 mol% CH <sub>2</sub> Cl <sub>2</sub>	81	21
11	<b>12.5 mol% CHCl<sub>3</sub></b>	<b>83</b>	<b>38</b>
12	12.5 mol% Glucosamin·HCl	100	11
13	iPr <sub>2</sub> O	69	32
14	Bu <sub>2</sub> O	65	17
15	CPME	83	48
16	Solvents 2-Methyl-THF	32	13
17	Dioxane	57	<1
18	Dioxolane	13	<1
19	TEGDME	18	2

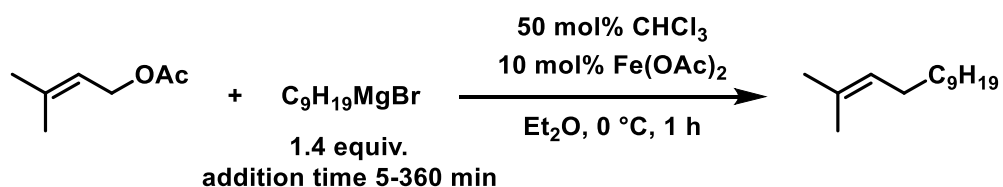
<sup>[a]</sup> Yields were determined by quantitative GC-FID vs. internal *n*-pentadecane.



Entry	CHCl <sub>3</sub> [mol%]	equiv. C <sub>9</sub> H <sub>19</sub> MgBr	Conversion[%] <sup>[a]</sup>	Yield [%] <sup>[a]</sup>
1	0	1.2	89	12
2		1.35	90	12
3	12.5	1.2	83	38
4		1.35	93	34
5	25	1.2	85	38
6		1.35	100	42
7		1.5	90	39
8	50	1.2	80	41
<b>9</b>		<b>1.35</b>	<b>89</b>	<b>46</b> (42 <sup>[b]</sup> , 43 <sup>[c]</sup> )
10		1.5	93	50
11		1.75	99	53
12	100	1.2	79	41
13		1.35	77	41
14		1.5	80	42
15		1.75	90	54
16	200	1.2	68	40
17		1.35	75	41
18		1.5	74	43
19		1.75	76	48

<sup>[a]</sup> Yields were determined by quantitative GC-FID vs. internal *n*-pentadecane. <sup>[b]</sup> Grignard concentration 0.5 M. <sup>[c]</sup> Grignard concentration 2.0 M.

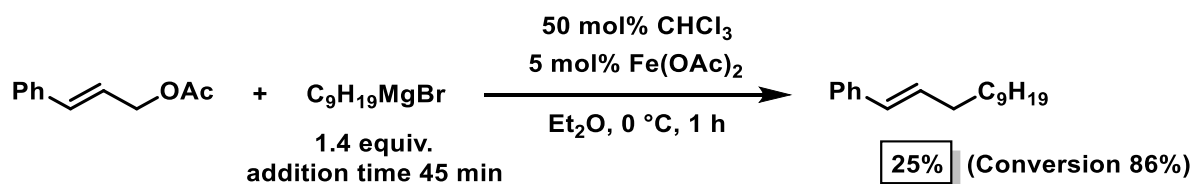
To remain in a reasonable amount of required chloroform and Grignard reagent, the reaction conditions were chosen to be 1.4 equiv. of the organomagnesiumbromide and 50 mol% CHCl<sub>3</sub>.

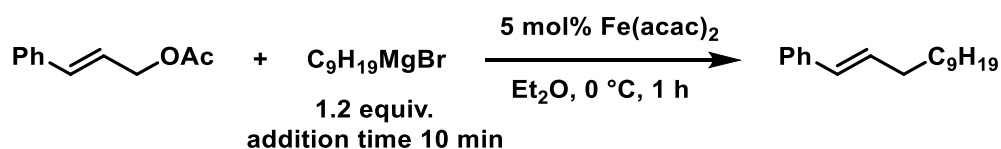


Entry	Addition time [min]	Conversion[%] <sup>[a]</sup>	Yield [%] <sup>[a]</sup>
1	5	68	22
2	10	89 (89 <sup>[b]</sup> )	45 (15 <sup>[b]</sup> )
3	20	84	52
4	30	100	50
<b>5</b>	<b>45</b>	<b>99</b> (100 <sup>[b]</sup> )	<b>64</b> (35 <sup>[b]</sup> )
6	60	94 (89 <sup>[b]</sup> )	61 (31 <sup>[b]</sup> )
7	180	100 <sup>[b]</sup>	50 <sup>[b]</sup>
8	360	100 <sup>[b]</sup>	62 <sup>[b]</sup>

<sup>[a]</sup> determined by quantitative GC-FID vs. internal *n*-pentadecane. <sup>[b]</sup> Without CHCl<sub>3</sub>.

#### Optimization experiments with aryl-substituted acetates



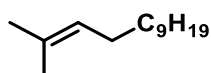


Entry	Change of reaction conditions	Conversion [%] <sup>[a]</sup>	Yield [%] <sup>[a]</sup>
1	Fe(OAc) <sub>2</sub>	65	9
2	Iron Precursor	<b>Fe(acac)<sub>2</sub></b>	<b>100</b>
3		FeCl <sub>2</sub>	100
4		FeBr <sub>2</sub>	100
5		12.5 mol% PPh <sub>3</sub>	100
6	Additives	12.5 mol% IPr·HCl	100
7		12.5 mol% NEt <sub>3</sub>	100
8		6.25 mol% TMEDA	100
9		6.25 mol% DABCO	100
10		12.5 mol% CHCl <sub>3</sub>	85
11		12.5 mol% Glucosamin·HCl	100
12	Addition time [min]	5	100
13		20	100

*Isolated products*

## 2-methyltridec-2-ene

Synthesized according to procedure A.



C<sub>14</sub>H<sub>28</sub> 196.38 g/mol

**<sup>1</sup>H-NMR** (300 MHz, CDCl<sub>3</sub>) δ<sub>H</sub> [ppm] = 5.18 - 5.06 (m, 1H), 2.01 - 1.90 (m, 2H), 1.69 (d, *J* = 1.0 Hz, 3H), 1.60 (s, 3H), 1.26 (s, 16H), 0.88 (t, *J* = 6.7 Hz, 3H).

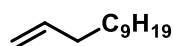
**<sup>13</sup>C-NMR** (101 MHz, CDCl<sub>3</sub>) δ<sub>C</sub> [ppm] = 131.1, 125.0, 31.9, 29.9, 29.7, 29.7, 29.6, 29.4, 29.4, 28.1, 25.7, 22.7, 17.6, 14.1.

**GC-MS** (EI, 70 eV, *m/z*): 196 [M]<sup>+</sup>, 111, 97, 83, 69, 56.

The data corresponds to the literature values.<sup>[69]</sup>

**dodec-1-ene**

Synthesized according to procedure A.



$C_{12}H_{24}$  168.32 g/mol

**$^1H$ -NMR** (400 MHz,  $CDCl_3$ )  $\delta_H$  [ppm] = 5.82 (ddt,  $J$  = 16.9, 10.2, 6.7 Hz, 1H), 4.99 (ddd,  $J$  = 17.1, 3.6, 1.6 Hz, 1H), 4.93 (ddt,  $J$  = 10.2, 2.2, 1.2 Hz, 1H), 2.08 - 2.00 (m, 2H), 1.41 - 1.22 (m, 16H), 0.88 (t,  $J$  = 6.8 Hz, 3H).

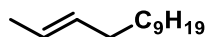
**$^{13}C$ -NMR** (101 MHz,  $CDCl_3$ )  $\delta_C$  [ppm] = 139.3, 114.1, 33.8, 31.9, 29.6, 29.6, 29.5, 29.4, 29.2, 29.0, 22.7, 14.1.

**GC-MS** (EI, 70 eV,  $m/z$ ): 168  $[M]^+$ , 140, 111, 97, 83, 69, 56.

The data corresponds to the literature values.<sup>[70]</sup>

**tridec-2-ene**

Synthesized according to procedure A.



$C_{13}H_{26}$  182.35 g/mol

**$^1H$ -NMR** (300 MHz,  $CDCl_3$ )  $\delta_H$  [ppm] = 5.44 - 5.37 (m, 2H), 2.00 - 1.90 (m, 2H), 1.66 - 1.62 (m, 3H), 1.36 - 1.21 (m, 16H), 0.88 (t,  $J$  = 6.7 Hz, 3H).

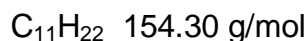
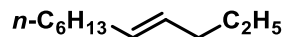
**$^{13}C$ -NMR** (75 MHz,  $CDCl_3$ )  $\delta_C$  [ppm] = 131.7, 124.5, 32.6, 31.9, 31.0, 29.7, 29.7, 29.6, 29.4, 29.2, 22.7, 18.0, 14.1.

**GC-MS** (EI, 70 eV,  $m/z$ ): 182  $[M]^+$ , 125, 111, 97, 83, 69, 55.

The data corresponds to the literature values.<sup>[70]</sup>

**(E)-octadec-7-ene**

Synthesized according to procedure A. Product purification by filtration over silica (hexanes).



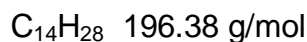
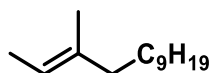
**<sup>1</sup>H-NMR** (300 MHz, CDCl<sub>3</sub>) δ<sub>H</sub> [ppm] = 5.45 – 5.30 (m, 2H), 2.06 – 1.84 (m, 4H), 1.38 – 1.21 (m, 10H), 0.88 (t, *J* = 7.4 Hz, 6H).

**<sup>13</sup>C-NMR** (75 MHz, CDCl<sub>3</sub>) δ<sub>C</sub> [ppm] = 130.6, 130.1, 34.7, 32.7, 31.8, 29.7, 28.9, 22.8, 22.7, 14.1, 13.7.

**GC-HRMS** (EI, 70 eV *m/z*): found 154.17198 [M]<sup>+</sup> (calculated 154.17160).

**(E)-3-methyltridec-2-ene**

Synthesized according to procedure A.



**<sup>1</sup>H-NMR** (300 MHz, Chloroform-*d*) δ 5.17 – 5.06 (m, 1H), 1.87 (m, 2H), 1.54 – 1.42 (m, 6H), 1.19 (m, 16H), 0.86 – 0.75 (m, 3H).

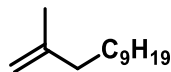
**<sup>13</sup>C-NMR** (75 MHz, CDCl<sub>3</sub>) δ 136.22, 117.93, 39.72, 31.94, 29.67, 29.60, 29.37, 28.02, 22.71, 15.57, 14.14, 13.33.

**GC-MS** (EI, 70 eV, *m/z*): 196 [M]<sup>+</sup>, 111, 97, 83, 70, 55.

The data corresponds to the literature values.<sup>[70]</sup>

**2-methyldodec-1-ene**

Synthesized according to procedure A. The purified product contains octadecane, wherein the separation has failed.



$C_{13}H_{26}$  182.35 g/mol

**$^1H$ -NMR** (300 MHz, Chloroform- $d$ )  $\delta$  4.65 – 4.55 (m, 2H), 1.93 (t,  $J$  = 7.5 Hz, 2H), 1.65 – 1.62 (m, 3H), 1.28 – 1.10 (m, 16H), 0.87 – 0.75 (m, 3H).

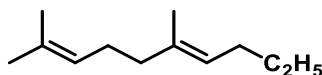
**$^{13}C$ -NMR** (75 MHz,  $CDCl_3$ )  $\delta$  146.4, 109.5, 37.9, 31.9, 29.6, 29.4, 27.7, 22.7, 22.4, 14.1.

**GC-MS** (EI, 70 eV,  $m/z$ ): 182  $[M]^+$ , 154, 126, 111, 97, 83, 69, 56.

The data corresponds to the literature values.<sup>[71]</sup>

**(*E*)-2,6-dimethyldeca-2,6-diene**

Synthesized according to procedure A.



$C_{12}H_{22}$  166.31 g/mol

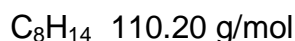
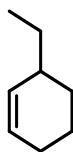
**$^1H$ -NMR** (300 MHz, Chloroform- $d$ )  $\delta$  5.10 – 5.00 (m, 2H), 2.05 – 1.80 (m, 6H), 1.64 – 1.59 (m, 6H), 1.56 – 1.54 (s, 3H), 1.34 – 1.20 (m, 2H), 0.86 – 0.69 (m, 3H).

**$^{13}C$ -NMR** (75 MHz,  $CDCl_3$ )  $\delta$  135.1, 131.5, 125.4, 124.4, 32.0, 30.0, 26.7, 25.7, 23.4, 23.2, 17.6, 13.9.

**GC-HRMS** (EI, 70 eV  $m/z$ ): found 166.17172  $[M]^{+*}$  (calculated 166.17160).

**3-ethylcyclohex-1-ene**

Synthesized according to procedure A.



**$^1\text{H-NMR}$**  (300 MHz, Chloroform- $d$ )  $\delta$  5.72 – 5.51 (m, 2H), 2.03 – 1.89 (m, 3H), 1.85 – 1.10 (m, 6H), 0.91 (t,  $J$  = 7.4 Hz, 3H).

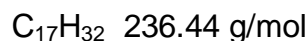
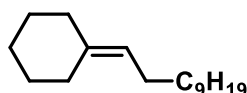
**$^{13}\text{C-NMR}$**  (75 MHz,  $\text{CDCl}_3$ )  $\delta$  132.1, 126.74, 36.9, 29.1, 28.7, 25.5, 21.6, 11.5.

**GC-MS** (EI, 70 eV,  $m/z$ ): 110  $[\text{M}]^+$ , 95, 81, 67, 53.

The data corresponds to the literature values.<sup>[72]</sup>

**Undecylidenecyclohexane**

Synthesized according to procedure A. The purified product contains octadecane, wherein the separation has failed.



**$^1\text{H-NMR}$**  (300 MHz, Chloroform- $d$ )  $\delta$  5.06 (tt,  $J$  = 7.3, 1.3 Hz, 1H), 2.16 – 1.89 (m, 6H), 1.57 – 1.41 (m, 6H), 1.26 (m, 16H), 0.94 – 0.82 (m, 3H).

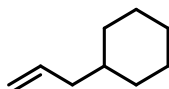
**$^{13}\text{C-NMR}$**  (75 MHz,  $\text{CDCl}_3$ )  $\delta_{\text{C}}$  [ppm] = 130.6, 130.1, 34.7, 32.7, 31.8, 29.7, 28.9, 22.8, 22.7, 14.1, 13.7.

**GC-HRMS** (EI, 70 eV,  $m/z$ ): found 236.2500  $[\text{M}]^{+*}$  (calculated 235.2499).



**Allylcyclohexane**

Synthesized according to procedure A.



$C_9H_{16}$  124.23 g/mol

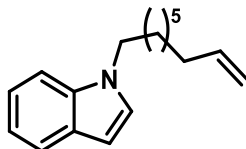
**$^1H$ -NMR** (300 MHz, Chloroform- $d$ )  $\delta$  5.72 (ddt,  $J$  = 17.4, 10.4, 7.2 Hz, 1H), 4.96 – 4.81 (m, 2H), 1.87 (m, 2H), 1.65 (s, 5H), 1.29 – 0.98 (m, 4H), 0.95 – 0.71 (m, 2H).

**$^{13}C$ -NMR** (75 MHz,  $CDCl_3$ )  $\delta$  137.71, 115.13, 41.95, 37.67, 33.07, 26.58, 26.34.

**GC-MS** (EI, 70 eV,  $m/z$ ): 124  $[M]^+$ , 83, 67, 55.

**1-(non-8-en-1-yl)-1*H*-indole**

Synthesized according to procedure A. The purified product contains 1-hexyl-1*H*-indole, wherein the separation has failed.



$C_{17}H_{23}N$  241.38 g/mol

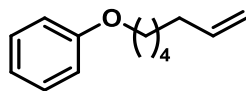
**TLC**  $R_f$  = 0.3 (hexanes/ethylacetate = 200/1)

**$^1H$ -NMR** (300 MHz, Chloroform- $d$ )  $\delta$  7.62 – 6.91 (m, 5H), 6.41 (d,  $J$  = 3.1 Hz, 1H), 5.81 – 5.61 (m, 1H), 4.99 – 4.78 (m, 2H), 4.03 (td,  $J$  = 7.1, 2.2 Hz, 2H), 1.97 (dq,  $J$  = 14.1, 7.0 Hz, 2H), 1.83 – 1.68 (m, 2H), 1.35 – 1.04 (m, 8H).

**GC-HRMS** (EI, 70 eV,  $m/z$ ): found 241.1824  $[M]^{+*}$  (calculated 241.1825).

**(hept-6-en-1-yloxy)benzene**

Synthesized according to procedure A. The purified product contains butoxybenzene, wherein the separation has failed.

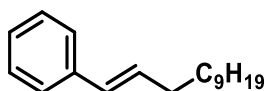


$C_{13}H_{18}O$  190.29 g/mol

<b><math>^1H</math>-NMR</b>	(300 MHz, Chloroform- $d$ ) $\delta$ 7.26 – 7.11 (m, 2H), 6.91 – 6.73 (m, 3H), 5.74 (ddt, $J$ = 16.9, 10.2, 6.6 Hz, 1H), 5.02 – 4.80 (m, 2H), 3.88 (t, $J$ = 6.5 Hz, 2H), 2.00 (m, 2H), 1.80 – 1.62 (m, 2H), 1.40 (m, 4H).
<b><math>^{13}C</math>-NMR</b>	(75 MHz, $CDCl_3$ ) $\delta$ 159.11, 138.85, 129.41, 120.49, 114.50, 67.77, 33.72, 29.18, 28.69, 25.60.
<b>GC-HRMS</b>	(EI, 70 eV $m/z$ ): found 190.13483 $[M]^{+*}$ (calculated 190.13522).

**(*E*)-1-phenyldodec-1-ene**

Synthesized according to procedure B.

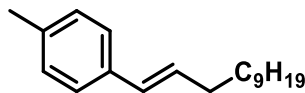


$C_{18}H_{28}$  244.42 g/mol

<b>TLC</b>	$R_f$ = 0.8 (hexanes)
<b><math>^1H</math>-NMR</b>	(300 MHz, $CDCl_3$ ) $\delta_H$ [ppm] = 7.41 - 7.14 (m, 5H), 6.38 (d, $J$ = 15.8 Hz, 1H), 6.23 (dt, $J$ = 15.8, 6.7 Hz, 1H), 2.21 (td, $J$ = 7.7, 1.0 Hz, 2H), 1.56 - 1.40 (m, 2H), 1.28 (s, 14H), 0.89 (t, $J$ = 6.7 Hz, 3H).
<b><math>^{13}C</math>-NMR</b>	(101 MHz, $CDCl_3$ ) $\delta_C$ [ppm] = 138.0, 131.3, 129.7, 128.5, 126.7, 125.9, 33.1, 31.9, 29.6, 29.6, 29.4, 29.4, 22.7, 14.1.
<b>GC-MS</b>	(EI, 70 eV, $m/z$ ): 244 $[M]^+$ , 171, 145, 129, 117, 104, 91, 77, 67, 55. The data correspond to the literature values. <sup>[73]</sup>

**(E)-1-(4-methylphenyl)-dodec-1-ene**

Synthesized according to procedure B. The purified product contains octadecane, wherein the separation has failed.



$C_{19}H_{30}$  258.45 g/mol

**TLC**

$R_f$  = 0.8 (hexanes)

 **$^1H$ -NMR**

(300 MHz,  $CDCl_3$ )  $\delta_H$  [ppm] = 7.26 - 7.20 (m, 2H), 7.10 (d,  $J$  = 8.0 Hz, 2H), 6.38 - 6.30 (m, 1H), 6.17 (dt,  $J$  = 15.8, 6.9 Hz, 1H), 2.32 (s, 3H), 2.19 (q,  $J$  = 6.8 Hz, 2H), 1.50 - 1.22 (m, 16H), 0.88 (t,  $J$  = 6.7 Hz, 3H).

 **$^{13}C$ -NMR**

(75 MHz,  $CDCl_3$ )  $\delta_C$  [ppm] = 136.4, 135.2, 130.3, 129.5, 129.2, 125.7, 33.1, 32.0, 29.7, 29.7, 29.6, 29.5, 29.4, 29.3, 22.7, 21.2, 14.2.

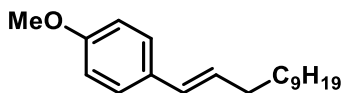
**GC-MS**

(EI, 70 eV,  $m/z$ ): 258  $[M]^+$ , 143, 131, 115, 106, 91, 77, 67, 55.

The data correspond to the literature values.<sup>[74]</sup>

**(E)-1-(4-methoxyphenyl)-dodec-1-ene**

Synthesized according to procedure B. The purified product contains octadecane, wherein the separation has failed.



$C_{19}H_{30}O$  274.45 g/mol

**TLC**

$R_f$  = 0.7 (hexanes)

 **$^1H$ -NMR**

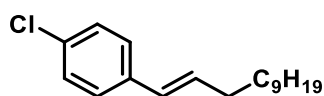
(300 MHz,  $CDCl_3$ )  $\delta_H$  [ppm] = 7.34 - 7.21 (m, 2H), 6.89 - 6.76 (m, 2H), 6.40 - 6.24 (m, 1H), 6.08 (dt,  $J$  = 15.8, 6.8 Hz, 1H), 3.81 (s, 3H), 2.25 - 2.09 (m, 2H), 1.49 - 1.16 (m, 16H), 0.88 (t,  $J$  = 6.7 Hz, 3H).

**$^{13}\text{C-NMR}$**  (75 MHz,  $\text{CDCl}_3$ )  $\delta_{\text{C}}$  [ppm] = 158.6, 130.8, 129.1, 129.0, 126.9, 113.9, 55.3, 33.1, 32.0, 29.7, 29.7, 29.7, 29.6, 29.4, 29.3, 22.7, 14.2.

**GC-MS** (EI, 70 eV,  $m/z$ ): 274  $[\text{M}]^+$ , 159, 147, 134, 121, 103, 91, 78, 67, 55.  
The data correspond to the literature values.<sup>[75]</sup>

**(E)-1-(4-chlorophenyl)-dodec-1-ene**

Synthesized according to procedure B.



$\text{C}_{18}\text{H}_{27}\text{Cl}$  278.86 g/mol

**TLC**  $R_f$  = 0.8 (hexanes)

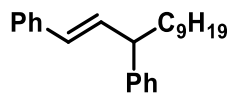
**$^1\text{H-NMR}$**  (300 MHz, Chloroform- $d$ )  $\delta$  7.18 (s, 4H), 6.25 (d,  $J$  = 15.9 Hz, 1H), 6.12 (dt,  $J$  = 15.8, 6.6 Hz, 1H), 2.12 (q,  $J$  = 7.0 Hz, 2H), 1.38 (t,  $J$  = 7.2 Hz, 2H), 1.29 – 1.14 (m, 14H), 0.88 – 0.73 (m, 3H).

**$^{13}\text{C-NMR}$**  (75 MHz,  $\text{CDCl}_3$ )  $\delta$  136.44, 132.24, 132.02, 128.57, 128.50, 127.09, 33.05, 31.93, 29.64, 29.54, 29.37, 29.31, 29.26, 22.72, 14.15.

**GC-HRMS** (EI, 70 eV  $m/z$ ): found 278.17889  $[\text{M}]^{+*}$  (calculated 278.17958).

**(E)-dodec-1-ene-1,3-diyl dibenzene**

Synthesized according to procedure B.



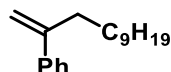
$\text{C}_{24}\text{H}_{32}$  320.52 g/mol

**TLC**  $R_f$  = 0.8 (hexanes)

<b><math>^1\text{H-NMR}</math></b>	(300 MHz, Chloroform- $d$ ) $\delta$ 7.33 – 7.02 (m, 10H), 6.38 – 6.17 (m, 2H), 3.32 (q, $J$ = 7.2 Hz, 1H), 1.75 (s, 2H), 1.19 (m, 14H), 0.85 – 0.74 (m, 3H).
<b><math>^{13}\text{C-NMR}</math></b>	(75 MHz, $\text{CDCl}_3$ ) $\delta$ 144.77, 137.63, 134.51, 129.22, 128.68, 128.47, 128.45, 128.31, 127.64, 126.99, 126.13, 125.74, 49.21, 35.92, 31.90, 29.62, 29.56, 29.33, 27.65, 22.70, 14.14.
<b>GC-HRMS</b>	(EI, 70 eV, $m/z$ ): found 320.2483 $[\text{M}]^{++}$ (calculated 320.2499).

**dodec-1-en-2-ylbenzene**

Synthesized according to procedure B.



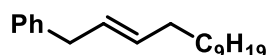
$\text{C}_{18}\text{H}_{28}$  244.42 g/mol

<b>TLC</b>	$R_f$ = 0.8 (hexanes)
<b><math>^1\text{H-NMR}</math></b>	(300 MHz, Chloroform- $d$ ) $\delta$ 7.46 – 7.20 (m, 5H), 5.26 (d, $J$ = 1.6 Hz, 1H), 5.05 (q, $J$ = 1.4 Hz, 1H), 2.49 (td, $J$ = 7.4, 1.3 Hz, 2H), 1.44 (s, 1H), 1.43 – 1.19 (m, 15H), 0.93 – 0.82 (m, 3H).
<b><math>^{13}\text{C-NMR}</math></b>	(75 MHz, $\text{CDCl}_3$ ) $\delta$ 148.78, 141.47, 128.21, 127.22, 126.11, 112.00, 35.37, 31.93, 29.63, 29.48, 29.38, 28.28, 22.72, 14.16.
<b>GC-MS</b>	(EI, 70 eV, $m/z$ ): 244 $[\text{M}]^+$ , 143, 131, 118, 103, 91, 77, 77, 55.

The data correspond to the literature values.<sup>[76]</sup>

**(E)-tridec-2-en-1-ylbenzene**

Synthesized according to procedure B.



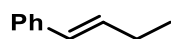
$\text{C}_{19}\text{H}_{30}$  258.45 g/mol

<b>TLC</b>	$R_f$ = 0.8 (hexanes)
------------	-----------------------

<b><math>^1\text{H-NMR}</math></b>	(300 MHz, Chloroform- $d$ ) $\delta$ 7.40 – 7.24 (m, 2H), 7.24 – 7.09 (m, 3H), 5.67 – 5.42 (m, 2H), 3.33 (d, $J$ = 5.3 Hz, 2H), 2.09 – 1.95 (m, 2H), 1.40 – 1.20 (m, 16 H), 0.96 – 0.83 (m, 3H).
<b><math>^{13}\text{C-NMR}</math></b>	(75 MHz, $\text{CDCl}_3$ ) $\delta$ 141.16, 132.19, 128.64, 128.48, 128.32, 125.84, 39.09, 32.55, 31.95, 29.66, 29.54, 29.51, 29.38, 29.23, 22.73, 14.17.
<b>GC-HRMS</b>	(EI, 70 eV, $m/z$ ): found 258.2337 $[\text{M}]^{+}$ (calculated 258.2342).

**(*E*)-but-1-en-1-ylbenzene**

Synthesized according to procedure B.



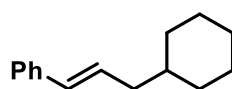
$\text{C}_{10}\text{H}_{12}$  132.21 g/mol

<b>TLC</b>	$R_f$ = 0.8 (hexanes)
<b><math>^1\text{H-NMR}</math></b>	(300 MHz, Chloroform- $d$ ) $\delta$ 7.41 – 7.32 (m, 2H), 7.32 – 7.14 (m, 3H), 6.45 – 6.33 (m, 1H), 6.28 (dt, $J$ = 15.9, 6.1 Hz, 1H), 2.32 – 2.15 (m, 2H), 1.10 (t, $J$ = 7.5 Hz, 3H).
<b><math>^{13}\text{C-NMR}</math></b>	(75 MHz, $\text{CDCl}_3$ ) $\delta$ 137.93, 132.66, 128.76, 128.48, 126.76, 125.90, 26.10, 13.68.
<b>GC-MS</b>	$R_t$ = 5.72 min (EI, 70 eV, $m/z$ ): 132 $[\text{M}]^+$ , 117, 104, 91, 77, 63, 51.

The data correspond to the literature values.<sup>[77]</sup>

**(*E*)-(3-cyclohexylprop-1-en-1-yl)benzene.**

Synthesized according to procedure B.

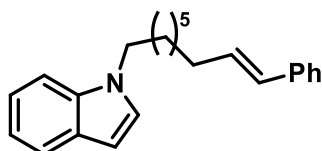


$\text{C}_{15}\text{H}_{20}$  200.33 g/mol

<b><sup>1</sup>H-NMR</b>	(300 MHz, Chloroform-d) $\delta$ 7.18 (ddt, $J$ = 27.9, 14.1, 7.3 Hz, 5H), 6.28 (d, $J$ = 15.8 Hz, 1H), 6.14 (dt, $J$ = 15.4, 7.1 Hz, 1H), 2.01 (dd, $J$ = 15.6, 8.7 Hz, 2H), 1.63 (q, $J$ = 13.2, 12.3 Hz, 5H), 1.32 (ddd, $J$ = 11.0, 7.3, 3.6 Hz, 1H), 1.15 (dt, $J$ = 20.3, 7.1 Hz, 3H), 1.00 – 0.74 (m, 2H).
<b><sup>13</sup>C-NMR</b>	(75 MHz, CDCl <sub>3</sub> ) $\delta$ 137.94, 130.68, 129.78, 128.46, 126.74, 125.91, 41.08, 38.22, 33.23, 26.59, 26.38.
<b>GC-MS</b>	(EI, 70 eV, $m/z$ ): 200 [M] <sup>+</sup> , 141, 128, 115, 104, 91, 83, 77, 65, 55. The data correspond to the literature values. [78]

**(*E*)-1-(9-phenylnon-8-en-1-yl)-1*H*-indole**

Synthesized according to procedure B.

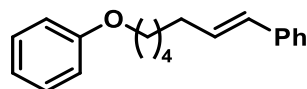


C<sub>23</sub>H<sub>27</sub>N 317.48 g/mol

<b>TLC</b>	$R_f$ = 0.3 (hexanes/ethylacetate = 200/1)
<b><sup>1</sup>H-NMR</b>	(300 MHz, Chloroform-d) $\delta$ 7.64 (d, $J$ = 7.8 Hz, 1H), 7.40 – 7.03 (m, 9H), 6.49 (s, 1H), 6.37 (d, $J$ = 15.9 Hz, 1H), 6.21 (dt, $J$ = 15.8, 6.8 Hz, 1H), 4.19 – 4.01 (m, 2H), 2.26 – 2.04 (m, 2H), 1.86 (q, $J$ = 8.1, 7.0 Hz, 2H), 1.51 – 1.39 (m, 2H), 1.38 – 1.21 (m, 6H).
<b><sup>13</sup>C-NMR</b>	(75 MHz, CDCl <sub>3</sub> ) $\delta$ 137.87, 135.92, 131.02, 129.80, 128.49, 127.81, 126.80, 125.90, 121.28, 120.93, 119.14, 109.38, 100.82, 46.42, 32.98, 30.26, 29.27, 29.15, 29.07, 26.99.
<b>GC-HRMS</b>	(EI, 70 eV $m/z$ ): found 317.21286 [M] <sup>+</sup> (calculated 317.21380).

**(E)-(7-phenoxyhept-1-en-1-yl)benzene**

Synthesized according to procedure B.

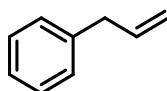


$C_{19}H_{22}O$  266.38 g/mol

<b>TLC</b>	$R_f = 0.4$ (hexanes/ethylacetate = 200/1)
<b><math>^1H</math>-NMR</b>	(300 MHz, Chloroform- $d$ ) $\delta$ 7.40 – 7.27 (m, 6H), 7.27 – 7.11 (m, 1H), 7.07 – 6.84 (m, 3H), 6.46 – 6.33 (m, 1H), 6.23 (dt, $J = 15.8$ , 6.8 Hz, 1H), 3.97 (t, $J = 6.5$ Hz, 2H), 2.25 (tdd, $J = 7.0$ , 5.6, 1.4 Hz, 2H), 1.90 – 1.72 (m, 2H), 1.65 – 1.44 (m, 4H).
<b><math>^{13}C</math>-NMR</b>	(75 MHz, $CDCl_3$ ) $\delta$ 159.05, 137.81, 130.79, 129.97, 129.42, 128.49, 126.83, 125.92, 120.48, 114.47, 67.73, 32.97, 29.19, 29.13, 25.68.
<b>GC-HRMS</b>	(EI, 70 eV, $m/z$ ): found 266.1661 $[M]^{+}$ (calculated 266.1665).

**Allylbenzene**

Synthesized according to procedure B.



$C_9H_{10}$  118.18 g/mol

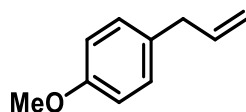
<b><math>^1H</math>-NMR</b>	(300 MHz, Chloroform- $d$ ) $\delta$ 7.30 – 6.96 (m, 5H), 5.89 (m, 1H), 5.09 – 4.89 (m, 2H), 3.31 (d, $J = 6.6$ Hz, 2H).
<b><math>^{13}C</math>-NMR</b>	(75 MHz, $CDCl_3$ ) $\delta$ 140.07, 137.48, 128.61, 128.44, 126.08, 115.80, 40.28.
<b>GC-MS</b>	(EI, 70 eV, $m/z$ ): 118 $[M]^{+}$ , 91, 65.

The data corresponds to the literature values.<sup>[79]</sup>



**4-allylanisole**

Synthesized according to procedure B.



$C_{10}H_{12}O$  148.21 g/mol

**TLC**

$R_f = 0.6$  (hexanes/ethylacetate 20/1)

 **$^1H$ -NMR**

(300 MHz,  $CDCl_3$ )  $\delta_H$  [ppm] = 7.16 - 7.08 (m, 2H), 6.89 - 6.81 (m, 2H), 5.96 (ddt,  $J = 16.8, 10.4, 6.6$  Hz, 1H), 5.12 - 5.06 (m, 1H), 5.04 (d,  $J = 0.7$  Hz, 1H), 3.80 (s, 3H), 3.34 (d,  $J = 6.6$  Hz, 2H).

 **$^{13}C$ -NMR**

(75 MHz,  $CDCl_3$ )  $\delta_C$  [ppm] = 158.0, 137.9, 132.1, 129.5, 115.5, 113.8, 55.3, 39.4.

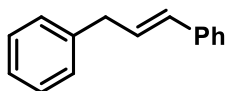
**GC-MS**

(EI, 70 eV,  $m/z$ ): 148  $[M]^+$ .

The data corresponds to the literature values.<sup>[80]</sup>

**(*E*)-prop-1-ene-1,3-diylidibenzene**

Synthesized according to procedure B.



$C_{15}H_{14}$  194.28 g/mol

**TLC**

$R_f = 0.3$  (hexanes)

 **$^1H$ -NMR**

(300 MHz,  $CDCl_3$ )  $\delta_H$  [ppm] = 7.30 - 7.08 (m, 10H), 6.42 - 6.27 (m, 2H), 3.47 (d,  $J = 6.4$  Hz, 2H).

 **$^{13}C$ -NMR**

(75 MHz,  $CDCl_3$ )  $\delta$  140.18, 137.49, 131.09, 129.24, 128.76, 128.51, 127.18, 126.19, 126.14, 39.37.

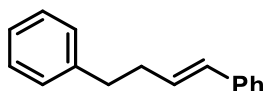
**GC-MS**

(EI, 70 eV,  $m/z$ ): 194  $[M]^+$ , 179, 165, 115, 102, 91, 78, 65, 51.

The data corresponds to the literature values.<sup>[81]</sup>

**(E)-but-1-ene-1,4-diylidibenzene**

Synthesized according to procedure B.



$C_{16}H_{16}$  208.30 g/mol

**$^1H$ -NMR** (300 MHz, Chloroform- $d$ )  $\delta$  7.32 (m Hz, 10H), 6.47 (d,  $J$  = 16.0 Hz, 1H), 6.32 (dt,  $J$  = 15.1, 6.7 Hz, 1H), 2.84 (t,  $J$  = 7.8 Hz, 2H), 2.58 (q,  $J$  = 7.4 Hz, 2H).

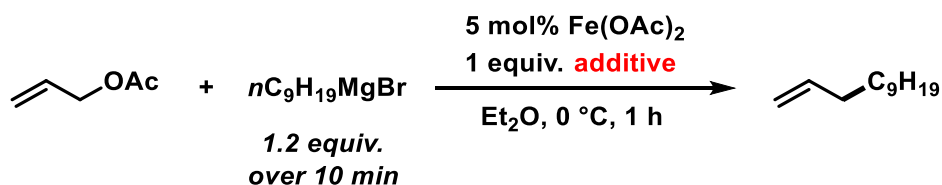
**$^{13}C$ -NMR** (75 MHz,  $CDCl_3$ )  $\delta$  141.78, 137.74, 130.40, 129.99, 128.50, 128.38, 126.96, 126.02, 125.91, 35.91, 34.91.

**GC-MS** (EI, 70 eV,  $m/z$ ): 208  $[M]^+$ , 117, 102, 91, 77, 65, 51.

The data corresponds to the literature values.<sup>[81]</sup>

**3.4.3 Mechanistic Investigations**

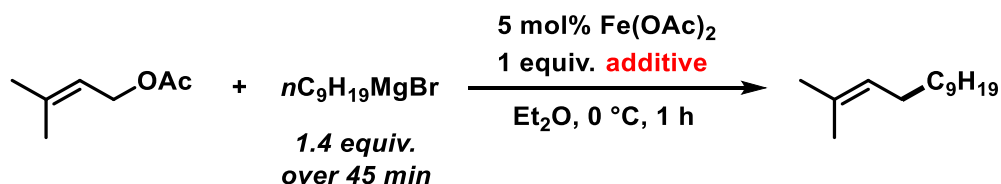
External Functional Group Test / Effect of electrophiles



A suspension of  $\text{Fe}(\text{OAc})_2$  (0.025 mmol, 4.3 mg) in absolute  $\text{Et}_2\text{O}$  (2 mL) was cooled to 0 °C under a nitrogen atmosphere in a flame dried reaction tube. After the addition of freshly distilled allyl acetate (0.5 mmol, 54  $\mu\text{L}$ ) and additive, a 1.0 M  $n$ -nonylmagnesium bromide solution (0.6 mmol, 0.6 mL) in  $\text{Et}_2\text{O}$  was added dropwise over a period of 10 minutes and the mixture was stirred at 0 °C for 1 hour. The reaction mixture was then hydrolyzed with a saturated  $\text{NH}_4\text{Cl}$  solution and the aqueous phase was extracted with  $\text{EtOAc}$ . Products were analyzed via GC-MS and GC-FID.

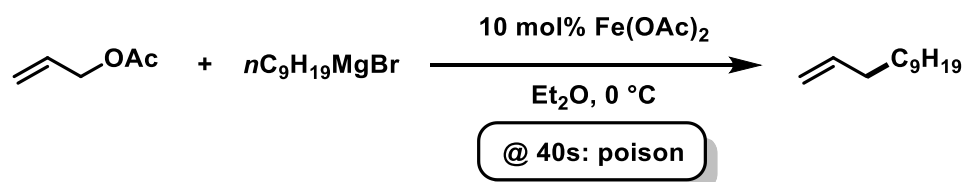
Entry	Additive	Additive conversion [%] <sup>a</sup>	Yield [%] <sup>a</sup>
1	-	-	77
2	PhCN	0	21
3	<i>n</i> -C <sub>3</sub> H <sub>7</sub> CN	9	49
4	PhNO <sub>2</sub>	90	<1
5	EtNO <sub>2</sub>	87	8
6	PhNH <sub>2</sub>	77	9
7	<i>n</i> -C <sub>6</sub> H <sub>13</sub> NH <sub>2</sub>	0	80
8	PhCHO	100	16
9	<b>PhCO<sub>2</sub>Me</b>	<b>0</b>	<b>82</b>
10	<i>n</i> -C <sub>3</sub> H <sub>7</sub> CO <sub>2</sub> Me	4	72
11	PhOH	0	75 <sup>b</sup>
12	<i>n</i> -C <sub>5</sub> H <sub>11</sub> OH	6	79 <sup>b</sup>

<sup>a</sup> Yields were determined by quantitative GC-FID vs. internal *n*-pentadecane. <sup>b</sup> 2.2 equiv. *n*-C<sub>9</sub>H<sub>19</sub>MgBr.

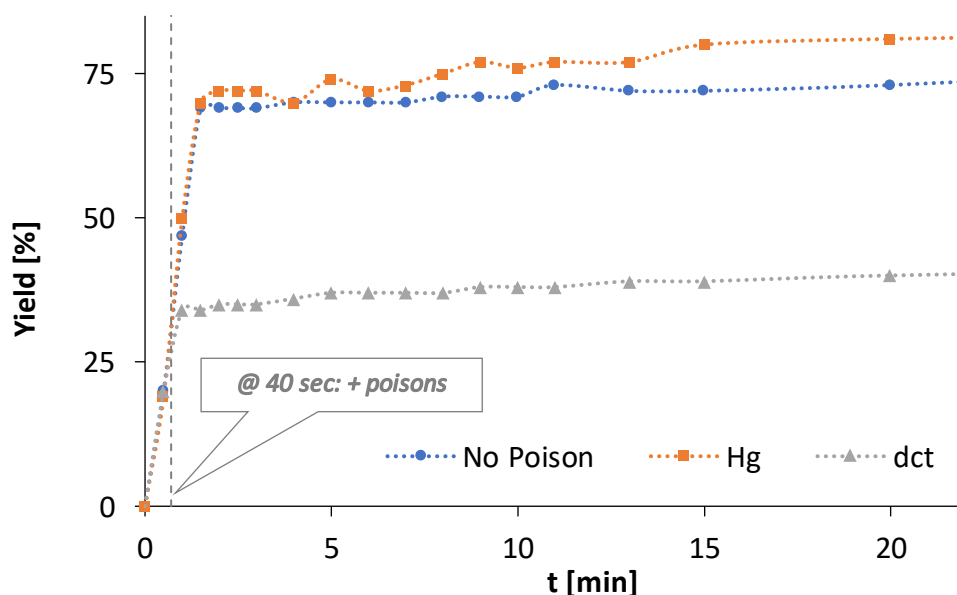


Entry	Additive	Yield [%] <sup>a</sup>	Estimated sideproduct <sup>b</sup>
1	-	27	-
2	1,2- Dichloroethane	27	-
3	Chlorobenzene	24	-
4	Chloroform	58	 m/z = 266
5	Air	37	 m/z = 126 <sup>c</sup>
6	PhCO <sub>2</sub> Me	31	 m/z = 342

<sup>a</sup> Yields were determined by quantitative GC-FID vs. internal *n*-pentadecane. <sup>b</sup> Masses recorded by GC-MS. <sup>c</sup> Retention time at 6.0 min vs. actual Nonenes at 3.7-4.0 min.

*Kinetic Poisoning*

A suspension of  $\text{Fe}(\text{OAc})_2$  (0.05 mmol, 8.7 mg) and *n*-pentadecane (0.18 mmol, 50  $\mu\text{L}$ ) in absolute  $\text{Et}_2\text{O}$  (4 mL) was cooled to 0  $^\circ\text{C}$  under a nitrogen atmosphere in a flame dried schlenk flask. After the addition of freshly distilled allyl acetate (0.50 mmol, 54  $\mu\text{L}$ ), a 1.0 M *n*-nonylmagnesium bromide solution (0.50 mmol, 0.5 mL) in  $\text{Et}_2\text{O}$  was added dropwise over a period of 2 minutes and the mixture was stirred at 0  $^\circ\text{C}$ . Samples of 0.1 mL were taken out during the reaction and hydrolyzed with a saturated  $\text{NH}_4\text{Cl}$  solution. In case of poisoning, the Hg (5.00 mmol, 148  $\mu\text{L}$ ) or Dibenzocyclooctatetrene (dct, 0.25 mmol, 51 mg, dissolved in 0.4 mL absolute  $\text{Et}_2\text{O}$ ) respectively was added after 40 seconds. The yields were determined by quantitative GC-FID vs. *n*-pentadecane as internal standard.

*Filtration Test*

A suspension of  $\text{Fe}(\text{OAc})_2$  (0.05 mmol, 8.7 mg) in absolute  $\text{Et}_2\text{O}$  (2 mL) was cooled to 0  $^\circ\text{C}$  under a nitrogen atmosphere in a flame dried schlenk flask. After the addition of

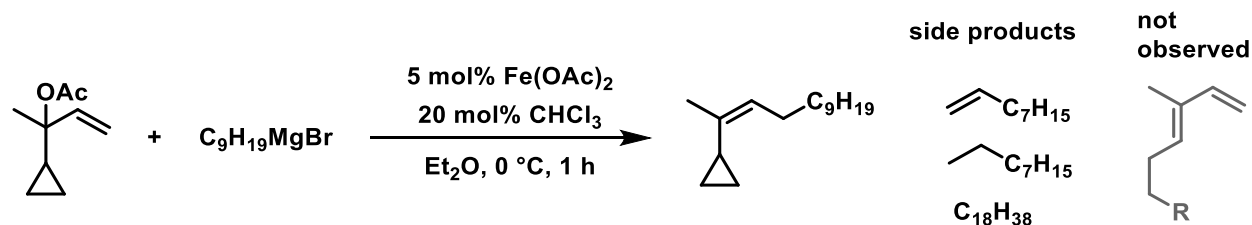
freshly distilled allyl acetate (0.50 mmol, 54  $\mu$ L), a 1.0 M *n*-nonylmagnesium bromide solution (0.50 mmol, 0.5 mL) in Et<sub>2</sub>O was added dropwise over a period of 10 minutes and the mixture was stirred at 0 °C for 1 hour. A sample was taken out (Yield coupling product 78%) and the reaction mixture was filtered.

To the filtrate another 0.5 mmol of allyl acetate and *n*-nonylmagnesium bromide (over 10 min) was added at 0 °C and another reaction cycle was run (Yield 2<sup>nd</sup> cycle filtrate 61%).

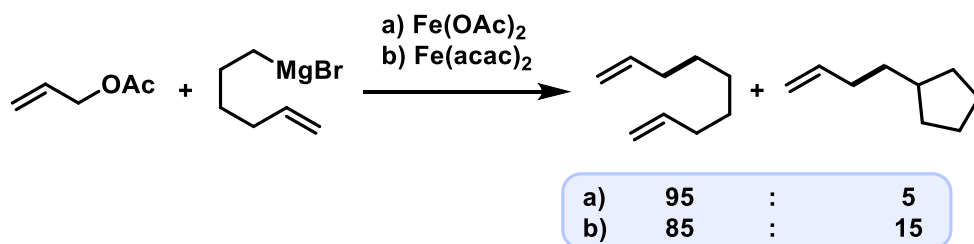
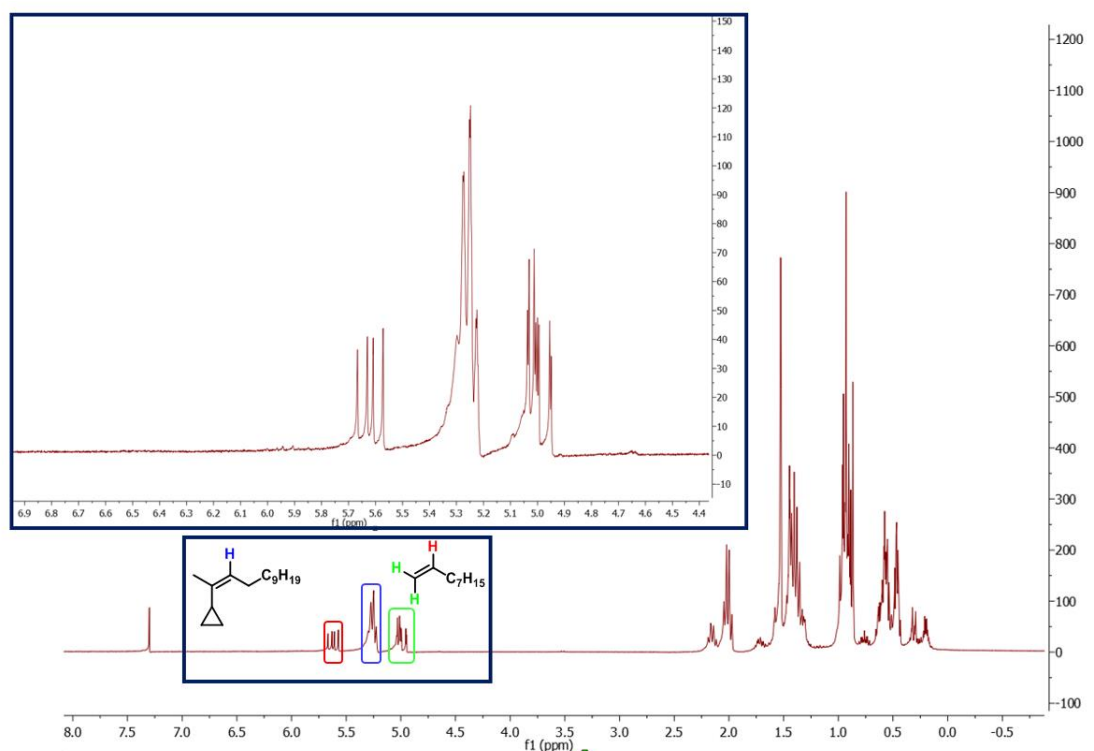
The residue of the filtration was washed with absolute Et<sub>2</sub>O (2 x 2 mL) and added to 0.5 mmol allyl acetate in 2 mL absolute Et<sub>2</sub>O. 0.5 mmol of *n*-nonylmagnesium bromide was added at 0 °C over 10 min and another reaction cycle was run (Yield 2<sup>nd</sup> cycle residue 45%).

The yields were determined by quantitative GC-FID vs. *n*-pentadecane as internal standard.

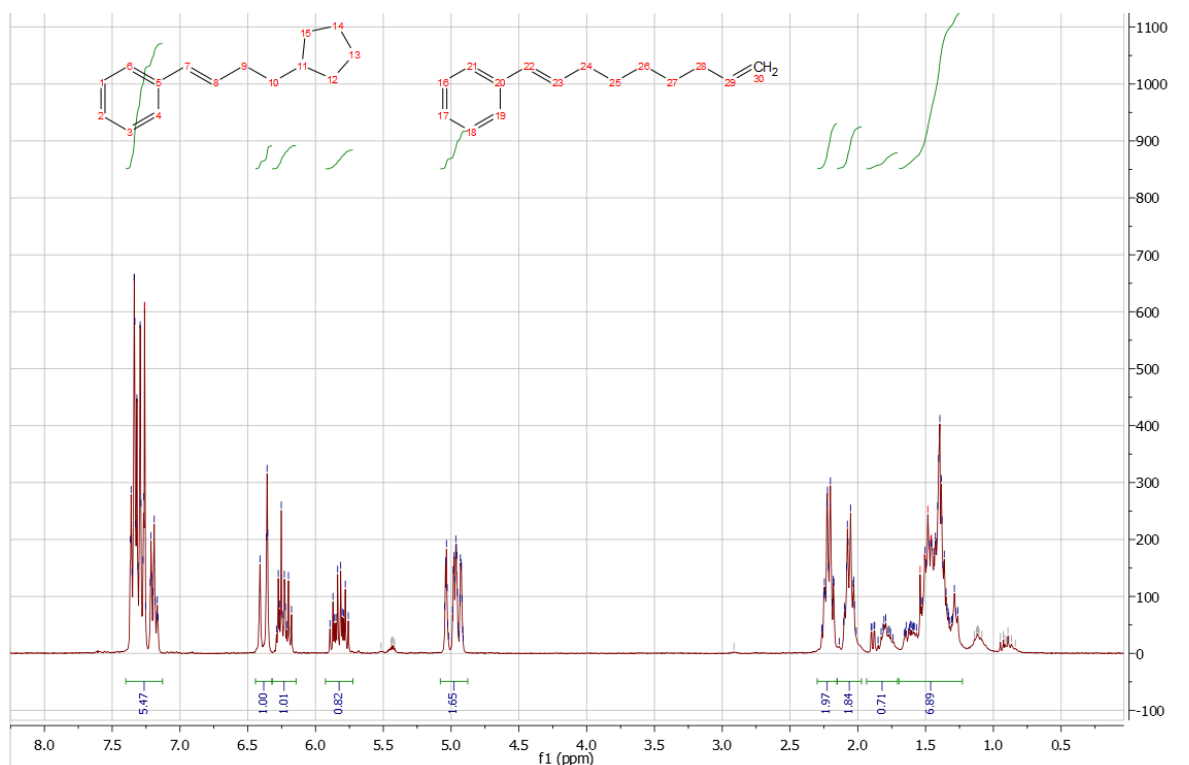
#### Radical Clock Experiments



The reaction was carried out as described in Protocol A. The crude NMR showed no ring opening of the cyclopropane as no signal evolved at around 6.X ppm, which would indicate the presence of the diene moiety.<sup>[82]</sup>



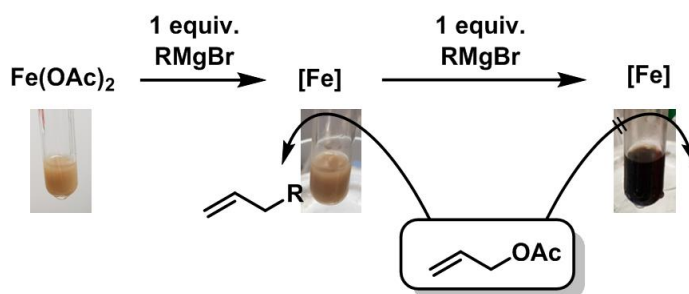
The reaction was carried out as described in a) Protocol A without addition of  $\text{CHCl}_3$  and b) Protocol B. The Grignard reagent (2% ring closure) and the reactions were analyzed by GC-MS and GC-FID. When using cinnamylacetate as the starting material, isolation and NMR analysis of the coupling products was possible, showing roughly 15% of additional ring closure.



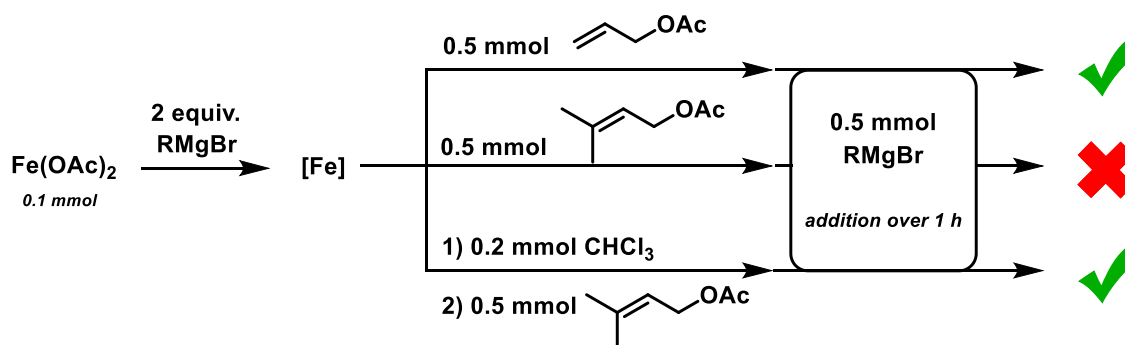
#### *Stoichiometric Reduction Experiments*

For determining the oxidation states of the active catalyst, the following experiments have been done:

A solution of  $\text{Fe}(\text{OAc})_2$  (17.4 mg, 0.1 mmol) in 1 mL diethylether was mixed with **A**) 1 equiv. or **B**) 2 equiv. of  $\text{C}_9\text{H}_{19}\text{MgBr}$  (1 M in diethylether).

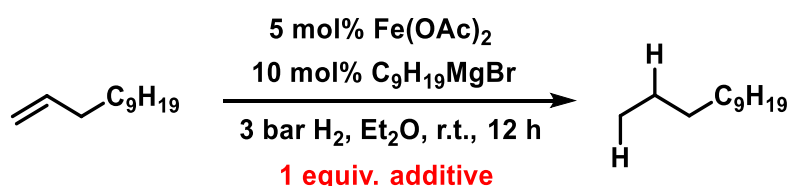


- These suspensions were then added dropwise to separate solutions of allylacetate (0.1 mmol) in 1 mL diethylether. In case of **A** formation of cross coupling product dodecene could be observed (29%), whereas in **B** only traces could be observed.



- To a solution of **B** was added **B1**) 0.5 mmol of allylacetate, **B2**) 0.5 mmol prenyl acetate or **B3**) 0.2 mmol chloroform and 0.5 mmol prenylacetate. To these solutions was added 0.5 mmol  $\text{C}_9\text{H}_{19}\text{MgBr}$  over a period of 1 hour. In case of **B1** and **B3** catalytic activity was observed, whereas in **B2** it was not, showing that allylacetate could possibly reoxidize the catalyst, where in the case of prenylacetate  $\text{CHCl}_3$  was necessary as an oxidizing agent.

#### Hydrogenation Poisoning studies



1-Dodecene (0.25 mmol), 5 mol%  $\text{Fe}(\text{OAc})_2$  and 1 equiv. of additive were mixed in a flame dried autoclave vial in an argon-filled glovebox. 10 mol% of  $\text{C}_9\text{H}_{19}\text{MgBr}$  was added and the mixture was stirred vigorously for 2 min. The rubber septum was penetrated with a cannula and the reaction vial was put into an autoclave, which was set under a pressure of 3 bar of  $\text{H}_2$ . The reaction was stirred overnight at r.t. and then quenched with aqueous  $\text{NH}_4\text{Cl}$  solution. The organic phase was extracted with ethyl acetate, dried over sodium sulfate and filtered over a short layer of silica. The yields were determined by quantitative GC-FID vs. *n*-pentadecane as internal standard.

Entry	Additive	Conversion [%]	Yield [%]
1	-	100	77
2	$\text{MgBr}_2$	19	<1
3	$\text{MgCl}_2$	100	72
4	$\text{LiBr}$	3	<1



### 3.5 References

- [1] A. d. Meijere, F. Diederich, *Metal-catalyzed cross-coupling reactions*, 2. Auflage, Wiley-VCH, Weinheim **2004**.
- [2] E.-i. Negishi, *Angew. Chem. Int. Ed.* **2011**, *50*, 6738–6764.
- [3] C. C. C. Johansson Seechurn, M. O. Kitching, T. J. Colacot, V. Snieckus, *Angew. Chem. Int. Ed.* **2012**, *51*, 5062–5085.
- [4] A. Fürstner, *ACS Cent. Sci.* **2016**, *2*, 778–789.
- [5] W. M. Czaplik, M. Mayer, J. Cvengros, A. Jacobi von Wangelin, *ChemSusChem* **2009**, *2*, 396–417.
- [6] I. Bauer, H.-J. Knölker, *Chem. Rev.* **2015**, *115*, 3170–3387.
- [7] R. Jana, T. P. Pathak, M. S. Sigman, *Chem. Rev.* **2011**, *111*, 1417–1492.
- [8] M. D. Greenhalgh, A. S. Jones, S. P. Thomas, *ChemCatChem* **2015**, *7*, 190–222.
- [9] A. S. Jones, J. F. Paliga, M. D. Greenhalgh, J. M. Quibell, A. Steven, S. P. Thomas, *Org. Lett.* **2014**, *16*, 5964–5967.
- [10] B. Plietker, M. Beller, *Iron Catalysis. Fundamentals and Applications*, Springer-Verlag Berlin Heidelberg, Berlin, Heidelberg **2011**.
- [11] D.-G. Yu, B.-J. Li, Z.-J. Shi, *Acc. Chem. Res.* **2010**, *43*, 1486–1495.
- [12] A. L. Silberstein, S. D. Ramgren, N. K. Garg, *Org. Lett.* **2012**, *14*, 3796–3799.
- [13] T. Mesganaw, N. K. Garg, *Org. Process Res. Dev.* **2013**, *17*, 29–39.
- [14] T. Agrawal, S. P. Cook, *Org. Lett.* **2013**, *15*, 96–99.
- [15] M. Mayer, W. M. Czaplik, A. Jacobi von Wangelin, *Adv. Synth. Catal.* **2010**, *352*, 2147–2152.
- [16] D. Gärtner, A. L. Stein, S. Grupe, J. Arp, A. Jacobi von Wangelin, *Angew. Chem. Int. Ed.* **2015**, *54*, 10545–10549.
- [17] S. N. Kessler, J.-E. Bäckvall, *Angew. Chem. Int. Ed.* **2016**, *55*, 3734–3738.
- [18] B. Plietker, *Angew. Chem. Int. Ed.* **2006**, *45*, 1469–1473.
- [19] G. K. Jarugumilli, S. P. Cook, *Org. Lett.* **2011**, *13*, 1904–1907.
- [20] S. J. Ladoulis, K. M. Nicholas, *J. Organomet. Chem.* **1985**, *285*, C13–C16.
- [21] J. L. Roustan, J. Y. Mérour, F. Houlihan, *Tetrahedron Lett.* **1979**, *20*, 3721–3724.
- [22] Y. Xu, B. Zhou, *J. Org. Chem.* **1987**, *52*, 974–977.
- [23] B. Plietker, *Angew. Chem. Int. Ed.* **2006**, *45*, 6053–6056.
- [24] R. Trivedi, J. A. Tunge, *Org. Lett.* **2009**, *11*, 5650–5652.
- [25] M. Jegelka, B. Plietker, *Org. Lett.* **2009**, *11*, 3462–3465.
- [26] B. Plietker, A. Dieskau, K. Möws, A. Jatsch, *Angew. Chem. Int. Ed.* **2008**, *47*, 198–201.
- [27] L. Qi, E. Ma, F. Jia, Z. Li, *Tetrahedron Lett.* **2016**, *57*, 2211–2214.
- [28] K. G. Dongol, H. Koh, M. Sau, C. L. L. Chai, *Adv. Synth. Catal.* **2007**, *349*, 1015–1018.
- [29] M. Guisán-Ceinos, F. Tato, E. Buñuel, P. Calle, D. J. Cárdenas, *Chem. Sci.* **2013**, *4*, 1098.

- [30] T. Hatakeyama, T. Hashimoto, K. K. A. D. S. Kathriarachchi, T. Zenmyo, H. Seike, M. Nakamura, *Angew. Chem. Int. Ed.* **2012**, *51*, 8834–8837.
- [31] T. N. Gieshoff, U. Chakraborty, M. Villa, A. Jacobi von Wangelin, *Angew. Chem. Int. Ed.* **2017**, *56*, 3585–3589.
- [32] S. C. Bart, E. Lobkovsky, P. J. Chirik, *J. Am. Chem. Soc.* **2004**, *126*, 13794–13807.
- [33] R. J. Trovitch, E. Lobkovsky, E. Bill, P. J. Chirik, *Organometallics* **2008**, *27*, 1470–1478.
- [34] P.-H. Phua, L. Lefort, J. A. F. Boogers, M. Tristany, J. G. de Vries, *Chem. Commun.* **2009**, 3747–3749.
- [35] C. Rangheard, C. de Julián Fernández, P.-H. Phua, J. Hoorn, L. Lefort, J. G. de Vries, *Dalton Trans.* **2010**, *39*, 8464–8471.
- [36] A. Welther, A. Jacobi von Wangelin, *Curr. Org. Chem.* **2013**, *17*, 326–335.
- [37] A. J. MacNair, M.-M. Tran, J. E. Nelson, G. U. Sloan, A. Ironmonger, S. P. Thomas, *Org. Biomol. Chem.* **2014**, *12*, 5082–5088.
- [38] W. Schlenk, W. Schlenk, *Ber. dtsch. Chem. Ges. A/B* **1929**, *62*, 920–924.
- [39] J. Kleimark, P.-F. Larsson, P. Emamy, A. Hedström, P.-O. Norrby, *Adv. Synth. Catal.* **2012**, *354*, 448–456.
- [40] Y. Gartia, S. Pulla, P. Ramidi, C. C. Farris, Z. Nima, D. E. Jones, A. S. Biris, A. Ghosh, *Catal. Lett.* **2012**, *142*, 1397–1404.
- [41] R. H. Crabtree, *Chem. Rev.* **2012**, *112*, 1536–1554.
- [42] J. A. Widegren, R. G. Finke, *J. Mol. Catal. A: Chem.* **2003**, *198*, 317–341.
- [43] S. Mørup, S. Linderöth, J. Jacobsen, M. Holmblad, *Hyperfine Interact.* **1992**, *69*, 489–492.
- [44] S. Linderöth, S. Morup, *J. Phys.: Condens. Matter* **1992**, *4*, 8627–8634.
- [45] D. R. Anton, R. H. Crabtree, *Organometallics* **1983**, *2*, 855–859.
- [46] G. Franck, M. Brill, G. Helmchen in *Organic Syntheses Based on Name Reactions* (Hrsg.: A. Hassner, C. Stumer), Elsevier, Burlington **2002**.
- [47] A. Hedström, Z. Izakian, I. Vreto, C.-J. Wallentin, P.-O. Norrby, *Chem. Eur. J.* **2015**, *21*, 5946–5953.
- [48] R. B. Bedford, *Acc. Chem. Res.* **2015**, *48*, 1485–1493.
- [49] P. G. N. Neate, M. D. Greenhalgh, W. W. Brennessel, S. P. Thomas, M. L. Neidig, *J. Am. Chem. Soc.* **2019**, *141*, 10099–10108.
- [50] D. Griller, K. U. Ingold, *Acc. Chem. Res.* **2002**, *13*, 317–323.
- [51] R. P. Yu, J. M. Darmon, J. M. Hoyt, G. W. Margulieux, Z. R. Turner, P. J. Chirik, *ACS Catal.* **2012**, *2*, 1760–1764.
- [52] A. Welther, M. Bauer, M. Mayer, A. Jacobi von Wangelin, *ChemCatChem* **2012**, *4*, 1088–1093.
- [53] T. N. Gieshoff, M. Villa, A. Welther, M. Plois, U. Chakraborty, R. Wolf, A. Jacobi von Wangelin, *Green Chem.* **2015**, *17*, 1408–1413.
- [54] D. Gärtner, A. Welther, B. R. Rad, R. Wolf, A. Jacobi von Wangelin, *Angew. Chem. Int. Ed.* **2014**, *53*, 3722–3726.
- [55] P. J. Chirik, *Acc. Chem. Res.* **2015**, *48*, 1687–1695.
- [56] K. Junge, K. Schröder, M. Beller, *Chem. Commun.* **2011**, *47*, 4849–4859.

- [57] G. Rai, C. J. Thomas, W. Leister, D. J. Maloney, *Tetrahedron Lett.* **2009**, 50, 1710–1713.
- [58] N. Shimojoh, Y. Imura, K. Moriyama, H. Togo, *Tetrahedron* **2011**, 67, 951–957.
- [59] W. Lölsberg, S. Ye, H.-G. Schmalz, *Adv. Synth. Catal.* **2010**, 352, 2023–2031.
- [60] O. Geiseler, J. Podlech, *Tetrahedron* **2012**, 68, 7280–7287.
- [61] D. Francová, G. Kickelbick, *Monatsh. Chem.* **2009**, 140, 413–422.
- [62] Watson, Iain D G, A. K. Yudin, *J. Am. Chem. Soc.* **2005**, 127, 17516–17529.
- [63] S. Magens, M. Ertelt, A. Jatsch, B. Plietker, *Org. Lett.* **2008**, 10, 53–56.
- [64] D. Pan, A. Chen, Y. Su, W. Zhou, S. Li, W. Jia, J. Xiao, Q. Liu, L. Zhang, N. Jiao, *Angew. Chem. Int. Ed.* **2008**, 47, 4729–4732.
- [65] D. D. Rowan, H. P. Lane, J. M. Allen, S. Fielder, M. B. Hunt, *J. Agric. Food Chem.* **1996**, 44, 3276–3285.
- [66] N. Marion, R. Gealageas, S. P. Nolan, *Org. Lett.* **2007**, 9, 2653–2656.
- [67] M. Brookhart, B. Grant, A. F. Volpe, *Organometallics* **1992**, 11, 3920–3922.
- [68] B. E. Love, E. G. Jones, *J. Org. Chem.* **1999**, 64, 3755–3756.
- [69] T. Hatakeyama, N. Nakagawa, M. Nakamura, *Org. Lett.* **2009**, 11, 4496–4499.
- [70] G. Cahiez, C. Duplais, A. Moyeux, *Org. Lett.* **2007**, 9, 3253–3254.
- [71] M. Sada, S. Komagawa, M. Uchiyama, M. Kobata, T. Mizuno, K. Utimoto, K. Oshima, S. Matsubara, *J. Am. Chem. Soc.* **2010**, 132, 17452–17458.
- [72] I. L. Lysenko, K. Kim, H. G. Lee, J. K. Cha, *J. Am. Chem. Soc.* **2008**, 130, 15997–16002.
- [73] D. M. Hodgson, M. J. Fleming, S. J. Stanway, *J. Am. Chem. Soc.* **2004**, 126, 12250–12251.
- [74] K. Ishizuka, H. Seike, T. Hatakeyama, M. Nakamura, *J. Am. Chem. Soc.* **2010**, 132, 13117–13119.
- [75] A. Krasovskiy, B. H. Lipshutz, *Org. Lett.* **2011**, 13, 3818–3821.
- [76] A. Krasovskiy, B. H. Lipshutz, *Org. Lett.* **2011**, 13, 3822–3825.
- [77] N. Sakai, T. Moriya, T. Konakahara, *J. Org. Chem.* **2007**, 72, 5920–5922.
- [78] V. B. Phapale, M. Guisán-Ceinos, E. Buñuel, D. J. Cárdenas, *Chem. Eur. J.* **2009**, 15, 12681–12688.
- [79] S. K. Pandey, A. E. Greene, J.-F. Poisson, *J. Org. Chem.* **2007**, 72, 7769–7770.
- [80] D. Seomoon, K. Lee, H. Kim, P. H. Lee, *Chem. Eur. J.* **2007**, 13, 5197–5206.
- [81] D. Habrant, B. Stengel, S. Meunier, C. Mioskowski, *Chem. Eur. J.* **2007**, 13, 5433–5440.
- [82] K. K. Wang, C. Liu, Y. G. Gu, F. N. Burnett, P. D. Sattsangi, *J. Org. Chem.* **1991**, 56, 1914–1922.

## 4 Thesis Summary

### 4.1 Summary

The aim of this thesis was to investigate alternative catalyst systems based on cheaper and more environmentally friendly metals to the established noble metal catalysts.

The first chapter deals with bis(imino)acenaphthene (BIAN) ligands and their application in catalysis. This ligand offers excellent coordinative properties and can be easily customized to satisfy individual requirements. It is also redox-active, making it a powerful tool for the substitution of noble metals in catalysis. The given examples illustrate many possible applications of this “non innocent” ligand.

The second chapter presents a bimetallic lithium aluminum hydride complex with a reduced BIAN ligand. This complex shows catalytic activity in various hydroboration reactions and in the hydrogenation of imines. While the former only deliver moderate results, the literature-known protocols for aluminum-catalyzed imine hydrogenations are surpassed by this system with regard to substrate scope. The high catalytic activity is said to be based on a) easier activation of the molecular hydrogen through the presence of the lithium cation and b) the sterically demanding ligand, which inhibits the formation of inactive dimer complexes.

The third chapter describes an iron-catalyzed system for the cross-coupling of allylic acetates with alkylgrignard reagents. Iron(II)-acetate or -acetylacetonate is used as the precatalyst, which is reduced to the active catalyst species by the grignard compound. Radical clock, poisoning and stoichiometric experiments indicate a homogeneous catalyst with iron in the +1 oxidation state. Subsequent iron-catalyzed hydrogenation provides formal  $sp^3$ - $sp^3$  coupling products, which constitute challenging reactions to this day.

## 4.2 Zusammenfassung

Das Ziel der vorliegenden Arbeit bestand darin, alternative Katalysatorsysteme auf Basis billigerer und umweltfreundlicherer Metalle zu den bereits etablierten Edelmetallkatalysatoren zu untersuchen.

Das erste Kapitel befasst sich mit Bis(imino)acenaphthen (BIAN) Liganden und deren Anwendung in der Katalyse. Dieser Ligand besitzt hervorragende koordinative Eigenschaften und kann leicht individuellen Ansprüchen angepasst werden. Er ist außerdem redoxaktiv und wird dadurch zu einem potenten Hilfsmittel für die Substitution von Edelmetallen in der Katalyse. Die vielfältigen Einsatzmöglichkeiten dieses „non-innocent“ Liganden werden an den aufgeführten Beispielen deutlich.

Im zweiten Kapitel wird ein bimetallischer Lithiumaluminiumhydridkomplex mit einem reduziertem BIAN Liganden vorgestellt. Dieser Komplex zeigt katalytische Aktivität in verschiedenen Hydroborierungsreaktionen und in der Hydrierung von Iminen. Während Erstere nur moderate Ergebnisse liefern, werden literaturbekannte Vorschriften für Aluminium-katalysierte Iminhydrierungen hinsichtlich Substratspektrum von diesem System übertroffen. Begründet wird die hohe katalytische Aktivität durch a) die erleichterte Aktivierung des molekularen Wasserstoffs durch die Anwesenheit des Lithiumkations und b) den sterisch anspruchsvollen Liganden, der die Bildung inaktiver Dimerkomplexe hemmt.

Das dritte Kapitel beschreibt ein Eisen-katalysiertes System für die Kreuzkupplung von allylischen Acetaten mit Alkyl-Grignardreagenzien. Als Präkatalysator wird Eisen(II)-acetat oder -acetylacetonat verwendet, welches nach der Reduktion durch die Grignardverbindung in die aktive Katalysatorspezies übergeht. Experimente mit Radikaluhren, Vergiftungs- und stöchiometrische Experimente deuten auf einen homogenen Katalysator mit Eisen in der Oxidationsstufe +1 hin. Eine direkt anschließende Eisen-katalysierte Hydrierung liefert formelle  $sp^3$ - $sp^3$  Kupplungsprodukte, welche bis heute schwer zugänglich sind.

## 5 Appendix

### 5.1 List of Abbreviations

<b>acac</b>	acetylacetonate
<b>BIAN</b>	bis(imino)acenaphthene
<b>Bn</b>	benzyl
<b>bpy</b>	2,2'-bipyridine
<b>CI</b>	chemical ionization
<b>COD</b>	1,5-cyclooctadiene
<b>CPME</b>	cyclopentylmethylether
<b>DAB</b>	1,4-diazabutadiene
<b>DABCO</b>	1,4-diazabicyclo[2.2.2]octane
<b>DCM</b>	dichloromethane
<b>dct</b>	dibenzo[a,e]cyclooctatetraene
<b>DFT</b>	density functional theory
<b>DiBAI-H</b>	diisobutyl aluminium hydride
<b>dipp</b>	2,6-diisopropylphenyl
<b>DMAP</b>	4-dimethylaminopyridine
<b>DME</b>	1,2-dimethoxyethane
<b>dppe</b>	1,2-bis(diphenylphosphino)ethane
<b>e.g.</b>	<i>exempli gratia</i>
<b>EDG</b>	electron donating group
<b>EA</b>	elemental analysis
<b>EI</b>	electron ionization
<b>equiv.</b>	equivalent(s)
<b>Et</b>	ethyl
<b>FID</b>	flame ionization detector
<b>GC</b>	gas chromatography
<b>h</b>	hour(s)
<b>HR</b>	high resolution
<b><i>i</i>Pr</b>	isopropyl
<b>IR</b>	infrared radiation
<b>LIFDI</b>	liquid injection field desorption ionization

<b>Me</b>	methyl
<b>min</b>	minute(s)
<b>MS</b>	mass spectrometry
<b>MTBE</b>	methyltertbutylether
<b>μW</b>	microwave
<b>NMP</b>	N-methyl-2-pyrrolidone
<b>NMR</b>	nuclear magnetic resonance
<b>o.n.</b>	over night
<b>ORTEP</b>	Oak Ridge Thermal Ellipsoid Plot
<b>PDI</b>	pyridinediimine
<b>Ph</b>	phenyl
<b>phen</b>	1,10-phenanthroline
<b>ppm</b>	part(s) per million
<b>R<sub>f</sub></b>	retention factor
<b>r.t.</b>	room temperature
<b>s</b>	second(s)
<b>t</b>	time
<b>T</b>	temperature
<b>tBu</b>	tertbutyl
<b>TEGDME</b>	tetraethyleneglycoldimethylether
<b>THF</b>	tetrahydrofuran
<b>TLC</b>	thin layer chromatography
<b>TMEDA</b>	N,N,N',N'-tetramethylethylenediamin
<b>TMS</b>	trimethylsilyl
<b>UV</b>	ultraviolet radiation
<b>Vis</b>	visible radiation

## 5.2 Acknowledgements

First of all, my profound thanks go to Axel for the given opportunities to take part in these interesting research topics and for the patient guidance and support provided during the past years.

My sincere thanks to Apl. Prof. Rainer Müller, Jun.-Prof. Ivana Fleischer and Prof. Frank-Michael Matysik for finding the time to review my thesis and to take part in my defense committee.

Huge thanks go to the whole AJvW group for the great atmosphere and the unforgettable memories collected during these years. My special thanks go to Matteo, Dominik and Dieter for helping me develop, to Patrick, Michael and Bernhard for the precious kitchen time and to all the other members of the group. Every one of you has made my past years truly extraordinary.

Zu guter Letzt gilt mein Dank meiner Familie, insbesondere meiner Frau Simone, die mich auf diesem Weg durch alle guten und schlechten Zeiten begleitet hat, und meinen Eltern Renate und Josef, deren Vertrauen und bedingungsloser Unterstützung ich mir zu jedem Zeitpunkt sicher sein konnte.



## 5.3 Curriculum Vitae

### Personal Data

Name	Josef Bernauer
Date of Birth	12.12.1990
Place of Birth	Passau (Germany)
Nationality	German

### Education

12/2015 – present	<p>Doctoral Thesis in Organic Chemistry at the University of Regensburg under supervision of Prof. Dr. Axel Jacobi von Wangelin</p> <p><i>“Aluminium and Iron Catalysts as sustainable Alternatives in Synthetic Processes”</i></p>
10/2013 – 10/2015	<p>Master’s degree at the University of Regensburg (1.6)</p> <p>Master Thesis in Organic Chemistry at the University of Regensburg under supervision of Prof. Dr. Axel Jacobi von Wangelin (1.1)</p> <p><i>“Eisen-katalysierte Kreuzkupplung allylischer Acetate“</i>  <i>(“Iron-catalyzed Cross Coupling of allylic Acetates”)</i></p>
10/2010 – 09/2013	Bachelor’s degree at the University of Regensburg (2.1)
09/2001 – 06/2010	General higher education entrance qualification at the Wilhelm-Diess-Gymnasium Pocking (2.1)

## List of Publications

*“Iron-Catalyzed Allylation-Hydrogenation Sequences as Masked Alkyl-Alkyl Cross-Couplings”*, J. Bernauer, G. Wu, A. Jacobi von Wangelin, *RSC Adv.* **2019**, 9, 31217-31223.

*“Application of Reduced Bis(imino)acenaphthene (BIAN) Aluminium Hydride Complexes in Catalysis”*, J. Bernauer, D. Schaarschmidt, A. Jacobi von Wangelin, *in preparation*.

*“Bis(imino)acenaphthene (BIAN) Ligands in Catalysis”* J. Bernauer, A. Jacobi von Wangelin, *in preparation*.

## Conference Contributions

J. Bernauer, A. Jacobi von Wangelin, *“Iron-Catalyzed Cross-Coupling Reactions of Allylic Acetates”*, Wissenschaftsforum Chemie (WiFO), **2015**, Dresden (Germany). (Poster)

J. Bernauer, A. Jacobi von Wangelin, *“Iron-Catalyzed Cross-Coupling Reactions of Allylic Acetates”*, Liebig-Vereinigung für Organische Chemie (ORCHEM), **2016**, Weimar (Germany). (Poster)

J. Bernauer, G. Wu, A. Jacobi von Wangelin, *“Iron-Catalyzed Pseudo  $sp^3$ - $sp^3$  Coupling Reactions”*, Wissenschaftsforum Chemie (WiFO), **2017**, Berlin (Germany). (Poster)

J. Bernauer, D. Schaarschmidt, A. Jacobi von Wangelin, *“Characterisation and Application of Reduced Bis(imino)acenaphthene (BIAN) Al-Complexes”*, Liebig-Vereinigung für Organische Chemie (ORCHEM), **2018**, Berlin (Germany). (Poster)

## 5.4 Eidesstattliche Erklärung

- I. Ich erkläre hiermit an Eides statt, dass ich die vorliegende Arbeit ohne unzulässige Hilfe Dritter und ohne Benutzung anderer als der angegebenen Hilfsmittel angefertigt habe; die aus anderen Quellen direkt oder indirekt übernommenen Daten und Konzepte sind unter Angabe des Literaturzitats gekennzeichnet.
- II. Bei der Auswahl und Auswertung haben mir die in den jeweiligen Kapiteln aufgeführten Personen in der beschriebenen Art und Weise unentgeltlich geholfen.
- III. Weitere Personen waren an der inhaltlich-materiellen Herstellung der vorliegenden Arbeit nicht beteiligt. Insbesondere habe ich hierfür nicht die entgeltliche Hilfe eines Promotionsberaters oder anderer Personen in Anspruch genommen. Niemand hat von mir weder unmittelbar noch mittelbar geldwerte Leistungen für Arbeiten erhalten, die im Zusammenhang mit dem Inhalt der vorgelegten Dissertation stehen.
- IV. Die Arbeit wurde bisher weder im In- noch im Ausland in gleicher oder ähnlicher Form einer anderen Prüfungsbehörde vorgelegt.

---

Regensburg, den 10.06.2020